UAB
Universitat Autònoma de Barcelona

Molecular mechanisms controlling the diurnal oscillation of R-loop formation in Arabidopsis thaliana

Wenguan Zhou

ADVERTIMENT. L'accés als continguts d'aquesta tesi queda condicionat a l'acceptació de les condicions d'ús establertes per la següent llicència Creative Commons: https://creativecommons.org/licenses/?lang=ca

ADVERTENCIA. El acceso a los contenidos de esta tesis queda condicionado a la aceptación de las condiciones de uso establecidas por la siguiente licencia Creative Commons: https://creativecommons.org/licenses/?lang=es

WARNING. The access to the contents of this doctoral thesis it is limited to the acceptance of the use conditions set by the following Creative Commons license: https://creativecommons.org/licenses/?lang=en

Universitat Autònoma de Barcelona

CRAG CENTRO DE INVESTIGACIÓN EN AGRIGENÓMICA

Molecular mechanisms controlling the diurnal oscillation of R-loop formation in *Arabidopsis thaliana*

PhD Thesis

Wenguan Zhou

Barcelona, 2024

Universidad Autónoma de Barcelona

Facultad de Biociencias

Departamento de Biología Animal, Biología Vegetal y Ecología

Programa de Doctorado en Biología y Biotecnología Vegetal

Molecular mechanisms controlling the diurnal oscillation of R-loop formation in *Arabidopsis thaliana*

Thesis Director:

Dr. Paloma Mas

PhD Candidate:

Wenguan Zhou

Barcelona, 2024

TABLE OF CONTENTS

TABLE OF CONTENTS

Acknowledgements....11
Introduction....15
1. Overview of the circadian system....17
2. The plant circadian clock....20
2.1 The Arabidopsis central oscillator....21
2.2 Circadian input pathways....25
2.2.1 Light input to the clock....25
2.2.1.1 Phytochromes entrain the plant clock....27
2.2.1.2 Cryptochromes entrain the plant clock....28
2.2.2 Temperature input to the plant clock....31
2.3 Circadian clock outputs....34
2.3.1 Circadian regulation of seedling growth by photoreceptors....35
2.3.2 Circadian regulation of flowering by photoreceptors....36
2.3.3 Connection of the circadian clock with DNA damage and genome stability....38
3 Brief overview on transcription....41
3.1 Transcription initiation and elongation....41
3.2 Functional connection of chromatin structure and transcription....43
3.3 General overview of the FACT (FAcilitates Chromatin Transcription) complex....44
3.3.1 Basic features and functions of FACT....45
3.3.2 FACT regulates plants development and growth....49
3.4 Connection between circadian clock and transcription....50
4 General overview of R-loops....51
4.1 Formation and removal of R-loops....54
4.2 The relationship between R-loops and N^6-methyladenine modifications....57
5. R-loops in plants....58
5.1 Genomic distribution of R-loops....59
5.2 The connection between R-loops and epigenetic modifications....59
5.3 Connection of R-loops with plant development and stress responses....60
5.3.1 Connection between R-loops and flowering time....61
5.3.2 Connection between R-loops and root development....63
5.3.3 R-loop response to stresses....64
5.3.4 R-loop regulation of RNA processing....65
5.4 R-loop connection with genome stability in plants....65

Table of contents

Objectives 69

Results 73

1. Diurnal accumulation of R-loops assayed by dot-blot analyses 75

1.1 Dot-blot analysis of R-loop accumulation in *Arabidopsis thaliana* 75

1.2 Diurnal accumulation of R-loops in *Arabidopsis thaliana* 80

1.3 Generation of *RNase H1A* over-expressing plants 81

1.4 Over-expression of *RNase H1A* reduces R-loop accumulation in Arabidopsis 83

2. Identification of the molecular components involved in the diurnal accumulation of R-loops 84

2.1 Phytochrome B and Cryptochrome 1 and 2 regulate the diurnal accumulation of R-loops 84

2.2 CCA1 represses R-loop accumulation during the day 87

2.3 PRRs are required for R-loop accumulation during the day 88

2.4 ELF3 represses R-loop accumulation at both day and night 89

3. Connection of transcription and R-loop accumulation 91

3.1 Mutation of LNKs reduces R-loop accumulation in Arabidopsis 91

3.2 Decreased accumulation of RNA Pol II at genomic loci correlates with reduced R-loop abundance 92

3.3 The diurnal changes in R-loop levels correlate with the accumulation of RNA Pol II-CTD S2P and S5P .. 94

3.4 Diurnal changes in chromatin compaction 95

3.5 Mutation of the transcription elongation factor *TFIIs* increases R-loop accumulation 96

4. Identifying the molecular link between transcription and the diurnal accumulation of R-loops 98

4.1 SSRP1 sustains the diurnal accumulation of R-loops 98

4.2 Mutation of *SSRP1* alters the chromatin compaction 100

4.3 Mutation of *SSRP1* induces changes in histone modifications 101

4.4 Mutation of *SSRP1* increases RNA Pol II S5P and S2P accumulation 102

4.5 Mutation of *SSRP1* suppresses m^6A accumulation 103

4.6 Mutation of *SSRP1* affects leaf emergence after DNA damage 105

Discussion 107

Conclusions 121

Resumen en Castellano 125

Summary in English 129

Materials and methods 133

1. Plant material and growth conditions 135

2. Dot-blot assay for R-loops analysis 135

3. Plasmid construction and plant transformation 137

4. RNA extraction and real-time quantitative PCR analysis 139

5. Flavopiridol (FLAP) treatments 140
6. DRIP (DNA-RNA Immunoprecipitation)-qPCR assay 140
7. Chromatin Immunoprecipitation (ChIP) 142
8. Western blot analyses 144
9. DAPI staining and image acquisition 146
10. Dot-blot analysis of N6-methyladenosine RNA modification 147
11. Leaf emergence analyses 148
References 159

ACKNOWLEDGEMENTS

Acknowledgements

Completing this doctoral thesis has been an extraordinary journey, marked by numerous challenges and significant personal growth. This milestone in my life would not have been possible without the unwavering support of many individuals, to whom I am deeply indebted.

First and foremost, I would like to express my heartfelt gratitude to my esteemed supervisor, Dr. Prof. Paloma Mas, for giving me the opportunity to pursue my Ph. D studies within her research group. Her profound knowledge, astute guidance, insightful feedback, and patience have been invaluable in shaping this study. I appreciate her taking time out of her busy schedule to meticulously revise my thesis. Without her mentorship, this thesis would not have been possible.

I am also immensely grateful to all the past and present members of our group at the Centre for Research in Agricultural Genomics (CRAG). Your assistance, companionship, and wisdom have contributed significantly to the best memories of my Ph.D. journey. Deeply thankful to everyone who has contributed to this journey in various ways. Your support, encouragement, and belief in my abilities have been invaluable.

I extend my sincere thanks to CRAG for providing an academically stimulating atmosphere. My appreciation also extends to the participants of my study for their invaluable help and support. Special thanks to the dedicated greenhouse managers, Gloria Villalba and Alejandro Alonso; the microscopy and imaging administrator, Montse Amenós; and the capillary sequencing manager, Mercè Miquel. Their hard work and contributions behind the scenes have ensured the smooth operation of

the experimental processes, paving the way for this study.

To my friends and family, I owe a debt of gratitude that words can scarcely express. Your unwavering support, understanding, and encouragement sustained me through the inevitable peaks and valleys of this academic odyssey.

Lastly, I would like to extend my profound thanks to the China Scholarship Council (CSC) for their financial support, which enabled me to conduct this study.

INTRODUCTION

1. Overview of the circadian system

Nearly all organisms, from bacteria to humans, have evolved a sophisticated mechanism that allows them to detect the daily changes in environmental signals and generate biological rhythms with a 24-hour period (Young, 2000; Vitaterna et al., 2001; Más, 2005). This mechanism, known as circadian clock, plays a crucial role in synchronizing the organism's physiology and metabolism to anticipate daily environmental changes, particularly fluctuations in light and temperature. Circadian oscillations offer an adaptive advantage to organisms, facilitating the coordination of simultaneous, sequential, or temporarily incompatible processes (Gerhart-Hines and Lazar, 2015). The circadian clock controls the rhythmic oscillation of numerous essential processes, including among many others, the sleep and wake cycle (Zhu and Zee, 2012), the immune system (Rijo-Ferreira and Takahashi, 2019), metabolism, and plant responses to abiotic and biotic stresses (de Montaigu et al., 2010).

In 1971, Konopka and Benzer identified the first clock mutant in *Drosophila melanogaster* (Konopka and Benzer, 1971). In the following years, the first circadian gene was identified in mammals (King et al., 1997). Over the years, with the discovery of other clock components, the basic core clock oscillator has been established in a variety of organisms, including mammals, plants, and fungi. These components, along with other interacting proteins form a complex regulatory network that generates the oscillations in gene expression, creating the internal circadian rhythms. Circadian rhythms vary among different cells, tissues, and organs, but coordinate their activity with each other (Kumar and Sharma, 2018). The circadian system in plants and mammals exhibits a hierarchical structure, with a central master clock governing circadian rhythms of distal organs. In mammals,

the suprachiasmatic nuclei (SCN) play a crucial role in coordinating the clocks of other organs (Aton and Herzog, 2005). Similarly, in plants, the shoot apex acts as a master clock that modulates the rhythms in roots (Takahashi et al., 2015).

The circadian function has been organized into three main broad components: the input pathways, the self-sustaining central oscillators, and the output pathways (Figure 1) (Hsu and Harmer, 2014). Although this organization is an over-simplification, it provides a good model for understanding how the clock works. Light and temperature diurnal changes serve as major signals for resetting the circadian clock through the input pathways, which are responsible for transmitting the environmental information to the central oscillator. The central oscillator consists of regulatory loops that receive the environmental information from the input pathways to synchronize the internal rhythms with the external day-night cycle. The central oscillator generates circadian rhythms through multiple output pathways, which establish the connection between the oscillator and metabolism and physiology (Figure 1).

The rhythmic expression and function of clock components play a crucial role in generating biological oscillations. Circadian regulation occurs through different molecular regulatory mechanisms, including among others, transcriptional, post-transcriptional, post-translational, chromatin modification, and protein movement (Seo and Mas, 2014; Chen et al., 2020). These mechanisms ensure that biological rhythms occur approximately every 24 hours in synchronization with the external day and night cycles.

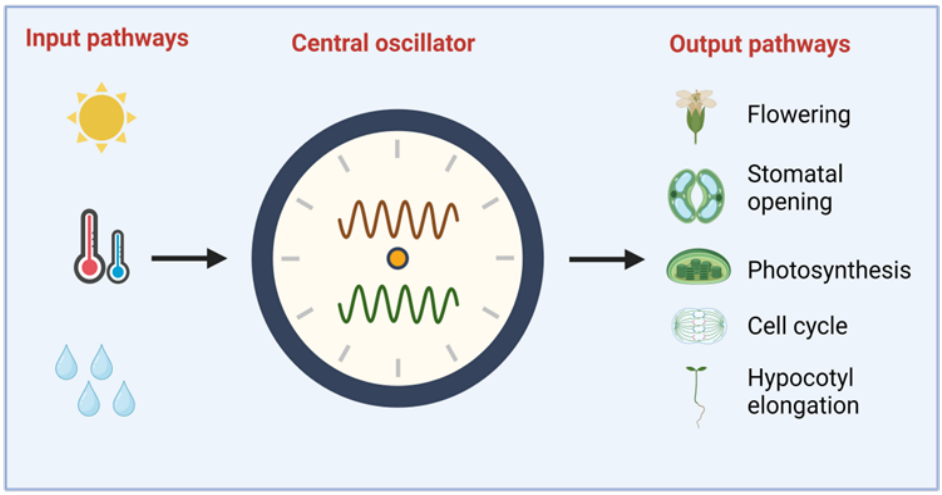


Figure 1. Simplified model of the *Arabidopsis* circadian system. The daily environmental changes, such as light, temperature as well as humidity are transmitted to the central oscillator through the input pathways. The central oscillator generates the circadian rhythms in a diverse array of biological processes or clock outputs. Created with Biorender.

Circadian rhythms are sinusoidal waves that can be mathematically defined by their period, phase, and amplitude. The phase of the circadian rhythm is defined as the position of the peaks or troughs relative to a reference rhythm (Vitaterna et al., 2001). The amplitude of the clock refers to the distance between the peak or trough and the midline of the waveform, while the period represents the time required to complete one cycle, typically measured between two adjacent peaks or troughs (Golden and Canales, 2003) (Figure 2).

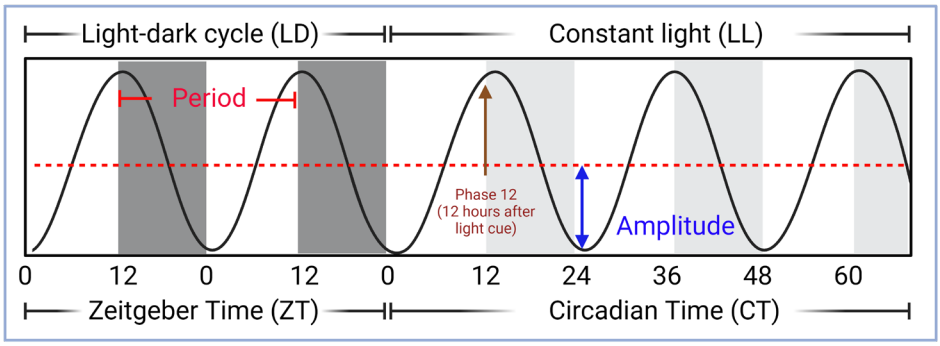


Figure 2. Mathematical parameters of circadian rhythms. The sinusoidal waves are defined by the period, phase, and amplitude (see text for further details). Zeitgeber time refers to the time cues or external signals that organisms use to synchronize their internal biological rhythms with the 24-hour day. Circadian time is the internal biological timekeeping system that operates on a roughly 24-hour cycle. This figure was modified from (Saini et al., 2019) and created with Biorender. White and dark gray boxes indicate periods of day and night, respectively. Constant light conditions are represented by alternating white (subjective day) and pale gray boxes (subjective night).

2. The plant circadian clock

Plants, as sessile organisms, have evolved a diverse array of adaptive mechanisms to effectively respond to environmental changes and secure their survival. One of these mechanisms, the circadian clock, is responsible for the regulation of plant growth, development, and responses to abiotic and biotic stress (de Montaigu et al., 2010; Johansson and Staiger, 2015; Kim et al., 2017; Yang et al., 2021). The model plant *Arabidopsis thaliana* shows more chlorophyll content, a fast growth rate, fixed more carbon and displays enhanced growth survival when the circadian period correctly matches the external period of the day-night cycle (Dodd et al., 2005). Moreover, the circadian clock in plants also plays a crucial role in controlling the functioning of cellular organelles such as mitochondria or

chloroplasts (Fukushima et al., 2009; Atkins and Dodd, 2014; Cervela-Cardona et al., 2021a; Cervela-Cardona et al., 2021b). In this section, we briefly describe the functioning of the circadian central oscillator, along with its input and output pathways, placing particular emphasis on the role of photoreceptors.

2.1 The Arabidopsis central oscillator

The central oscillator in *Arabidopsis* is governed by a set of interconnected genes known as the "core clock genes." These genes regulate the timing of various physiological and developmental processes in response to diurnal cycles (Figure 3). The Arabidopsis central oscillator exhibits a remarkable complexity, with numerous transcription factors organized into multiple regulatory loops. One main regulatory module is composed by the morning-expressed single-MYB transcriptional factors, CIRCADIAN CLOCK ASSOCIATED1 (CCA1) (Wang and Tobin., 1998), LATE ELONGATED HYPOCOTYL (LHY) (Schaffer et al., 1998) and the evening-expressed TIMING OF CAB EXPRESSION 1/PSEUDO-RESPONSE REGULATOR 1 (TOC1/PRR1) (Strayer et al., 2000) (Figure 3). CCA1 and LHY have partially redundant functions (Alabadí et al., 2002; Mizoguchi et al., 2002). They bind to the promoters of the evening-expressed target genes and repress their expression in the morning (Hazen et al., 2005; Li et al., 2011; Lu et al., 2012). For instance, CCA1 and LHY repress *TOC1* expression by directly binding to the Evening Element (EE) motif in the *TOC1* promoter (Alabadí et al., 2001; Perales and Mas, 2007). Furthermore, CCA1 and LHY repress each other as well as their own expression (Schaffer et al., 1998). The DE-ETIOLATED 1 (DET1) protein, a member of the COP10-DET1-DDB1 (CDD) complex, is required for the repressive activity of CCA1 and LHY on their target genes, including central clock genes and multiple output genes (Lau et al., 2011;

Nagel et al., 2015). Consistent with their important function within the clock, the *CCA1* over-expressing (*CCA1-ox*) and *LHY-ox* plants are arrhythmic (Schaffer et al., 1998; Wang and Tobin, 1998). The *cca1* and *lhy* mutant plants show a shorter circadian period phenotype (Green and Tobin, 1999; Mizoguchi et al., 2002) while the period of the *cca1lhy* double mutant is shorter than either single mutant (Lu et al., 2009).

In addition to CCA1 and LHY, other single-MYB transcription factor proteins known as REVEILLE (RVE) (McClung, 2014) show circadian-regulated expression (Rawat et al., 2011). Previous studies suggest that *RVE1*, *RVE2,* and *RVE7* mainly function in the regulation of circadian outputs (Kuno et al., 2003; Zhang et al., 2007; Rawat et al., 2009; Tian et al., 2022). Others, like RVE8 (known as LHY-CCA1-LIKE 5, LCL5), plays a role within the central oscillator. Over-expression or mutation of *RVE8/LCL5* affects the rhythmic expression of *CCA1* and *TOC1* (Farinas and Mas, 2011; Rawat et al., 2011). Additionally, RVE8/LCL5 and CCA1 have opposing effects on the regulation of the *TOC1* gene expression by modulating chromatin modification (Farinas and Mas, 2011). RVE8/LCL5 enhances *TOC1* expression by binding to the *TOC1* promoter, which correlates with increased histone H3 acetylation (Farinas and Mas, 2011). In contrast, CCA1 represses the expression of *TOC1* by promoting histone deacetylation (Farinas and Mas, 2011). Following studies demonstrated that RVE8 interacts with the NIGHT LIGHT-INDUCIBLE AND CLOCK-REGULATED1 (LNK1) and LNK2, thereby activating the expression of evening-expressed *PRR5* and *TOC1* by recruitment of the transcriptional machinery (Xie et al., 2014).

TOC1 in turn represses the expression of *CCA1* and *LHY* (Gendron et al., 2012; Huang et al., 2012). Notably, when *TOC1* is over-expressed, it causes a reduction

in the expression of nearly all oscillator genes (Huang et al. 2012). The *toc1* mutant and *TOC1* RNAi plants both exhibit a shorter circadian period when exposed to white light and blue light, whereas they show arrhythmia under continuous darkness or exposed to varying intensities of red light (Strayer et al., 2000; Más et al., 2003). The *TOC1 minigene* plants (TMG, expressing additional copies of *TOC1* under its native promoter) show a delayed pace of the clock, while constitutive over-expression of *TOC1* (*TOC1-ox*) leads to arrhythmia (Más et al., 2003).

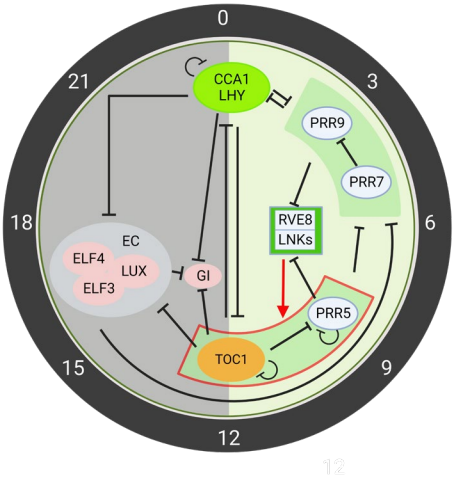


Figure 3. The main regulatory transcriptional network of the *Arabidopsis* central oscillator. The central oscillator is composed of reciprocal regulatory loops. See the text for further details. Transcriptional activation is represented by red arrows while transcriptional repression is represented by lines ending in perpendicular dashes. Created with Biorender.

Additional regulatory modules include the one consisting of CCA1, LHY, and other members of the TOC1 family, namely PRR7, and PRR9, which are expressed early in the morning and during the day (Wang and Tobin., 1998; Akinori Matsushika et al., 2000). CCA1 and LHY repress the expression of *PRR9* and *PRR7* by binding to their promoters. In turn, PRR9, PRR7, and the close-to-dusk-expressed PRR5 repress *CCA1* and *LHY* through interaction with TOPLESS/TOPLESS-RELATED (TPL/TPR) proteins (Farré et al., 2005; Nakamichi et al., 2010; Wang et al., 2013). A recent study has shown that PRR9, PRR7, and PRR5 interact with the B-BOX proteins BBX28 and BBX29 in the

nucleus, enhancing the transcriptional repressive activities of PRRs (Yu et al., 2023). In turn, PRR proteins directly repress the expression of *BBX28* and *BBX29* (Yu et al., 2023). On the other hand, the co-activators LIGHT-REGULATED WD1 (LWD1) and LWD2 play a role in the transcriptional activation of *CCA1* by direct interaction with TEOSINTE BRANCHED 1-CYCLOIDEA-PCF20 (TCP20) and TCP22 (Wu et al., 2016). The expression levels of *PRR9* and *PRR7* are also lower in the *lwd* mutant, suggesting that LWD1 also acts as a positive regulator of *PRR9* and *PRR7* (Wang et al., 2011).

Another regulatory module consists of the clock components GIGANTEA (GI), TOC1, PRR5, EARLY FLOWERING 3 (ELF3), ELF4, as well as LUX ARRHYTHMO (LUX) (Strayer et al., 2000; Nusinow et al., 2011b; Herrero et al., 2012). These genes are expressed close to dusk or in the evening. As mentioned above, TOC1 not only represses the morning-expressed genes expression but also represses the evening-expressed genes *ELF4*, *GI*, and *LUX* by binding to their promoters (Huang et al., 2012). ELF3 interacts with LUX and ELF4 *in vivo*, forming the Evening Complex (EC) (Nusinow et al., 2011a). The EC represses the expression of *PRR9*, *PRR7* and *LUX*, among other genes (Dixon et al., 2011; Helfer et al., 2011; Nusinow et al., 2011a). Extensive overlap in binding sites across the entire genome has been observed for ELF3, ELF4, and LUX through chromatin immunoprecipitation assays followed by sequencing (ChIP-seq) (Ezer et al., 2017). These studies suggest that the EC serves as a central hub that governs various biological processes, including photosynthesis, light perception, hormone signaling, circadian rhythms, and temperature responses (Ezer et al., 2017). Further RNA-sequencing data have revealed that the expression of most EC target genes is increased in the *elf3* and *lux* mutants (Ezer et al., 2017). This suggests

that the EC complex primarily functions as a repressor. Furthermore, the EC not only suppresses targets during the early evening but also transmits temperature information in this regulation (Ezer et al., 2017). Consistently, ELF3 functions as a thermosensor (Jung et al., 2020). Under normal conditions, ELF3 exhibits rapid and reversible binding to the promoter of its target genes, leading to the repression of gene expression under normal ambient temperatures (Jung et al., 2020). At elevated temperatures, ELF3 drives the formation of nuclear speckles, leading to the reduction of transcriptional repression on its target genes (Jung et al., 2020).

2.2 Circadian input pathways

The circadian input pathways in Arabidopsis transmit time-keeping signals from the surrounding environment to the central oscillator, aiding in synchronizing the central oscillator with diurnal environmental cues to ensure that circadian function is appropriately timed (Devlin, 2002). These signals typically originate from predictable shifts between the day and night, including, among others, light, temperature as well as humidity (Gould et al., 2006; Bieniawska et al., 2008; Portoles and Mas, 2010; Mwimba et al., 2018). In this section, we will briefly describe how light and temperature entrain the circadian clock in Arabidopsis.

2.2.1 Light input to the clock

Light serves as the primary signal for resetting the biological clock, and multiple studies have demonstrated a strong connection between photoreceptors and the clock in various organisms. Light entrains the circadian clock through two distinct mechanisms, non-parametric entrainment and parametric entrainment (Comas et al., 2008; Oakenfull and Davis, 2017). Parametric entrainment involves gradual entrainment of the clock, such as increasing or decreasing the pace of the clock

with changes in light intensity, as Aschoff's rule states (Aschoff, 1979). Typically, the circadian period of diurnal organisms under free-running (constant light or constant dark) tends to be longer at lower light intensities and shorter at higher light intensities. The circadian period in plants becomes significantly longer under constant darkness (Millar et al., 1995).

In addition to the gradual alteration of the clock's speed, light has the capability to induce rapid resetting of the clock, occurring within minutes to hours. This phenomenon is referred to as non-parametric entrainment or entrainment to discrete light pulses (Pittendrigh, 1960). Non-parametric entrainment involves the readjustment of the clock through daily phase changes and from light to dark or dark to light (Comas et al., 2008; Roenneberg et al., 2010). Phase response curves (PRC) can be accurately obtained by utilizing short light pulses, and they offer satisfactory explanations for the entrainment phenomenon (Aschoff, 1999). PRCs are constructed by observing and recording the circadian phase and period during light pulses (Oakenfull and Davis, 2017). The shape of the PRC is determined by the intensity of the resetting stimulus it receives. For instance, when weaker light pulses are administered during the subjective night, they elicit smaller phase shifts compared to the larger phase shifts induced by more intense light pulses (Johnson, 1992).

The central oscillator receives light input through various types of photoreceptors, including cryptochromes, phytochromes, and the ZTL family proteins (Fankhauser and Staiger, 2002; Inoue et al., 2017). Phytochrome and cryptochrome photoreceptors control red (600-700 nm wavelength) and blue light (400-500 nm wavelength) signaling to the clock, respectively (Somers et al., 1998;

Devlin and Kay, 2000; Yanovsky et al., 2000). In Arabidopsis, five phytochromes (PHYA to PHYE) and at least two members of the cryptochrome gene family (CRY1 and CRY2) have been identified (Ahmad and Cashmore, 1993; Lin et al., 1998; Eichenberg et al., 2000; Wang et al., 2001). Both phytochrome and cryptochrome photoreceptors play a crucial role in regulating the circadian clock (Bognar et al., 1999; Ceriani et al., 1999).

2.2.1.1 Phytochromes entrain the plant clock

Phytochromes are activated by red light, converting the inactive Pr form to the active Pfr form. Far-red light deactivates phytochromes by converting the Pfr form back to the Pr form (Inoue et al., 2017). The purification of phytochromes from plants has confirmed the existence of two spectrally interconvertible forms (Butler et al., 1959). Phytochromes are classified into two groups: type I (PHYA in Arabidopsis), which is light-labile, and type II (PHYB to PHYE in Arabidopsis), which is light-stable (Hirschfeld et al., 1998). PHYA highly accumulates in etiolated seedlings (Quail, 1991), and plays a crucial role during seed germination, seedling establishment, and response to low red light (Whitelam et al., 1993; Johnson et al., 1994). PHYA is unstable in the presence of light and rapidly degrades under high-light conditions (Sharrock and Clack, 2002). The *phyA* mutant exhibits a longer circadian period than the wild type under low red light free-running conditions (Somers et al., 1998). In *phyB* mutants, the circadian period is longer than in the wild type under high red light conditions (Somers et al., 1998). *PHYB* over-expression results in a shorter period length in a fluence-dependent manner compared to the wild type (Somers et al., 1998). The *phyABCDE* quintuple mutants display a shorter period under low red light conditions (Hu et al., 2013; Jones et al., 2015).

The phytochrome signaling intermediates FHY3 (FAR-RED ELONGATED HYPOCOTYL3) and its paralog FAR1 (FAR-RED IMPAIRED RESPONSE1) are also crucial for circadian clock gene expression under continuous white light conditions (Allen et al., 2006; Li et al., 2011). FHY3 and FAR1 directly bind to the promoters of *ELF4* and *CCA1*, activating their expression (Li et al., 2011; Liu et al., 2020b). Furthermore, the phytochrome-interacting factors (PIFs) connect the circadian clock with environmental light signaling (Shor et al., 2017; Liu et al., 2020b). The light-signaling repressor PIF5, along with TOC1, physically interacts with FHY3 and FAR1, repressing their transcriptional activity, further reducing the *CCA1* expression (Liu et al., 2020b). Under diurnal ambient conditions, the high expression level of *FHY3* and *FAR1* combined with low levels of *PIF5* and *TOC1* before dawn, contributes to the peak expression of the morning gene *CCA1*. The rhythmic expression of *PIF5* and *PIF4* is regulated by the EC (Nusinow et al., 2011a). The EC binds to the promoters of *PIF4* and *PIF5* through the recruitment of LUX, reducing the expression of *PIF4* and *PIF5* during the night (Nusinow et al., 2011a). Additionally, PHYB represses the post-translational levels of *PIF4* and *PIF5* (Sakuraba et al., 2014).

2.2.1.2 Cryptochromes entrain the plant clock

Besides phytochromes, cryptochromes are also crucial factors involved in circadian entrainment. *CRY1* and *CRY2* perceive blue light signals that regulate the clock (Devlin and Kay, 2000). CRY1 exhibits high stability at high intensities of blue light (Lin et al., 1998) whereas CRY2 protein rapidly decreases under high-light conditions (Lin et al., 1998). Under low blue light conditions, the *cry2* mutant displays a shorter circadian period length, while the *cry1* mutant exhibits

a longer period length compared to the wild type under both low and high blue light conditions (Devlin and Kay, 2000). Similarly, the *cry1cry2* double mutant shows a longer period under both low and high blue light conditions (Devlin and Kay, 2000). Over-expression of *CRY1* in Arabidopsis leads to a shorter circadian period length and increased sensitivity to blue light (Lin et al., 1996). It is worth noting that the *cry1cry2* double mutant still maintains robust rhythmicity, suggesting that CRY1 and CRY2 serve as important factors in the input pathway of the plant circadian system.

Notably, the *cry1* mutant demonstrates a deficiency in perceiving low fluence-rate white light, similar to the observed response in the *phyA* mutant (Devlin and Kay, 2000). This suggests that both CRY1 and PHYA are required to respond to low fluence white light. In white light, the double mutant of *phyAcry1* confirms the absence of additivity between the *phyA* and *cry1* mutations, suggesting that CRY1 operates downstream of the photoreceptor PHYA, likely functioning as a signal transduction element (Devlin and Kay, 2000). Indeed, the yeast two-hybrid experiment showed that CRY1 interacted with PHYA, and phosphorylation of CRY1 by recombinant oat PHYA *in vitro* (Ahmad et al., 1998). Additionally, PHYB and CRY2 also engage in light-dependent nuclear speckle formation through their interaction, which controls flowering time, hypocotyl elongation, and circadian period by the clock (Mas et al., 2000). A subsequent study demonstrated that PHYB physically interacts with clock components, such as CCA1, LHY, GI, TOC1, LUX, and ELF3 (Yeom et al., 2014). Furthermore, the results indicated that CCA1 and TOC1 preferentially interact with PHYB under red light, while LUX exhibits a preferential interaction under far-red light (Yeom et al., 2014).

CRYs play a pivotal role in mediating the blue-light regulation of the RNA N6-methyladenosine (m^6A) modification of at least 10% of the Arabidopsis transcriptome. Interestingly, this modification is especially enriched in circadian clock-regulated genes (Wang et al., 2021b). The abundance of m^6A decreased markedly in the *cry1cry2* double mutant compared to wild type plants under blue light conditions (Wang et al., 2021b). To exert its regulation, CRY2 interacts with the subunit of the m^6A RNA methyltransferase (writer of m^6A) messenger RNA (mRNA) adenosine methylase A (MTA), mRNA adenosine methylase B (MTB), and FKBP12 INTERACTING PROTEIN 37 (FIP37), and undergoes liquid-liquid phase separation (LLPS) *in vivo* (Wang et al., 2021b). Both *cry1cry2* and *mta* mutants show a long-period phenotype, decreased m^6A abundance, and accelerated degradation of *CCA1* mRNA (Wang et al., 2021b) (Figure 4).

A recent study showed that CRY2 plays an important role in regulating the phosphorylation of PRR9 by competitively interacting with PHOTOREGULATORY PROTEIN KINASEs (PPKs) in a light-dependent manner (He et al., 2022). Furthermore, CRY2 reduces the repressing activity of PRR9 by directly interacting with PRR9 and effectively blocking the interaction between PRR9 and TPL (He et al., 2022) (Figure 4). CRY2 also engages in photobody formation together with TCP22 (Wu et al., 2016) in response to blue light (Mo et al., 2022). PPK1 regulates the CRY2-TCP22 photobodies by phosphorylating both CRY2 and TCP22 (Mo et al., 2022). As mentioned above, LWDs interact with TCP22 (Wu et al., 2016), especially with phosphorylated TCP22 (Mo et al., 2022). This suggests that PPK1 enhances the interaction between LWDs and TCP22 and increases the partition ratio and size of LWD1-CRY2-TCP22 photobodies both *in vitro* and *in vivo* (Mo et al., 2022). Further, this

interaction positively regulates the expression of *CCA1* (Mo et al., 2022) (Figure 4). CRY2 also interacts with CRYPTOCHROME-INTERACTING basic helix-loop-helix 1 (CIB1) and activates the activity of the transcription factor CIB1 promoting the *FLOWERING LOCUS T* (*FT*) gene expression (Liu et al., 2013) (Figure 4). ZTL prevents the degradation of CIB1 through the 26S proteasome in response to blue light (Liu et al., 2013). Overall, CRY2 contributes to circadian gene expression in a light quality-dependent manner.

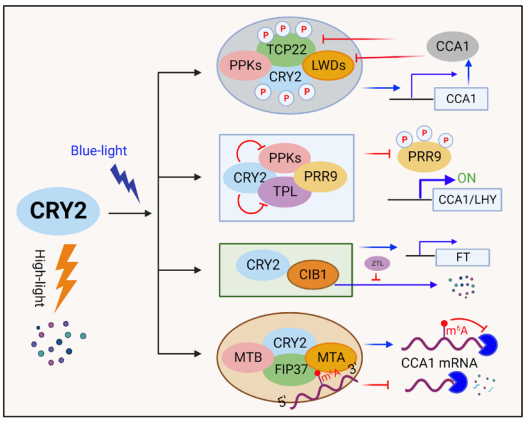


Figure 4. Diagram illustrating the connection of CRY2 with the circadian clock. The interaction of CRY2 with several factors contributes to the regulation of circadian clock gene expression. Red lines denote repression while blue arrows represent activation. For further details please consult the text. Created with Biorender.

2.2.2 Temperature input to the plant clock

In addition to light, temperature is another important cue that entrains the circadian clock. As mentioned above, even a small temperature change of four degrees can impact circadian rhythms (Brown et al., 2002; Thines and Harmon, 2010). A study demonstrated that a four-degree difference is sufficient to induce temperature entrainment (Thines and Harmon, 2010). Under free-running conditions, plants exhibit a circadian period of approximately 24 hours across a physiological range of temperatures (Gould et al., 2006), reflecting the endogenous cellular period of the circadian clock (Beaulé, 2009). It is somewhat counterintuitive that while the Arabidopsis circadian is entrained by rhythmic

temperature cycles, it can also buffer the free-running circadian period against ambient temperature changes (within a physiological range). This is an intrinsic feature of circadian clocks known as temperature compensation (Gould et al., 2006). Several mechanisms have been described thus far to explain how temperature compensation is achieved (Portoles and Mas, 2010; Salome et al., 2010).

The interaction between CCA1 and the protein kinase CK2 (CASEIN KINASE 2) provides a mechanism for temperature compensation in plants (Portoles and Mas, 2010). CCA1 undergoes phosphorylation by CK2, resulting in reduced binding of CCA1 to its target promoters (Portoles and Mas, 2010). High temperature increases both CK2 phosphorylation and CCA1 binding and conversely, low temperatures reduce both activities. Thus, there is a precise balance of counteracting activities that are similarly regulated by temperature. This co-regulatory mechanism provides a means for temperature compensation in Arabidopsis (Portoles and Mas, 2010). Further studies have also shown that PRR7 and PRR9 negatively regulate the expression of *CCA1* and *LHY* and contribute to temperature compensation as ambient temperature increases (Salome et al., 2010). The regulation of *CCA1* expression and activity at both transcriptional and post-transcriptional levels is essential in the control of clock temperature compensation. A previous study also identified that GI plays a role in maintaining the rhythms within a certain range of temperatures (Gould et al., 2006). The balance between GI and LHY is essential under high-temperature conditions while CCA1 functions at low temperatures (Gould et al., 2006).

Core clock components, such as TOC1, CCA1, LHY, and PRRs, display altered expression patterns when exposed to continuous light at 4°C, eventually leading

to arrhythmia (Bieniawska et al., 2008). As the ambient temperature rises from 17ºC to 27ºC, the mRNA expression levels of *GI* and *TOC1* increase, whereas the transcription level of *LHY* decreases (Gould et al., 2006). Conversely, the expression levels of *CCA1* and *LHY* increase as the temperature decreases from 17ºC to 12ºC (Gould et al., 2006). Temperature also exerts a significant influence on alternative splicing of circadian clock genes (Capovilla et al., 2015; Shang et al., 2017). Two transcript isoforms of *CCA1*, *CCA1α* and *CCA1β*, have been identified using RT-PCR and whole-genome sequencing (Filichkin et al., 2010; Seo et al., 2012). Similar to *CCA1α*, *CCA1β* also possesses a dimerization domain, but it lacks the N-terminal DNA-binding MYB motif (Filichkin et al., 2010; Seo et al., 2012). At high temperatures, the transcript level of the alternative splice variant *CCA1α* is increased, while the *CCA1β* transcripts are reduced (Seo et al., 2012). CCA1β acts as a repressor of CCA1α, by competing for interaction with CCA1α and LHY and forming nonfunctional CCA1α/CCA1β and CCA1β/LHY heterodimers (Seo et al., 2012). Over-expression of *CCA1β* results in a shortened circadian period similar to the *cca1/lhy* double mutant, and sensitivity to low temperature (Park et al., 2012; Seo et al., 2012). Under low-temperature conditions, the production of *CCA1β* is reduced, which enhances the function of *CCA1α* and contributes to freezing tolerance (Seo et al., 2012). This suggests that the redundant function of CCA1 and LHY is regulated by the temperature-dependent splice variants.

Other circadian clock components are subject to temperature-dependent alternative splicing as well. For example, the level of *ELF3β* is upregulated under high-temperature conditions and downregulated under low-temperature conditions (Kwon et al., 2014). The splicing variant level of *TOC1β* is increased

under both low- and high-temperature conditions (Kwon et al., 2014). The degradation of RNA splice variants of *TOC1* and *ELF3* occurs via the nonsense-mediated decay (NMD) pathway (Kwon et al., 2014). Heat stress induces significant upregulation of the splice variant *PRR7β*, which retains an intron whereas *PRR9* exhibits an increase in both full-length *PRR9α* and the splice variant *PRR9β* following both cold and heat stress (Kwon et al., 2014). *RVE8* is also subject to temperature-responsive alternative splicing, and cold stress promotes intron retention in *RVE8* (James et al., 2012).

As mentioned above, the EC component ELF3 acts as a thermo-sensor, forming condensates via LLPS, and triggering a temperature-dependent shift between active and inactive states (Jung et al., 2020). Under high temperatures, ELF3 forms nuclear speckles, reducing its repressing function on target genes, and thus allowing thermal-responsive transcription (Jung et al., 2020). Temperature also affects protein movement, as ELF4 moves from shoots to roots in a temperature-dependent manner to control the period of the clock in the roots (Chen et al., 2020). At low temperatures, ELF4 mobility is enhanced, leading to a slower clock in root, and conversely, at high temperatures, ELF4 movement is reduced, resulting in an accelerated clock in roots (Chen et al., 2020). Consequently, the ELF4 facilitates communication between shoots and roots and determines the pace of the clock in root tissues (Chen et al., 2020). Additionally, PHYB also acts as a thermo-sensor in Arabidopsis (Jung et al., 2016; Legris et al., 2016), with the activity of PHYB decreasing as the temperature increases (Legris et al., 2016).

2.3 Circadian clock outputs

The circadian clock exerts control over nearly all developmental stages of the

plant life cycle as well as over metabolism, physiology, and stress responses. In addition to the diurnally regulated outputs, seasonal processes regulated by changes in day-length or photoperiod are also coordinated by the circadian system. In this section, we briefly describe the diverse roles played by photoreceptors and the circadian system in the regulation of several biological processes.

2.3.1 Circadian regulation of seedling growth by photoreceptors

Miss-expression of the photoreceptors involved in the circadian input pathway alters plant growth. Under blue light conditions, the *cry1* mutant shows an elongated hypocotyl phenotype, while the *CRY1* over-expression exhibits a short hypocotyl phenotype (Ma et al., 2016). The *cry2* mutant displays an elongated hypocotyl phenotype under low fluence rates of blue light, whereas the *CRY2* over-expression plants exhibit reduced elongation (Lin et al., 1998). The hypocotyl length of the *cry2cry1* double mutant is significantly increased compared to the wild type, even longer than that of the *cry1* and *cry2* signal mutants (Mockler et al., 1999).

Under white light, PHYB is the primary phytochrome responsible for inhibiting hypocotyl elongation during seedling de-etiolation (Reed et al., 1993). *PHYB* over-expression seedlings exhibit a short hypocotyl phenotype compared to the wild type (Wagner et al., 1991). Previous studies demonstrated that CRY1 and PHYB directly interact with PIF4 in the presence of blue and red light, respectively, to regulate hypocotyl growth (de Lucas et al., 2008; Ma et al., 2016). Furthermore, CRY1 and PHYB physically interact with the Auxin Response Factors 6 (ARF6) and ARF8 to inhibit DNA binding activities under blue and red light, respectively (Mao et al., 2020). These interactions repress the ARFs target

gene expression, thereby regulating hypocotyl elongation (Mao et al., 2020). As mentioned above, CRY2 protein directly interacts with PHYB in nuclear speckles, contributing to the regulation of hypocotyl elongation (Mas et al., 2000). Under white light with low R/FR ratio conditions (mimicking shade-avoidance), the hypocotyl length of *cry2* is longer than that of the wild type (Mas et al., 2000).

2.3.2 Circadian regulation of flowering by photoreceptors

The transition from vegetative growth to a reproductive state is a critical stage in the plant life cycle. Many plants utilize day-length as a signal to synchronize their flowering with the appropriate season, thereby maximizing their reproductive success. In Arabidopsis, long-day promotes rapid flowering, while short-day delays flowering. The perception of day-length involves the circadian clock components and mutations in the clock genes often result in altered photoperiodic regulation of flowering time (Carr, 2001; Hayama and Coupland, 2003). *CONSTANS* (*CO*) is a flowering accelerator gene regulated by the circadian clock and day-length (Suarez-Lopez et al., 2001). The central role of CO is to trigger the flowering process in response to LgD conditions (Putterill et al., 1995; Robson et al., 2001). The *CO* transcript accumulates during the night under ShD, while the peak abundance of the *CO* transcript occurs mainly towards the end of the day under LgD (Suárez-López et al., 2001; Yanovsky and Kay, 2002). This suggests that *CO* is highly expressed during the day under LgD conditions, not under ShD (Valverde et al., 2004). The transcription of *FT* is activated by CO (Suárez-López et al., 2001). This is consistent with the earlier flowering phenotype of Arabidopsis under LgD conditions. These findings suggest that the synchronization of *CO* expression with light exposure is crucial for promoting flowering.

Photoreceptors play crucial roles in the regulation of flowering time in response to photoperiod. For instance, the Arabidopsis *phyA* mutant shows delayed flowering compared to the wild type under LgD conditions (Johnson et al., 1994; Neff and Chory, 1998). Conversely, the *phyB* mutant exhibits earlier flowering than the wild type under both LgD and ShD conditions (Goto et al., 1991; Mockler et al., 1999). Interestingly, plants with a monogenic *phyD* mutation do not exhibit any noticeable phenotype (Aukerman et al., 1997). However, mutation of both *PHYB* and *PHYD* genes exhibit an early flowering phenotype compared to *phyB* monogenic mutation under both LgD and ShD conditions (Aukerman et al., 1997; Devlin et al., 1999). Similar to PHYD, the signal *phyE* mutant shows no phenotypic alterations unless it is in the background of the *phyB* mutant. The flowering time of the *phyBphyE* double mutant is much earlier than the *phyB* single mutant under ShD conditions (Devlin et al., 1998). This suggests that the function of PHYD and PHYE are similar to that of PHYB, in the inhibition of flowering.

The precise role of CRY1 in flowering remains elusive, although it appears to have a promotive effect. The *cry1* mutant in the Landsberg *erecta* (L*er*) ecotype background exhibits a delayed flowering phenotype under ShD conditions (Mozley and Thomas, 1995). Similar results are also observed in the *cry1* mutant under the Col-0 background, particularly under ShD and quasi LgD (either day extensions or night breaks) conditions (Bagnall et al., 1996). Nevertheless, unlike other photoreceptors, the flowering time of the *cry1* mutant exhibits a significant degree of inconsistency (Goto et al., 1991; Mozley and Thomas, 1995; Bagnall et al., 1996; Zagotta et al., 1996; Mockler et al., 1999). In Arabidopsis, CRY2 is known to promote flowering. The *cry2* mutant is allelic to the photoperiod-

hypersensitive late-flowering *fha* mutant (Guo et al., 1998; Koornneef et al., 1998). *cry2* mutants exhibit a delayed flowering phenotype under LgD conditions but not under ShD conditions (Guo et al., 1998). However, when *CRY2* is over-expressed, plants show early flowering under ShD conditions but not under LgD conditions (Guo et al., 1998). These findings suggest that both mutation and over-expression of *CRY2* result in reduced sensitivity to the photoperiod.

2.3.3 Connection of the circadian clock with DNA damage and genome stability

DNA damage results in a series of defects in DNA structures. According to the type of DNA strand lesions, DNA damage has been classified into two main categories: DNA single-strand breaks (SSBs) and DNA double-strand breaks (DSBs) (Spampinato, 2017). Among the various types of DNA damage, DSBs are the most harmful, posing a threat to genomic integrity as they directly interfere with processes such as DNA replication and transcription (Waterworth et al., 2011). The occurrence of DNA replication or progression through mitosis in the presence of DSBs can result in the loss of chromosome fragments (Waterworth et al., 2011), leading to abnormal chromosome structures that ultimately affect the development and growth of the cell (Waterworth et al., 2011). Failure to appropriately repair DNA breaks affects both the chemical and physical structures of DNA, resulting in chromosomal rearrangements, alterations of the cell cycle, or cell death.

For adaptation to the surrounding environment and survival, organisms have evolved a diverse array of mechanisms to adeptly detect and repair DNA damage, which is crucial for maintaining genome integrity. A series of repair processes is

collectively known as the DNA damage repair (DDR) response. The signaling cascade of the general organization of the DDR is conserved between plants and animals (Nisa et al., 2019). Indeed, many environmental stresses are well-known to cause DNA damage in Arabidopsis (Jiang et al., 2011; Liu et al., 2012). Consistently, environmental temperature and day length significantly affect the DDR and genome stability in Arabidopsis (Boyko et al., 2005). Furthermore, the efficiency of DDR is age-dependent. With an increase in the age of plants, the rate of DNA repair decreases, leading to a significant increase in genomic instability (Golubov et al., 2010).

UV is one of the main factors affecting plant development and growth, although UV-B constitutes only a fraction of sunlight (Britt, 2002). Essential components such as DNA, proteins, and membranes within plants are vulnerable to the damaging effects of ultraviolet radiation (Jansen et al., 1998). A significant proportion of genes that are regulated by UV-B radiation are also subject to regulation by the circadian system (Feher et al., 2011; Takeuchi et al., 2014; Oztas et al., 2018).

In plants, the circadian clock regulates changes in gene expression mediated by UV-B (Feher et al., 2011; Takeuchi et al., 2014). In Arabidopsis, wild type plants are much more sensitive to UV-B radiation during the subjective night than during the subjective day (Takeuchi et al., 2014). When treated during the subjective night, plants exhibit sensitivity to UV-B in the absence of light, but not when exposed to light (Takeuchi et al., 2014). It suggests that the circadian clock confers UV-B resistance during the subjective day, while resistance during the subjective night requires the presence of light (Takeuchi et al., 2014).

The EC components function downstream of COP1, interacting with the UV-B photoreceptor UVR8 and regulating the circadian gating of the UV-B signaling pathway (Cloix et al., 2012). Additionally, EC directly binds to the promoter of the UV-B-induced genes *PRR9* and *ELIP1* (*EARLY LIGHT INDUCIBLE PROTEIN 1*), repressing their expression (Takeuchi et al., 2014). Moreover, mutations in the components of the EC lead to a constitutive response to UV-B irradiation (Takeuchi et al., 2014). The diel sensitivity difference in the *elf3-8* and *elf4-300* mutants disappears and is comparatively diminished in *lux-4* (Takeuchi et al., 2014), suggesting that the EC could be an important factor in gating the UV-B response (Takeuchi et al., 2014).

The precise timing and combinatorial accumulation of histone marks are important for both the circadian system (Hemmes et al., 2012; Malapeira et al., 2012; Song and Noh, 2012) and the DNA damage response (Waterworth et al., 2011). In Arabidopsis, in response to X-ray-induced DNA damage, there is an increase in the relative abundance of N-terminus H3 acetylation, and a global reduction in hyper-acetylated H4 levels (Drury et al., 2012). Mass spectrometric analysis of posttranslational modifications on histone proteins reveals that, following irradiation, UV-B-tolerant lines exhibit increased acetylation of UV-B-associated gene promoters and transcribed regions (Casati et al., 2008). Examination of *ATM* (ATAXIA-TELANGIECTASIA MUTATED) mutant plants revealed an elevation in histone acetylation following irradiation, thereby establishing a connection between the DNA damage response and alterations in histone modification in plants (Drury et al., 2012). Furthermore, studies revealed that the function of histone methyltransferase SET DOMAIN GROUP

2/ARABIDOPSIS TRITHORAX RELATED 3 (SDG2/ATXR3) is involved in both DNA repair and regulation of the circadian clock (Malapeira et al., 2012; Yao et al., 2013), establishing a molecular connection between these two pathways via chromatin remodeling.

3 Brief overview on transcription

Regulation of mRNA transcription is one of the key control points for proper responses to changing environments (Ohama et al., 2017; Kidokoro et al., 2022; Li et al., 2023). Nuclear-encoded genes undergo transcription by RNA polymerase II (RNA Pol II) activity (Hirose and Manley, 2000). This process necessitates the intricate interaction among numerous proteins essential for the successful assembly of the pre-initiation complex (PIC) at core promoter elements (CPEs) (Struhl, 1987; Roeder, 1991). Proteins responsible for modulating gene expression by specific binding to *cis*-acting elements within the promoter regions of target genes are referred to as transcription factors (TFs) (Hobert, 2004). General transcription factors (GTFs) from a group of transcription factors that bind to CPEs and play a crucial role in initiating basal transcription. GTFs are complex proteins with multiple subunits, that are essential for recognizing the core promoter, initiating the formation of the RNA Pol II transcriptional PIC, and initiating the transcription process. These GTFs are individually identified as TFIIA, TFIIB, TFIID, TFIIE, TFIIF, and TFIIH as well as some additional cofactors (Orphanides et al., 1996; Thomas and Chiang, 2006).

3.1 Transcription initiation and elongation

Although the establishment of a robust and stable PIC at gene promoters is

paramount for initiating transcription, its presence does not ensure transcriptional productivity. The largest subunit of RNA Pol II, known as Rpb1, contains a unique C-terminal domain (CTD) consisting of heptapeptide repeats of Tyr1-Ser2-Pro3-Thr4-Ser5-Pro6-Ser7 ($Y^1S^2P^3T^4S^5P^6S^7$) and plays a crucial role in the different stages of transcription (Allison et al., 1985; Corden et al., 1985; Egloff and Murphy, 2008). Indeed, the CTD serves as a platform for the coordination of various events during transcription, such as initiation, elongation, termination, and RNA processing (Hsin and Manley, 2012; Zhang et al., 2012). The unique structure of CTD allows it to undergo reversible phosphorylation at specific residues, contributing to the regulation of transcription (Hsin and Manley, 2012; Zhang et al., 2012; Heidemann et al., 2013).

Typically, the RNA Pol II C-terminal domain (CTD) undergoes phosphorylation predominantly at serine-5 (S5P) and serine-2 (S2P) residues (Chapman et al., 2007; Sogaard and Svejstrup, 2007). The S5P facilitates the release of RNA Pol II from the promoter elements (Sogaard and Svejstrup, 2007), favoring the initiation of transcription (Ohkuma and Roeder, 1994). The S2P plays a key role in orchestrating the sequential recruitment of factors involved in the elongation and termination phases of transcription (Komarnitsky et al., 2000; Mayer et al., 2012). Thus, following successful initiation, there is a gradual decrease in S5P along with a simultaneous increase in S2P within the CTD repeats. Once the transcription is finished, both RNA Pol II and the freshly synthesized RNA are released from the DNA template. This separation involves the targeted removal of phosphate groups from S2P and S5P in the CTD, a dephosphorylation process catalyzed by phosphatase enzymes.

3.2 Functional connection of chromatin structure and transcription

The dynamics of chromatin structure are tightly regulated through various mechanisms, including, among others, histone modification, incorporation of histone variants, and eviction of histones (Li et al., 2007a; Clapier and Cairns, 2009). A pivotal advancement in elucidating the impact of chromatin on gene regulation stems from the discovery that DNA methylation and post-translational modifications of histones induce the recruitment of protein complexes, which subsequently govern the transcription process (Berger, 2007). Based on the function of chromatin modifications that regulate transcription of the protein-encoding genome, these modifications have been broadly classified into two types: the ones involved in transcription activation and the ones connected with transcription repression (Lee et al., 2005; Berger, 2007).

DNA methylation and histone post-translational modifications of histones (histone PTMs) exhibit associations with either repressive or active transcriptional states. In general, DNA methylation occurs at cytosine residues, typically within CG dinucleotides or CNG trinucleotides, and acts as a transcriptional repressor (Bird, 2002). Multiple histone PTMs have been identified, which include acetylation, phosphorylation, methylation, ubiquitylation, and SUMOylation (Espinos et al., 1999; Shiio and Eisenman, 2003; Shilatifard, 2006). Lysine is a pivotal substrate in histone biochemistry due to its involvement in various exclusive modifications. Further, methylation can happen multiple times (mono-, di-, or trimethylation) on a single lysine side chain, and each degree of modification can result in distinct biological outcomes, some of which are well-established (Luo, 2018). For instance, histone acetylation has an overall activating effect on transcription (Struhl, 1998; Sterner and Berger, 2000; Stasevich et al.,

2014), while SUMOylation appears to be repressive (Shiio and Eisenman, 2003), with potential mutual interference between these two modifications (Wu and Chiang, 2009). In contrast, methylation and ubiquitylation exhibit variable effects on transcription, depending on the specific residues. For example, in general, the trimethylation of lysine 4 in histone H3 (H3K4me3) and H3K36me3 are considered to favor transcription (Xu et al., 2008; Zhang et al., 2009), while H3K27me3 and H4K20me3 are considered to repress transcription (Fuchs et al., 2006; Berger, 2007; Li et al., 2007a). Ubiquitylation in the C-termini of H2B is associated with transcriptional activation (Zhang, 2003; Xiao et al., 2005), while H2A ubiquitylation represses transcription (Berger, 2007; Higashi et al., 2010). Regarding histone phosphorylation, H3 phosphorylation (ph) has been extensively studied, with H3S10ph showing a correlation with both activated transcription and mitotic chromosome condensation (Zippo et al., 2009; Chen et al., 2017a). Initially, basic models proposed that specific molecular markers are responsible for determining whether chromatin is in an actively transcribing or inactive state. Nevertheless, an increasing number of findings indicate that the intricate functional epigenetic landscape is far more nuanced than previously envisioned.

3.3 General overview of the FACT (FAcilitates Chromatin Transcription) complex

FACT was originally identified in both mammalian and yeast cells (Brewster et al., 1998; Orphanides et al., 1998; Orphanides et al., 1999). The nomenclature of FACT is derived from its observed ability to enhance *in vitro* transcription from reconstituted chromatin templates (Orphanides et al., 1998; Orphanides et al., 1999; Belotserkovskaya et al., 2003). This enhancement occurs through the destabilization of nucleosomes, thereby promoting the passage of RNA Pol II

during the elongation phase (Orphanides et al., 1999; Belotserkovskaya et al., 2003). Through subsequent investigations, additional functions of FACT have been elucidated. In addition to its role in chromatin transcription, FACT has been found to participate in various chromatin-dependent processes, including recombination, DNA repair, and replication, among others (Formosa et al., 2001; Belotserkovskaya et al., 2004; Winkler et al., 2011; Gao et al., 2017; Obermeyer et al., 2023).

3.3.1 Basic features and functions of FACT

FACT complex functions as the most extensively studied histone chaperone, facilitating chromatin recovery during transcription (Hsieh et al., 2013). FACT consists of two subunits: the large subunit suppressor of Ty 16 (SPT16) and the small subunit structure-specific recognition protein 1 (SSRP1) in Arabidopsis. The SPT16 protein is evolutionarily conserved among eukaryotes, while SSRP1 contains an N-terminal domain responsible for dimerization with SPT16, a middle acidic domain, and a high-mobility group (HMG)-box domain facilitating interaction with DNA and nucleosomes in higher eukaryotes (Lichota and Grasser, 2001; Belotserkovskaya et al., 2003; Pfab et al., 2018b). In contrast, the SSRP1 homolog in yeast, POB3, lacks an HMG-box, and this specific function is fulfilled by the Nhp6 protein (Antosch et al., 2012; Formosa, 2012; Van Lijsebettens and Grasser, 2014). SSRP1 undergoes phosphorylation by protein kinase CK2, and the phosphorylation of the HMG-box domain regulates the structure-specific interaction with DNA (Krohn et al., 2003). In Arabidopsis cells, fluorescence recovery after photobleaching (FRAP) analysis revealed that both intact SSRP1 and SSRP1 without HMG-box domain (SSRP1ΔHMG) display the same mobility within nuclei (Pfab et al., 2018b). Furthermore, the expression of SSRP1ΔHMG

demonstrates nearly equivalent efficiency compared to that of full-length SSRP1 in promoting the normal development and growth of the otherwise nonviable *ssrp1-1* mutant (Pfab et al., 2018b). This suggests that the domain of HMG-box is not required under normal growth conditions in Arabidopsis. However, attaching a C-terminal HMG-box domain to Pob3 does not fully restore FACT activity (McCullough et al., 2018). Both human FACT and yeast FACT (incorporating the Pob3-HMG fusion) rely on Nhp6 for effective nucleosome reorganization (McCullough et al., 2018). This suggests that the SSRP1-SPT16 complex might require small HMGB proteins for assistance, similar to the collaboration between Nhp6 and Pob3 in yeast.

FACT is proposed to disassemble and assemble nucleosome structures during transcription (Belotserkovskaya et al., 2003). It plays a crucial role in overcoming and sustaining the barrier of nucleosomes linked to DNA-dependent activities in chromatin. FACT exhibits interactions with diverse nucleosomal components, such as DNA, H3-H4 tetramers, and H2A-H2B dimers (Jamai et al., 2009; Hondele et al., 2013; Kemble et al., 2015; Wang et al., 2018). The competitive interplay between FACT and DNA for histone binding emerges as a crucial factor in the reversible reorganization of nucleosomes and uncoiling of nucleosomal DNA from the histone core, typically resulting in enhanced DNA accessibility (Xin et al., 2009; Kemble et al., 2015; Valieva et al., 2016; Zhao et al., 2019).

Indeed, the FACT complex helps RNA polymerase to transcribe genes by temporarily disrupting nucleosomes ahead of the polymerase and then reassembling the nucleosomes behind it (Hsieh et al., 2013). This process allows efficient transcription and ensures that chromatin is properly reassembled after the transcription process. Nevertheless, the significant challenge lies in the proper

assembly of disassembled nucleosomes and the maintenance of histone PTMs during transcription. In this regard, the histone chaperone FACT plays a pivotal role recycling nucleosomes during transcription in yeast (Jeronimo et al., 2019). This function is reinforced by various RNA Pol II-associated elongation factors (Robert and Jeronimo, 2023). The localized recycling of modified histones by FACT during transcription is crucial for preserving the epigenetic landscape (Jeronimo et al., 2019). Mutations in FACT result in the redistribution of modified histones (Jeronimo et al., 2019).

PTMs may regulate the activity of the FACT complex. Mass spectrometry analysis reveals the identification of four acetylated lysine residues in the C-terminal region of SSRP1 and three phosphorylated serine/threonine residues in the C-terminal region of SPT16 (Michl-Holzinger et al., 2022). Examining the acetylation sites on SSRP1 through mutational analysis shows only mild phenotypic effects (Michl-Holzinger et al., 2022). However, the phosphorylation of SPT16, facilitated by protein kinase CK2, influences interactions with histones (Michl-Holzinger et al., 2022). A version of SPT16 that cannot undergo phosphorylation displays reduced binding to histones and is ineffective in complementing the growth and developmental phenotypes of *spt16* mutant plants (Michl-Holzinger et al., 2022). In plants expressing this non-phosphorylatable SPT16 version, there is an enrichment of histone H3 directly upstream of transcription start sites (TSSs) in a region that is usually nucleosome-depleted (Michl-Holzinger et al., 2022). This implies that for certain genes, the phosphorylation of the SPT16 acidic region is necessary to establish the proper nucleosome occupancy at the TSS of active genes.

Both SSRP1 and SPT16 are nuclear proteins with ubiquitous expression across most Arabidopsis tissues (Ikeda et al., 2011; Tripathi et al., 2015; Zhou et al., 2015b; Frost et al., 2018; Pfab et al., 2018a; Grasser, 2020). In indirect immunofluorescence microscopy, SSRP1 and SPT16 proteins are discernible within the euchromatic regions of interphase nuclei, but their presence isn't observed in the heterochromatic regions (Duroux et al., 2004). ChIP assays in Arabidopsis reveal the presence of SPT16 and SSRP1 along the regions transcribed by RNA Pol II (Duroux et al., 2004). However, this association is not observed in intergenic regions, or regions transcribed by RNA Pol I and III (Antosz et al., 2017). The interaction with active protein-coding gene chromatin occurs in a transcription-dependent manner (Perales and Mas, 2007; Lolas et al., 2010; Zhou et al., 2015b; Antosz et al., 2017). Furthermore, utilizing an affinity-purification method coupled with mass spectrometry demonstrates that FACT effectively co-purified with elongating RNA Pol II characterized by S2P and S5P (Antosz et al., 2017). This association is observed in Arabidopsis and concurrent interaction with recognized transcript elongation factors, such as transcript elongation factor IIS (TFIIs), SPT4/SPT5, and RNA polymerase-associated factor 1 complex (PAF1C) (Antosz et al., 2017; Obermeyer et al., 2023). The distribution pattern of SPT4/SPT5 along transcribed regions closely relates to that of RNA Pol II-S2P, whereas the presence of FACT and PAF1C is more closely associated with that of RNA Pol II-S5P (Obermeyer et al., 2023). Under transcriptionally challenging heat stress conditions, plants lacking the corresponding transcription elongation factors exhibit differential impairments in transcript synthesis (Obermeyer et al., 2023). FACT is especially crucial for promoting transcriptional upregulation and facilitating RNA Pol II transcription through +1 nucleosomes under stress conditions (Obermeyer et al., 2023).

Furthermore, *SSRP1* and *SPT16* are found to genetically interact with *TFIIs*, a gene encoding a modulator of RNA Pol II activity (Antosz et al., 2017), and with *HUB1/2*, genes responsible for catalyzing histone H2B mono-ubiquitination, a modification associated with elongation processes (Lolas et al., 2010). Above all, those findings suggest that FACT plays an important role in RNA Pol II transcriptional elongation in Arabidopsis (Van Lijsebettens and Grasser, 2014; Zhou et al., 2015b; Grasser and Grasser, 2018). This is consistent with the function of FACT regulating the synthesis of mRNA across various organisms (Reinberg and Sims, 2006; Gurova et al., 2018).

3.3.2 FACT regulates plants development and growth

In diverse organisms, including Arabidopsis, the viability of cells relies on the presence of FACT (Cao et al., 2003; Formosa, 2012; Frost et al., 2018; Goswami et al., 2022). In Arabidopsis, the homozygous transposon insertion in the first exon mutant *ssrp1-1* is lethal, while in the heterozygous state, it exhibits a wild-type phenotype (Lolas et al., 2010). While, the T-DNA insertion in the last exon results in reduced *SSRP1* expression (Lolas et al., 2010). T-DNA insertion mutants *spt16-1* and *spt16-2* in Arabidopsis show reduced expression levels of *SPT16* (Lolas et al., 2010). Both knockdown mutants of *ssrp1-1* and *spt16-1* or *spt16-2* exhibit diverse abnormalities in both vegetative and reproductive development (Zhou et al., 2015b; Pfab et al., 2018b). FACT plays a crucial role in two pivotal plant developmental transitions: the change from seed dormancy to germination and the transition from vegetative to reproductive growth. Freshly harvested seed germination assays demonstrated that the *ssrp1* seeds exhibit a decreased dormancy level (Michl-Holzinger et al., 2019). Consistent with this observation,

the seeds of *ssrp1* display reduced expression of the *DOG1*, a recognized locus influencing seed dormancy (Michl-Holzinger et al., 2019). The introduction of an additional copy of *DOG1* into *ssrp1* leads to elevated *DOG1* expression levels, resulting in enhanced seed dormancy levels (Michl-Holzinger et al., 2019). This finding suggests that SSRP1 is essential for seed dormancy by regulating the expression of *DOG1*. Mutations in *ssrp1* and *spt16* result in an increased number of leaves and inflorescences, early flowering, abnormal flowers and leaves, and adversely affect seed reproduction (Lolas et al., 2010). The early bolting phenotype in *ssrp1* and *spt16* plants is linked to a decrease in the expression of the floral repressor *FLC* compared to wild type (Lolas et al., 2010).

Transcript profiling of Arabidopsis *ssrp1* and *spt16* seedlings revealed that only a relatively small subset of genes exhibits differential expression in the mutants compared to the wild type (Pfab et al., 2018a). The transcript profiles of both mutants show strikingly similar changes, aligning with the established role of SSRP1 and SPT16 as a heterodimer (Pfab et al., 2018a). Among the downregulated genes, there is a notable overrepresentation of genes that encode enzymes involved in anthocyanin biosynthesis (Pfab et al., 2018a). In response to moderate high-light stress, the *ssrp1* and *spt16* plants exhibit reduced expression of anthocyanin biosynthetic genes compared to the wild type (Pfab et al., 2018a). Consequently, the FACT mutant plants exhibit reduced levels of anthocyanin pigments (Pfab et al., 2018a).

3.4 Connection between circadian clock and transcription

Circadian regulation of transcription is an important regulatory mechanism at the core of the circadian clock in nearly all organisms. Not only does precise

transcription of the components of the oscillator result in specific peak-phases during the day and night (Harmer and Kay, 2005) but also the coordinated circadian transcription plays a central role in the regulation of growth, physiology, and development (Covington et al., 2008; Thines and Harmon, 2011; Kinmonth-Schultz et al., 2013).

RVE8, an important regulator of the Arabidopsis circadian clock, contains a single-MYB domain and the so-called LHY/CCA1-LIKE (LCL) domain at the C terminal end (Farinas and Mas, 2011). The MYB domain of RVE8 is responsible for the binding to the promoter of *PRR5* and *TOC1*, while the interaction of RVE8 with LNKs is facilitated by the RVE8 LCL domain (Ma et al., 2018). ChIP-qPCR assays show that both RVE8 and LNK1 are highly enriched in the 5' region of *PRR5* and *TOC1* loci (Ma et al., 2018). LNK1 functions as a transcriptional coactivator by establishing direct interactions with RNA Pol II (Ma et al., 2018). The interaction with RNA Pol II isoforms, S5P and S2P, further implies that LNK1 may play a role in governing transcript initiation and elongation processes (Ma et al., 2018). RNA Pol II and CTD-phosphorylated isoforms S5P and S2P enrichment are reduced in the *lnk1lnk2* double mutant at the *TOC1* and *PRR5* loci (Ma et al., 2018). Furthermore, the FACT subunit, SSRP1, interacts with the LNK proteins (Ma et al., 2018). Thus, LNKs, RNA Pol II, and SSRP1 form a protein complex that rhythmically activates *PRR5* and *TOC1* expression (Ma et al., 2018). Mutation or inactivation of the protein complex components influences the nascent RNA expression of *TOC1* and *PRR5* (Ma et al., 2018).

4 General overview of R-loops

In addition to RNA, one of the by-products generated by transcription are the so-

called R-loops. R-loops are three-stranded nucleic acid structures composed of the DNA-RNA hybrid and the non-template single-stranded DNA (Wahba et al., 2016) (Figure 5). The first observation of R-loops was made in 1967 using X-ray diffraction (Milman et al., 1967). Subsequent studies demonstrated the presence of R-loops in nearly all organisms (Lima et al., 2016; Shafiq et al., 2017; Ariel et al., 2020). The structure of R-loops is considered to be relatively stable once they are formed, while the degradation of RNA in R-loops is thought to be necessary for their resolution (Hegazy et al., 2020). Over the past years, various techniques have been employed to detect R-loops and to investigate their biological function (Figure 5).

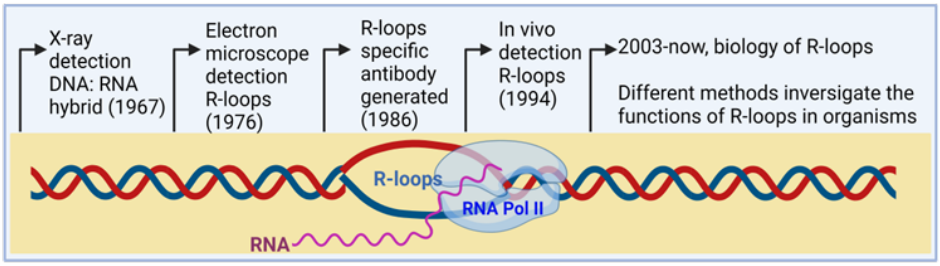


Figure 5. Research progress of R-loops. The diagram illustrates the key advancements or progress made in the understanding and studies of R-loops. Modified from Groh and Gromak 2014, and Gao et al. 2021. Created with Biorender.

The accumulation of R-loops can also compromise the integrity and stability of the genome (Sollier and Cimprich, 2015). When R-loops accumulate in an uncontrolled manner, they can lead to various diseases in humans (Groh and Gromak, 2014), including cancer, neurodegenerative disorders, and inflammatory conditions (Sollier and Cimprich, 2015). Generally, R-loops are present in approximately 5-10% of the genomic regions in mammals and also in plants (Sanz et al., 2016; Xu et al., 2017), suggesting that only a part of R-loops might be

"pathogenic" (Costantino and Koshland, 2015).

Over the years, R-loops have garnered significant attention due to studies showing an active function of R-loops rather than being mere transcriptional by-products as initially considered. R-loops are dynamic structures that play a crucial role in regulating diverse cellular processes in both plants and mammals (Figure 6). For instance, they participate in transcription termination, genome stability, and stress responses (Proudfoot, 2016; Hamperl et al., 2017; Belotserkovskii et al., 2018; Yang et al., 2019).

R-loops primarily undermine genome stability through DNA damage (Brambati et al., 2020), DNA recombination and rearrangement (Gan et al., 2011), as well as accumulation in front of the backtracked RNA Pol II (Zatreanu et al., 2019). Increased abundance of R-loops has been confirmed to impact transcription or replication in both plants and animals (Figure 6) (Yang et al., 2017; Belotserkovskii et al., 2018; Zatreanu et al., 2019). Interestingly, R-loops might also facilitate the DSB repair pathway (Yasuhara et al., 2018). Consistent with this, a decrease in R-loop levels leads to reduced efficiency in both NHEJ and HR (Lu et al., 2018). Thus, maintaining appropriate R-loop levels in the genome is important for organismal development and growth (Allison and Wang, 2019). As a result, organisms have developed intricate and precise mechanisms to balance R-loop formation and removal as described in the section below.

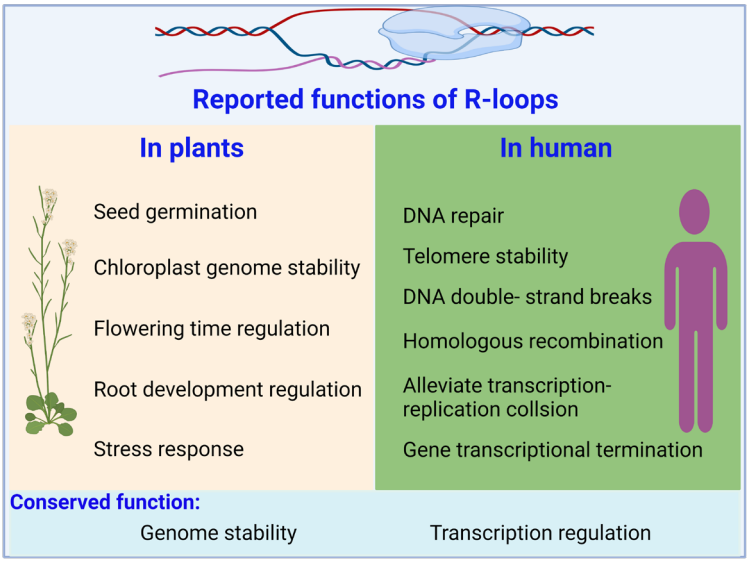


Figure 6. R-loop functions in plants (left) and in humans (right). The yellow panel represents the functions documented in plants, and the green panel represents the functions revealed in humans. The bottom panel shows the conserved functions shared by both plants and humans. This diagram is modified from Gao et al. (2021) and created using Biorender.

4.1 Formation and removal of R-loops

Studies in yeast and animals have shown that following the annealing of the nascent RNA with the complementary single-stranded DNA, the RNA-DNA hybrid is elongated and stabilized by a guanine-rich region (Zhang et al., 2014; Yadav et al., 2016; Allison and Wang, 2019). Other factors also contribute to R-loop formation. For instance, enhanced negative supercoiling downstream of the transcription bubble's trailing fork provides additional opportunities for interactions between the newly transcribed RNA and the template strand (Kuzminov, 2018). Additionally, non-template strand nicks can also contribute to the formation of R-loops between nascent RNA and the template strand *in vitro*

(Roy and Lieber, 2009).

Predictably, the formation of R-loops introduces structural lesions in the genome that can impact cellular processes (Allison and Wang, 2019). Organisms have developed multiple mechanisms to counteract R-loop formation and maintain transcriptional integrity, including nuclease and helicase activity, and resolution of topological stress. RNase H, an RNA-specific ribonuclease, plays a role in digesting hybridized RNA from R-loops (Zhao et al., 2018; Kucinski et al., 2020). Numerous studies have demonstrated that over-expression of RNase H1 can significantly reduce the accumulation of R-loops (Wahba et al., 2011; Yang et al., 2017). Senataxin (SETX) is a putative helicase in humans, which prevents R-loop accumulation by coordinating the activities of replication and transcription processes when replication forks come across the elongating RNA Pol II (Yüce and West, 2013; Hasanova et al., 2023). In yeast, the prototypical member of the PIF1 DNA helicases family, pif1p, exhibits a pronounced preference for unwinding R-loops compared to dsDNA (Boule and Zakian, 2007). Aquarius (AQR), as an RNA/DNA helicase, plays an essential role in regulating R-loop accumulation. Depleting AQR leads to an increase in the accumulation of R-loops and subsequent elevation in R-loop-dependent DNA damage levels in human cells (Sollier et al., 2014).

Topoisomerases, which are enzymes involved in controlling DNA topology, also play a role in the regulation of R-loop formation (Masse et al., 1997; El Hage et al., 2010; Manzo et al., 2018; Promonet et al., 2020) (Figure 7). These enzymes prevent the formation of R-loops by reducing negative supercoiling, which facilitates access to nascent mRNA on the template DNA (Allison and Wang, 2019). Consistently, studies in yeast have shown that the loss of the function of

Topoisomerase 1 (TOP1) blocks pre-rRNA synthesis and increases R-loop formation (El Hage et al., 2010). Moreover, the simultaneous occurrence of DNA replication and transcription can lead to significant genomic instability and increased accumulation of R-loops. To maintain the stability of the genome, organisms have evolved various mechanisms (García-Muse and Aguilera, 2016), which include factors that help or facilitate the progression of replication, as well as the transcription machinery itself (García-Muse and Aguilera, 2016). These factors function by removing RNA Pol II from chromatin to promote replication (Poli et al., 2016), and dephosphorylation or phosphorylation of the replication-related proteins (Canal et al., 2018).

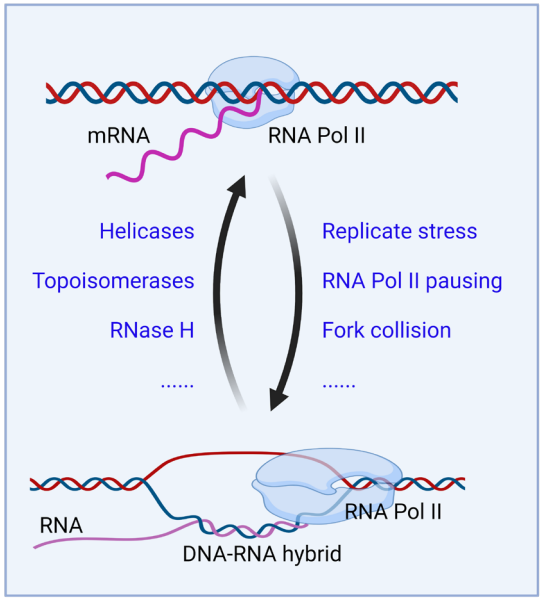


Figure 7. Scheme depicting several components involved in R-loop formation and removal. The factors involved in the removal of R-loops consist of multiple components, including topoisomerases, helicases, and RNase H, among others. During transcription, topoisomerases and helicases reduce the exposure time of single-stranded DNA, effectively preventing the formation of R-loops in the genome. RNase H contributes to the

reduction of R-loop accumulation by specifically digesting the RNA within R-loop structure. Factors that induce RNA Pol II pausing, backtracking, and arresting, such as replication stress and fork collision, are typically conducive to R-loop formation. Modified from Allison and Wang, 2019. Created with Biorender.

4.2 The relationship between R-loops and N^6-methyladenine modifications

In eukaryotic RNA, numerous modifications exist (Kadumuri and Janga, 2018). Among those modifications, N6 -methyladenosine (m^6A) is one of the most prevalent in eukaryotic mRNA, formed by the methylation of internal adenosine residues at the N6 position (Kierzek and Kierzek, 2003). M^6A nearly affects every aspect of mRNA metabolism, including pre-mRNA processing (Haussmann et al., 2016; Zhou et al., 2019), decay (Wang et al., 2014), and translation (Wang et al., 2015; Zhou et al., 2015a). Thereby, this modification plays a pivotal role in diverse fundamental biological processes in eukaryotes.

RNA m^6A modification is added by enzymes known as 'writers' such as methyltransferase-like 3 (METTL3) (Meyer and Jaffrey, 2017). This modification is subsequently identified by specific proteins referred to as 'readers', for example, YTH-domain family member 2 (YTHDF2) (Meyer and Jaffrey, 2017). The removal of m^6A is orchestrated by 'erasers' like fat mass and obesity-associated protein (FTO) (Jia et al., 2011; Meyer and Jaffrey, 2017).

Within mammalian cells, METTL3 initiates m^6A modification on newly synthesized transcripts in close proximity to the poly(A) site, enhancing the stability of R-loops to promote the regular termination of transcription (Yang et al., 2019). Moreover, METTL3 facilitates m^6A modifications on transient RNA:

DNA hybrids found at sites of DSBs. The m^{6}A reader YTHDC1 identifies and protects m^{6}A-modified RNAs, resulting in the accumulation of RNA: DNA hybrids at DSBs, thereby enhancing the efficiency of HR repair in human cells (Zhang et al., 2020). Knockout of YTHDF2 leads to increased R-loop levels, and the accumulation of γH2AX, a marker of DSB in mammalian cells (Abakir et al., 2020). The tonicity-responsive enhancer binding protein (TonEBP) recognizes R-loops and recruits METTL3 for m^{6}A RNA modification. Furthermore, TonEBP interaction with METTL3 and recruitment of RNase H1 promote R-loop resolution (Kang et al., 2021). Consistent with this, depletion of TonEBP or METTL3 in human cells increases the accumulation of R-loops and reduces survival when present UV light (Kang et al., 2021). Similarly, knockout of the writer *METTL 3* or the reader *YTHDC1* of m^{6}A in mouse cells not only increases chromatin accessibility but also activates transcription in an m^{6}A-dependent manner (Liu et al., 2020a). Consistently, two activation histone marks, H3K4me3 and H3K27ac, are elevated upon the depletion of *mettl3* and *ythdc1* (Liu et al., 2020a).

5. R-loops in plants

The fundamental biological function of R-loops in plants appears to be similar to that described in animals. R-loops in plants are connected with gene transcription through chromatin rearrangements and epigenetic modifications (Niehrs and Luke, 2020). They are also involved in maintaining plant genome stability (Yang et al., 2017; Yuan et al., 2019b; Yang et al., 2020) and regulating plant developmental transitions. In this section, the significance of plant R-loops is described.

5.1 Genomic distribution of R-loops

Genome-wide identification of R-loops in Arabidopsis revealed their enrichment in promoter and gene body regions, along with a high association with repetitive genomic regions and noncoding RNA (Xu et al., 2017). Furthermore, both Watson and Crick strand-specific R-loops are highly enriched in the DNA sequence motif GARGAAGx (R=G or A) (Xu et al., 2017), which is commonly found in Arabidopsis promoters (Hetzel et al., 2016). These findings are consistent with the preferential enrichment of R-loops in gene promoters. In Arabidopsis, R-loop formation is strongly associated with strand bias for GC skews near TTS (transcription termination site) and TSS regions (Xu et al., 2017). Similarly, a strong TA composition bias is also observed near TTS and TSS regions in the antisense direction (Xu et al., 2017). In rice, both sense or antisense (S/AS)-R-loops and antisense only (ASO)-R-loops exhibit peaks around transcription start sites (TSS), which are positively correlated with the transcription levels of overlapping genes (Fang et al., 2019).

5.2 The connection between R-loops and epigenetic modifications

The normal functioning of R-loops is closely connected to the epigenetic status at specific genomic regions in mammals and plants (Ginno et al., 2013; Xu et al., 2017). Genome-wide studies have demonstrated that the abundance of histone marks in Arabidopsis and rice are influenced by the type of R-loop or their genomic location (Xu et al., 2017; Fang et al., 2019). A study in rice reveals a positive correlation between R-loops and H3K9me2/3 levels (heterochromatin marks), and an inverse relationship between R-loops and histone acetylation (Fang et al., 2019). Certain RNA-DNA interactions originating from R-loops are strongly correlated with genomic regions displaying H3K4me3 enrichment in rice

(Xiao et al., 2022). In Arabidopsis, the majority of the peaks of R-loop are enriched in active histone marks, H3K9Ac, H3K36me3, H3K4me3, and H3K4me2 (Xu et al., 2017). Only a few R-loop peaks are found in regions with repressive/heterochromatic marks, such as H3K27me3, H3K27me1, and H3K9me2 (Xu et al., 2017). Compared to the gene body, R-loops exhibit a higher enrichment of those heterochromatic marks in the promoter, terminal, and intergenic regions (Xu et al., 2017).

R-loops exhibit a positive correlation with CHH (H=A, T, or C) methylation levels in the promoter regions of both non-TE (transposable element) and TE genes in rice (Fang et al., 2019). Although the analysis of DNA methylation in R-loop peaks reveals a weak correlation between DNA methylation (CG, CHG, and CHH) and R-loops in Arabidopsis (Xu et al., 2017), an anticorrelation between R-loops and CG methylation is observed near the TSS regions (Xu et al., 2017). Furthermore, CG methylation exhibited notable enrichment in both the upstream and downstream regions of R-loop peaks (Xu et al., 2017), suggesting a negative correlation between the regions of R-loop peaks and CG methylation.

5.3 Connection of R-loops with plant development and stress responses

R-loops are associated with various plant processes, such as flowering time, xylem formation, stress responses, and root development (Shafiq et al., 2017; Ariel et al., 2020; Xu et al., 2020b; Zhang et al., 2022). In this section, we will briefly describe the functions of R-loops in flowering time regulation, root development, stress response, and RNA processing.

5.3.1 Connection between R-loops and flowering time

Specifically, the function of R-loops in the regulation of flowering time by controlling the transcription of the *FLC* has been extensively investigated (Sun et al., 2013; Rosa et al., 2016; Xu et al., 2021; Zhang et al., 2022). The homeodomain protein NODULIN HOMEOBOX (AtNDX) regulates the expression of *COOLAIR*, the antisense transcripts from the 3' end *FLC*, by associating with the non-template single-stranded DNA from R-loops (Sun et al., 2013). AtNDX-associated R-loop negatively regulates the expression of *COOLAIR* (Sun et al., 2013). In comparison to the wild type, the mutation in *AtNDX* results in a delayed flowering time and an up-regulation of *FLC* expression (Sun et al., 2013). FLOWERING CONTROL LOCUS A (FCA) directly interacts with the canonical 3' end processing factor, FY/WDR33, to facilitate R-loop resolution over the *COOLAIR* proximal polyadenylation site (Xu et al., 2021). A recent study showed that hnRNP R-LIKE PROTEIN (HRLP) undergoes LLPS along with the splicing factor ARGININE/SERINE-RICH 45 (SR45) (Zhang et al., 2022). This process enhances R-loop formation close to the first intron of *FLC* by forming nuclear condensates, ultimately resulting in reduced recruitment of RNA Pol II levels and decreased *FLC* expression (Zhang et al., 2022) (Figure 8A).

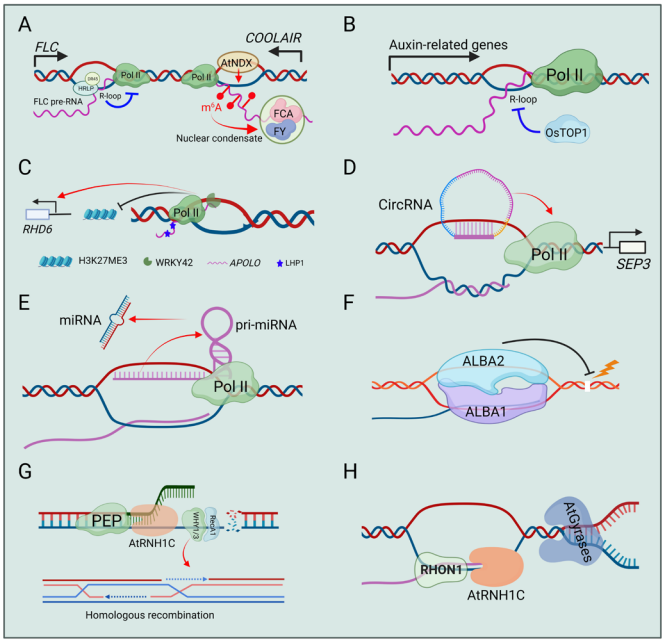


Figure 8. Several functions of R-loops have been observed in plant genomes. (A) AtNDX stabilizes *COOLAIR* R-loop to regulate *FLC* expression; HRLP and SR45 also regulate the *FLC* expression by promoting R-loop formation. (B) OsTOP1 regulates auxin-related gene expression by preventing the formation of R-loops. (C) *APOLO* and LHP1 have parallel functions in mediating R-loop formation, resulting in the alteration of chromatin conformation in Auxin-related genes. (D) The participation of R-loops in RNA processing, encompassing R-loops formed by circRNAs and their role in the exon-skipping process of *SEP3.3*, influences the regulation of Arabidopsis floral organ development. (E) R-loops initiated by pri-miRNAs and their involvement in miRNA processing within Arabidopsis. (F) Arabidopsis ALBA1/2 heterodimers function as readers of genic R-loops, serving to maintain genome stability. (G) PEP promotes R-loop formation at chloroplast DNA break sites, AtRNH1C removes R-loops and thus recruits WHY1/3 and RacA1 proteins for homologous recombination repair. (H) In Arabidopsis chloroplasts, AtRNH1C and RHON1 possess similar functions, working in parallel to remove R-loops. For further details please find them in the text. Created with Biorender.

5.3.2 Connection between R-loops and root development

DNA topology is a crucial factor regulating gene expression and development through R-loops. TOP1 exhibits a remarkable degree of conservation across diverse organisms, including yeast, plants, and animals (Shafiq et al., 2017). Miss-expression of OsTOP1 in rice alters the expression of the auxin transporter *OsABCB13/14* and signaling gene *OsARF19*, resulting in increased R-loop accumulation and morphological defects in rice roots (Figure 8B) (Shafiq et al., 2017). Other auxin-related factors are also connected with R-loops and Arabidopsis root development. For example, the long non-coding RNA auxin-regulated promoter loop (*APOLO*) plays a crucial role in facilitating trans-R-loop formation by recruiting a component of the plant polycomb repressive complex 1, namely, LIKE HETEROCHROMATIN PROTEIN 1 (LHP1) (Ariel et al., 2020). This recruitment significantly affects the expression of auxin-responsive genes that are involved in lateral root development (Figure 8C) (Ariel et al., 2020). Moreover, *APOLO* directly identifies numerous distinct loci within the Arabidopsis genome and influences their three-dimensional chromatin structure, thereby inducing changes in transcriptional activity (Moison et al., 2021). *APOLO* recognizes the master regulator of root hair, *ROOT HAIR DEFECTIVE 6* (*RHD6*), and forms R-loops through sequence complementarity (Moison et al., 2021). *APOLO* exerts control over the transcriptional activity of *RHD6* by recruitment of the WRKY42, leading to increased elongation of root hairs in cold conditions in Arabidopsis (Moison et al., 2021) (Figure 8C). This process occurs due to the activation of the transcription factor genes *RHD6-like 2* (*RSL2*) and *RSL4* (Moison et al., 2021).

5.3.3 R-loop response to stresses

R-loops also exhibit dynamic responses to various stress treatments, such as fluctuations in temperature (both low and high), exposure to ABA, salicylic acid (SA), and UV-C irradiation in Arabidopsis (Xu et al., 2020b). The antisense R-loops near TSS exhibit a minor increase after heat treatment (37°C for 30 hours) and decrease at 12 hours and 84 hours after treatment (Xu et al., 2020a). This suggests that R-loops are related to plant responses to changes in environmental temperature. *APOLO* also interacts with the methylcytosine-binding protein VARIANT IN METHYLATION 1 (VIM1) for plant thermo-morphogenic responses (Fonouni-Farde et al., 2022). The *APOLO*-VIM1-LHP1 complex plays an essential role in regulating the transcription of the auxin biosynthesis gene *YUCCA2* (Fonouni-Farde et al., 2022) (Figure 8C). Under normal conditions, *APOLO* recognizes the auxin-related gene *YUCCA2* gene through sequence complementarity, leading to the formation of R-loops (Fonouni-Farde et al., 2022). The *APOLO*-VIM1-LHP1 complex represses the expression of *YUCCA2* by inducing DNA methylation and H3K27me3, while, under high-temperature conditions, *APOLO* transcription is reduced, and the capacity of the *APOLO*-VIM1-LHP1 complex to bind to the *YUCCA2* promoter is decreased (Fonouni-Farde et al., 2022). Consequently, there is an elevation in the transcriptional activity of *YUCCA2*, thereby facilitating auxin-dependent hypocotyl elongation in response to heat.

Analyses of plants grown under different light conditions (red, blue, and far-red), the antisense R-loops remain unaffected, while the sense R-loops exhibit significant variations between white light and darkness (Xu et al., 2020a). Furthermore, the sense R-loops exhibit significant decreases in flowers,

germinating seedlings and dark conditions particularly in RNA Pol III-transcribed tRNA and small nucleolar RNA (snoRNA) loci, (Xu et al., 2020a). The Pol III-transcribed differential R-loop genes also show considerable overlaps among these three samples, suggesting that the conserved changes in R-loops might be governed by common regulatory factors (Xu et al., 2020a).

5.3.4 R-loop regulation of RNA processing

The R-loop formation by non-coding RNA molecules, such as microRNAs (miRNAs) and circular RNAs (circRNAs), play a vital role in RNA processing (Conn et al., 2017; Liu et al., 2021; Gonzalo et al., 2022). The novel class of non-coding RNA, circRNA, drives R-loop formation from the 6th exon of *SEPALLATA3* (*SEP3*) through strong binding to the cognate DNA locus (Conn et al., 2017). This further contributes to the increased splicing of *SEP3*, which regulates the floral homeotic phenotypes in Arabidopsis (Conn et al., 2017) (Figure 8D). Similarly, the studies demonstrated that several R-loop peaks overlap with the stem-differentiating xylem (SDX)-related circRNAs in *Populus Trichocarpa*, which modulate alternative splicing (AS) in SDX (Liu et al., 2021). Moreover, R-loops play a broader role in RNA processing, extending to the co-transcriptional processing of primary microRNAs (pri-miRNAs) in plants (Gonzalo et al., 2022). In Arabidopsis, this processing is facilitated by R-loops that are formed at particular genomic sites encoding miRNAs (Gonzalo et al., 2022) (Figure 8E).

5.4 R-loop connection with genome stability in plants

R-loops play a crucial role in the regulation of plant genome stability, and their proper management is essential for maintaining genomic integrity. Excessive

accumulation of R-loops is a potential threat to genome stability. The evolutionarily conserved proteins ALBA1 and ALBA2 function as R-loop readers and specifically bind *in vivo* and *in vitro* to DNA: RNA hybrid and single-stranded DNA, respectively (Yuan et al., 2019a) (Figure 8F). Miss-expression of ALBA1 and ALBA2 show increased sensitivity to DNA damage agents (Yuan et al., 2019a) suggesting that the ALBA1 and ALBA2 proteins complex act as essential R-loop readers, playing a crucial role in maintaining genome stability in Arabidopsis.

RNase H is highly conserved in both prokaryotes and eukaryotes (Yang et al., 2017; Allison and Wang, 2019). In Arabidopsis, three RNase H proteins have been identified: AtRNH1A (AT3G01410), AtRNH1B (AT5G51080), and AtRNH1C (AT1G24090), and they are predominantly expressed in the nucleus, mitochondria and chloroplasts, respectively (Yang et al., 2017). In the *atrnh1c* mutant, the integrity of chloroplast DNA is decreased, leading to an increased R-loop accumulation within the chloroplast (Yang et al., 2017). Removal of chloroplast-localized R-loops by RNase H1C and AtGyrases is critical for R-loop homeostasis and maintenance of genome stability in Arabidopsis (Yang et al., 2017). Furthermore, plastid-encoded RNA polymerase (PEP) promotes the formation of DNA: RNA hybrids at DNA break sites (Wang et al., 2021a). Subsequently, AtRNH1C recognizes R-loop structures and cooperates with the recombinase HOMOLOG OF BACTERIAL RECA (RECA1) and ssDNA binding proteins WHIRLY (WHY)1/3 for HR repair (Wang et al., 2021a) (Figure 8G). Normally, AtRNH1C is mainly expressed in the chloroplast, but it could be translocated to mitochondria to remove R-loops when the cell lacks AtRNH1B, thus maintaining the stability of the mitochondrial genome (Cheng et al., 2021). Removing R-loops on the intermediate-sized repeat of mitochondrial DNA by AtRNH1B is important

for repressing ectopic HR and maintaining the stability of mitochondrial DNA (mtDNA) (Cheng et al., 2021). Apart from this, the bacterial Rho-like DNA-RNA helicase, RHON1, acts independently or in coordination with RNase H1 to restrict R-loops and stabilize the genome in Arabidopsis chloroplasts (Yang et al., 2020) (Figure 8H).

OBJECTIVES

The primary objective of this Doctoral Thesis is to uncover the components and mechanisms involved in the temporal regulation of R-loop homeostasis in *Arabidopsis thaliana*. This general aim comprises the following specific goals:

1. Development of a reliable and reproducible method for detecting R-loops in *Arabidopsis thaliana* using dot-blot assays with the S9.6 antibody.

2. Decipher the dynamics of R-loop accumulation in *Arabidopsis thaliana* during the day and night.

3. Elucidate the influence of Arabidopsis photoreceptors and morning- and evening-expressed clock components on the dynamic accumulation of R-loops.

4. Uncover the relationship between R-loop accumulation and active transcription.

5. Identify the molecular components linking the diurnal accumulation of R-loops with transcription and chromatin remodeling.

RESULTS

The results of this Doctoral Thesis can be grouped into four main sections, each one comprising a number of related subsections. In the first section, we describe the development of the dot-blot assay to efficiently detect R-loops and used this method to examine their diurnal accumulation in *Arabidopsis thaliana*. In the second section, we used relevant mutants to verify the influence of photoreceptors and the circadian clock in the control of the diurnal abundance of R-loops. A third section focused on clarifying whether the diurnal accumulation of R-loops is directly connected with active transcription, and lastly, a fourth section focused on the identification of a molecular component directly linking transcription with R-loop abundance.

1. Diurnal accumulation of R-loops assayed by dot-blot analyses

1.1 Dot-blot analysis of R-loop accumulation in *Arabidopsis thaliana*

To obtain a global view of R-loop accumulation in *Arabidopsis thaliana*, we performed dot-blot assays using the S9.6 primary antibody, which specifically recognizes R-loops (Konig et al., 2017; Bou-Nader et al., 2022) (Figure 9). After processing the samples (see Materials and Methods section), serial dilutions of genomic DNA were loaded onto a positively charged polyvinylidene difluoride (PVDF) membrane. Following the incubation with the S9.6 primary and secondary antibody, the intensity of the signals was quantified in order to obtain quantitative values of R-loop enrichment (Figure 9).

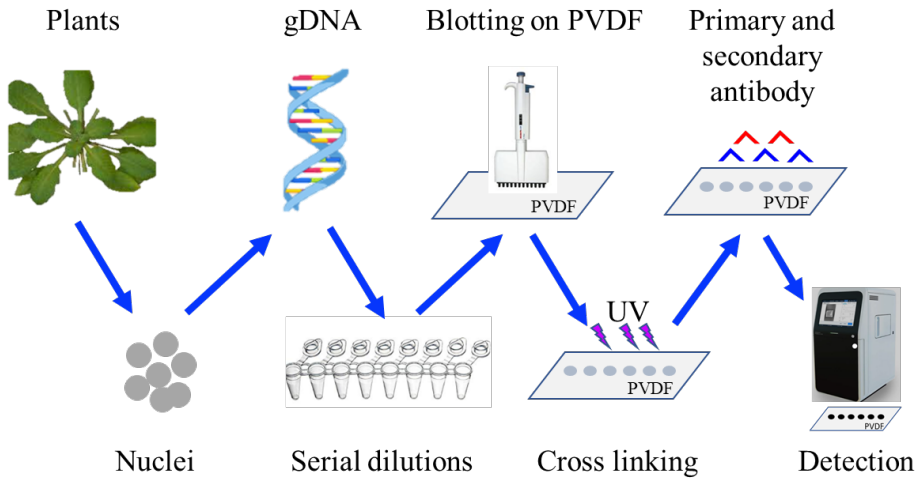


Figure 9. Schematic diagram depicting the dot-blot assay procedure to detect R-loops in *Arabidopsis thaliana*. Genomic DNA (gDNA) was isolated from plant nuclei and then subjected to serial dilutions. Subsequently, the diluted samples were directly applied onto the PVDF (polyvinylidene difluoride) membrane. Following UV light crosslinking, the membrane was incubated with the S9.6 primary and secondary antibodies. The signals were detected using the ImageQuant 800 imaging system.

Dot-blots were performed with 10-day-old seedlings grown under 12 hours of light and 12 hours of dark conditions (LD). Samples were collected during the day at Zeitgeber Time 7 (ZT7: 7 hours after lights-on). Quantification of the signals showed an effective detection fully consistent with the serially diluted samples (Figure 10A and B). Thus, the results suggest that the dot-blot technique with the S9.6 antibody can be used to specifically detect R-loop enrichment in Arabidopsis samples.

We also verified the reliability of the method by analyzing R-loop accumulation in samples treated with two commercial RNase H enzymes: RNase Ha (NEB) and RNase Hb (Thermo Fisher). RNase H selectively degrades the RNA strand in DNA:RNA hybrids, so that RNase H effectively eliminates R-loops from the genome (Amon and Koshland, 2016). Similar to the untreated control samples, serial dilutions of the RNase H-treated samples were prepared, and dot-blot assays were conducted. The quantification of the dot intensity following RNase H treatment revealed a much-reduced accumulation of R-loops compared to untreated samples (Figure 10A and B). As the signals for 200 ng appeared saturated, and the 25 ng signals were too weak, we used the concentrations of 100 ng and 50 ng for reliable quantification. Statistical analyses of the quantified signals (100 ng and 50 ng) revealed a significant decrease in R-loop enrichment for both RNase H-treated samples compared to untreated samples (Figure 10C). No significant differences were observed in comparisons between the two RNase H-treated samples (Figure 10C). We still observed residual signals remaining in the RNase H-treated samples, suggesting that the RNase H cannot effectively remove all the RNA from R-loops and/or that the S9.6 antibody might be detecting some minor unspecific signals.

To ensure that similar amounts of genomic DNA was loaded, the serially diluted samples were incubated with the double-stranded DNA (dsDNA) antibody. The dsDNA antibody effectively detected signals across the serially diluted samples (Figure 10D), revealing a clear correlation between the loaded concentration and the intensity of the dots (Figure 10D and E). Quantification of the relative intensity of samples with 100 ng and 50 ng demonstrated that RNase H-treated DNA loading amounts were similar to the untreated samples (Figure 10F).

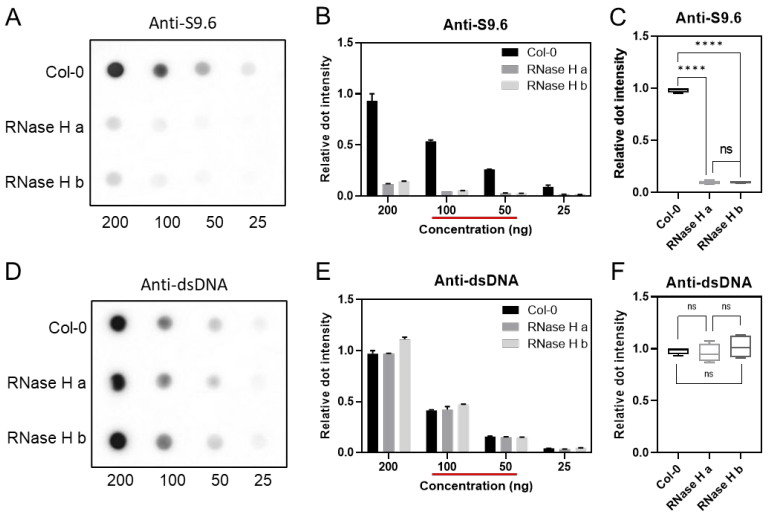


Figure 10. RNase H reduces R-loop accumulation in *Arabidopsis thaliana*. (A, D) Dot-blot analyses of R-loop accumulation in wild-type plants with or without RNase H treatment. Plants were grown under a 12-hour light and 12-hour dark cycle for 10 days, and samples were collected at ZT7. Detection was performed using S9.6 and dsDNA antibodies. (B, E) Quantification of signals detected by S9.6 and dsDNA antibodies. The values were normalized against the untreated samples. Data are shown as means + SEM. (C, F) Statistical analyses were conducted on the quantified signals from 100 ng and 50 ng, highlighted by the red line in panels B and E. Box plots show median and 25th and 75th percentiles with whiskers showing minimum and maximum values. Two biological replicates were performed, with plants grown independently, and with samples collected, processed, and analyzed at different times. Unpaired t-test was performed for the statistical analyses between RNase H-treated samples and untreated samples. **** p-value < 0.0001, ns: not significant.

We also analyzed R-loop accumulation using two S9.6 antibodies from different manufacturers: S9.6 I (Bio-Rad) and S9.6 II (Abcam). Our results showed that both antibodies successfully detected R-loop signals to a similar degree (Figure 11A, D). In line with our previous observations, the dilution factor and the dot intensity correlated well for both S9.6 antibodies (Figure 11A, B, D, and E). Signals were also significantly reduced in samples treated with RNase H (Figure

11C and F). No significant differences were observed in comparisons between the two RNase H-treated samples (Figure 11C and F). The consistency among the results obtained with the antibodies reinforces the reliability and reproducibility of the dot-blot technique, suggesting that it is a robust method for R-loop detection and quantification in *Arabidopsis thaliana*.

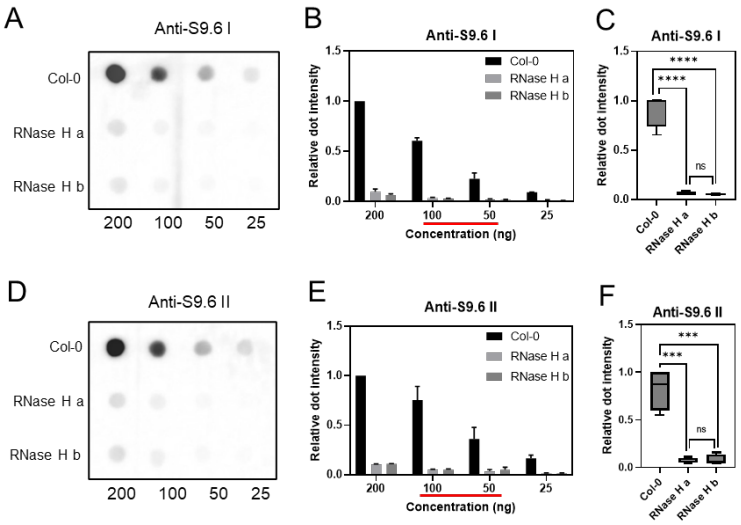


Figure 11. R-loop specific detection using two different commercially available S9.6 antibodies. (A, D) Dot-blot analyses of R-loop accumulation in wild-type plants with or without RNase H treatment. Plants were grown under a 12-hour light and 12-hour dark cycle for 10 days, and samples were collected at ZT7. Signals were detected with two different S9.6 antibodies from different suppliers. (B, E) Quantification of signals detected by S9.6 antibodies. The values were normalized against the untreated samples. Data are shown as means + SEM. (C, F) Statistical analyses on the quantified signals from 100 ng and 50 ng, highlighted by the red line in panels B and E. Box plots show median and 25th and 75th percentiles with whiskers showing minimum and maximum values. Two biological replicates were performed, with plants grown independently, and with samples collected, processed, and analyzed at different times. Unpaired t-test was performed for the statistical analyses between RNase H-treated samples and untreated samples. *** p-value < 0.001, **** p-value < 0.0001, ns: not significant.

1.2 Diurnal accumulation of R-loops in *Arabidopsis thaliana*

To investigate the possible diurnal changes in R-loop accumulation, seedlings grown under LD cycles were sampled at two time points: one during the day (ZT7) and another one during the night (ZT19: 7 hours after lights-off) (Figure 12A). Dot-blot assays using the S9.6 antibody showed a significantly increased signal at ZT19 compared to ZT7 (Figure 12B-D) while the genomic loading was similar for all samples, as assessed with the anti-dsDNA antibody (Figure 12E-G). The results suggest a diurnal accumulation of R-loops, with a significant enrichment during the night (ZT19) compared to the day (ZT7).

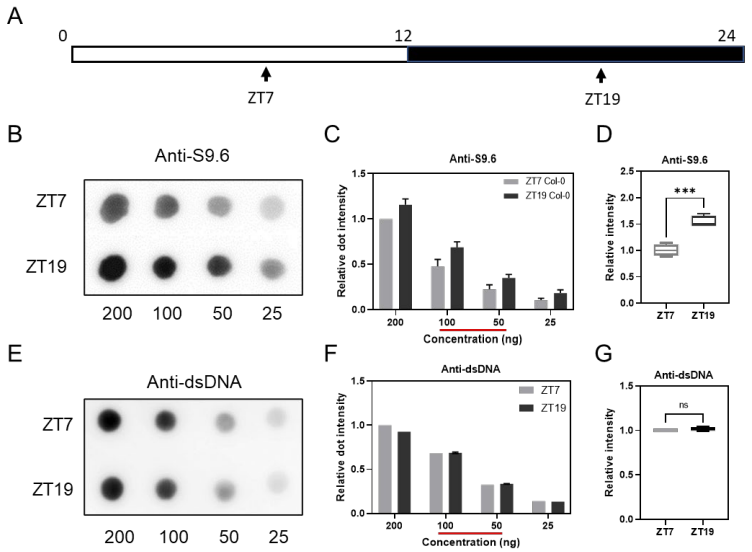


Figure 12. R-loop accumulation is higher during the night than during the day. (A) Schematic diagram illustrating the time points of sample collection during the day (ZT7) and night (ZT19) of plants grown under 12h light:12h dark cycle. The white bar represents the day, and the black bar indicates the night. (B, E) Dot-blot analyses of R-loop accumulation in samples collected at ZT7 and ZT19. Detection was performed using S9.6 and dsDNA antibodies, respectively. (C, F) Quantification of signals detected with the S9.6 and dsDNA antibodies. The values were normalized against the ZT7 samples. Data are shown as means + SEM. (D, G) Statistical analyses on the quantified signals from 100 ng and 50 ng, highlighted by the red line in panels C and F. Box plots

show median and 25th and 75th percentiles with whiskers showing minimum and maximum values. Two biological replicates were performed, with plants grown independently, and with samples collected, processed, and analyzed at different times. Unpaired t-test was performed for the statistical analyses between the day and night samples. *** p-value < 0.001, ns: not significant.

1.3 Generation of *RNase H1A* over-expressing plants

RNase H plays a crucial role resolving R-loops by cleaving the RNA strand within the RNA-DNA hybrid, leading to the removal of the RNA (Shen et al., 2017b). The Arabidopsis RNase H1 protein family is comprised of three members: RNase H1A, RNase H1B, and RNase H1C (Figure 13A). Similar to RNase H1 proteins in other organisms, the three RNase H1 proteins in Arabidopsis contain a DNA:RNA hybrid binding domain (HBD) and an RNase H1 activity domain (RNase H) (Figure 13B). This suggests a possible functional conservation of RNase H1 in Arabidopsis. Two of the RNases (RNase H1B and RNase H1C) were predicted to contain mitochondrial/chloroplast targeting signals (MTS/CTS) (Figure 13B). Prediction of protein localization showed that RNase H1A protein was likely a nuclear protein (Figure 13C) while RNase H1B likely localized in mitochondria (Figure 13D) and RNase H1C in chloroplasts (Figure 13E). Based on its predicted nuclear localization, we generated plants over-expressing the *RNase H1A* coding sequence (CDS) under the control of the cauliflower mosaic virus (CaMV) 35S promoter. Multiple independent homozygous lines of *RNase H1A*-ox lines with a single insertion were obtained. The lines exhibited varying degrees of over-expression as observed by reverse transcription polymerase chain reaction (RT-qPCR) analysis (Figure 13F).

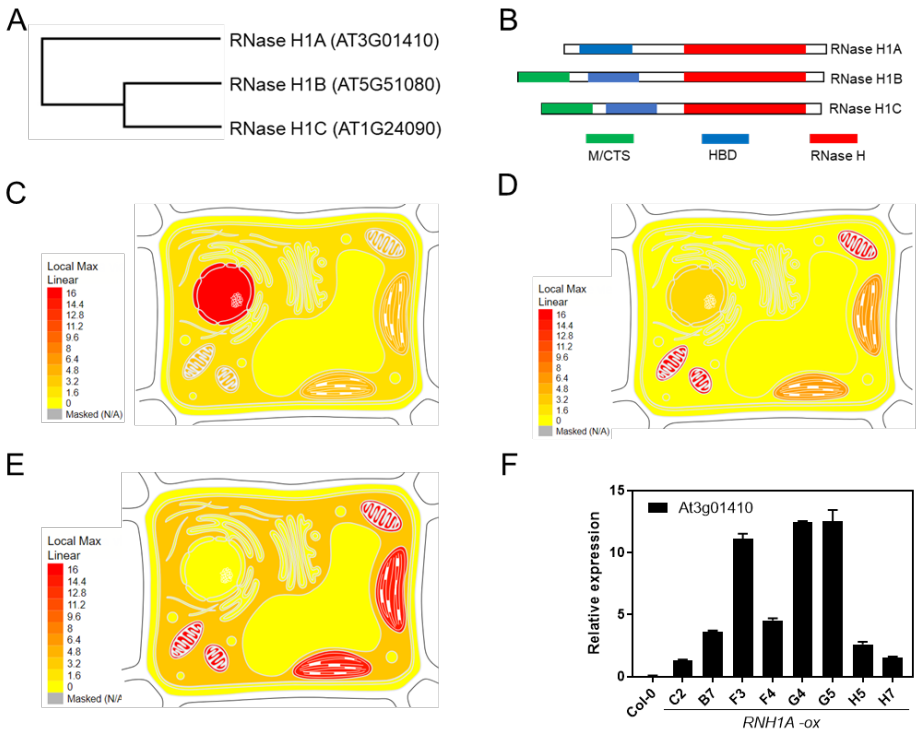


Figure 13. Analysis of RNase H1 proteins in Arabidopsis and generation of *RNase H1A* over-expressing lines. (A) Phylogenetic analysis of the Arabidopsis RNase H1 protein family. Protein sequences of three homologs were aligned using MUSCLE (multiple sequence comparison by logexpectation) (Edgar, 2004). (B) Schematic diagram of the RNase H1 proteins structure in Arabidopsis. Mitochondrion or chloroplast targeting sequences (M/CTS) are highlighted in green while the RNase H domains are highlighted in red, and the DNA:RNA hybrid binding domains (HBD) are highlighted in blue. (C-E) Subcellular localization prediction for RNase H1A, RNase H1B, and RNase H1C proteins. RPKM values from zero to local maximum across the cell (Hooper et al., 2017). Image obtained from the Cell eFP (bar.utoronto.ca/eplant) online tool (Waese et al., 2017). (F) RT-qPCR analysis of *RNase H1A* expression in wild-type (Col-0) and *RNase H1A -ox* lines. Plants were grown under a 12-hour light and 12-hour dark cycle for 10 days, and samples were collected at ZT7. Values were normalized to *IPP2* (*AT3G02780*, *ISOPENTENYL PYROPHOSPHATE: DIMETHYLALLYL PYROPHOSPHATE ISOMERASE 2*). Data are shown as means + SEM. Two biological replicates were performed, with plants grown independently, and with samples collected, processed, and analyzed at different times.

1.4 Over-expression of *RNase H1A* reduces R-loop accumulation in Arabidopsis

Two independent homozygous *RNase H1A-ox* lines, namely *RNase H1A-ox* B7 and *G4*, were selected based on their relatively low and high degree of over-expression compared to wild-type (Figure 13F). R-loop enrichment was examined at both day (ZT7) and night (ZT19). A significant reduction in R-loop accumulation was observed in the two *RNase H1A-ox* lines compared to wild-type at both time points (Figure 14A, C, and D). This effect appeared slightly more pronounced at ZT19 than at ZT7 (Figure 14D). However, no significant difference was observed between the two over-expression lines, despite the notable difference in *RNase H1A* over-expression (Figure 14D). Similar amounts of genomic DNA were loaded onto the membranes as shown by the dot-blot analyses using the anti-dsDNA antibody (Figure 14B, E, and F). Our results indicate that over-expression of the nuclear-localized RNase H1A reduces (albeit do not fully eliminate) the accumulation of R-loops in Arabidopsis.

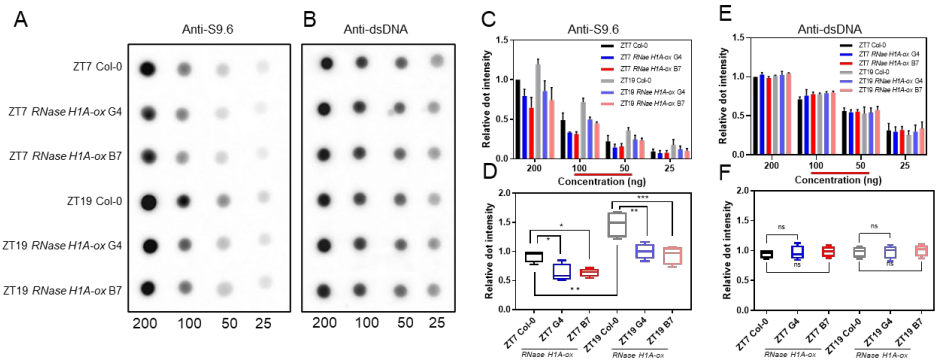


Figure 14. Reduced R-loop accumulation in *RNase H1A-ox* lines. (A, B) Dot-blot analyses of R-loop accumulation in wild-type and two independent *RNase H1A* over-expression lines (*RNase H1A-ox* B7 and *G4*). Plants were grown under a 12-hour light and 12-hour dark cycle for 10 days, and samples were collected at ZT7 and ZT19. (C, E) Quantification of signals detected by the S9.6

and dsDNA antibodies. The values were normalized against the ZT7 wild-type samples. Data are shown as means + SEM. (D, F) Statistical analyses on the quantified signals from 100 ng and 50 ng, highlighted by the red line in panels C and E. Box plots show median and 25th and 75th percentiles with whiskers showing minimum and maximum values. Two biological replicates were performed, with plants grown independently, and with samples collected, processed, and analyzed at different times. Unpaired t-test was performed for the statistical analyses between the *RNase H1A* over-expression lines and wild-type samples. * p-value <0.05, ** p-value<0.01, *** p-value<0.001 and ns: not significant.

2. Identification of the molecular components involved in the diurnal accumulation of R-loops

2.1 Phytochrome B and Cryptochrome 1 and 2 regulate the diurnal accumulation of R-loops

Based on the differential R-loop accumulation during the light and dark periods, we investigated whether the diurnal changes in R-loop accumulation required the photoreceptor function. We thus examined R-loop enrichment in the photoreceptor *cry2-1/hy4-B104* double mutant (*cry2cry1*) (Mockler et al., 1999) and in the photoreceptor *phyB* mutant (*phyB*). Our results showed that R-loop enrichment was significantly decreased in both *cry2cry1* and *phyB* mutants at both day and night (Figure 15A-C). R-loops accumulated similarly at both time points, suggesting that the photoreceptor mutants cannot distinguish the day and night. The decreased R-loop enrichment suggests that *PHYB* and *CRYs* are, directly or indirectly, activators of R-loop accumulation.

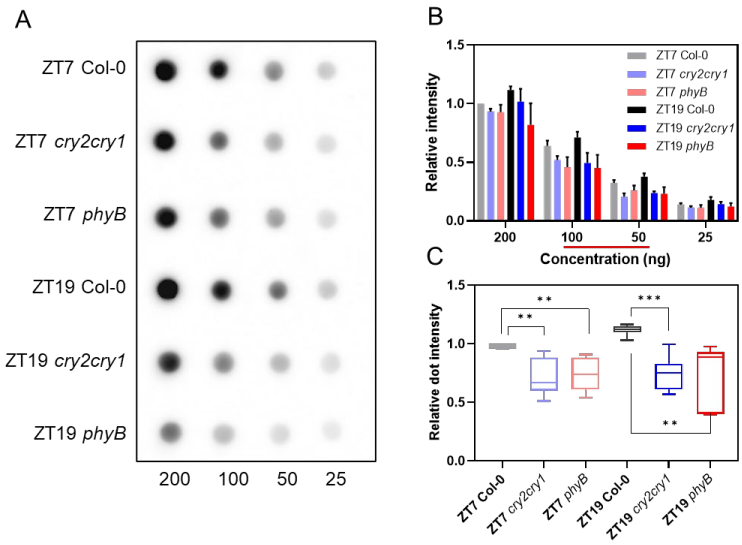


Figure 15. Reduced accumulation of R-loops in *cry2cry1* and *phyB* mutants under LD cycles. (A) Dot-blot analyses of R-loop accumulation in wild-type, *cry2cry1*, and *phyB* mutant plants grown under a 12-hour light and 12-hour dark cycle for 10 days. Samples were collected at ZT7 and ZT19 and signals were detected with the S9.6 antibody. (B) Quantification of signals detected by S9.6 antibody. The values were normalized against the ZT7 wild-type sample. Data are shown as means + SEM. (C) Statistical analyses were conducted on the quantified signals from 100 ng and 50 ng, highlighted by the red line in panel B. Box plots show median and 25th and 75th percentiles with whiskers showing minimum and maximum values. Two biological replicates were performed, with plants grown independently, and with samples collected, processed, and analyzed at different times. Unpaired t-test was performed for the statistical analyses between photoreceptor mutants and wild-type samples. ** p-value<0.01, *** p-value<0.001.

PHYB perceives red light while CRYs are involved in blue light perception (Chory, 1993; Briggs and Huala, 1999). Thus, we examined whether R-loop accumulation in photoreceptor mutant plants was also influenced by light quality. To that end, dot-blots were performed with plants synchronized under 12 hours of low blue light: 12 hours dark (BL/D) or 12 hours red light: 12 hours dark (RL/D) conditions. Our results showed that under BL/D conditions, the diurnal

accumulation of R-loops was sustained in wild-type plants, while R-loop accumulation was significantly decreased in *cry2-1* and *cry2cry1* double mutants during the day (Figure 16A-C). Similarly, the accumulation of R-loops was reduced in *phyB* mutant during the day under RL/D conditions (Figure 17A-C). The reduced accumulation of R-loops was not so evident during the night for both cryptochrome mutant and *phyB* mutant under BL or RL, respectively (Figure 16 and 17). Overall, the results indicate that PHYB and CRYs are important for maintaining the accumulation of R-loops under specific light qualities particularly during the day.

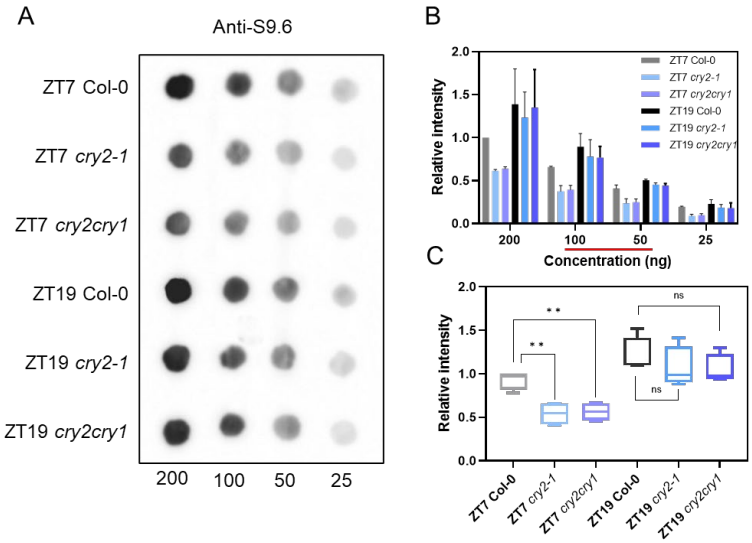


Figure 16. Reduced accumulation of R-loops in *cry2-1* and *cry2cry1* double mutants during the day under blue light/dark conditions. (A) Dot-blot analyses of R-loop accumulation in wild-type, *cry2-1*, and *cry2cry1* mutant seedlings. Plants were grown under a 12-hour low blue light (5 μmol/m^2/s) and 12-hour dark cycle for 10 days, and samples were collected at ZT7 and ZT19. (B) Quantification of signals detected by the S9.6 antibody. The values were normalized against the ZT7 wild-type sample. Data are shown as means + SEM. (C) Statistical analyses were conducted on the quantified results from 100 ng and 50 ng, highlighted by the red line in panel B. Box plots show median and 25th and 75th percentiles with whiskers showing minimum and maximum values. Two biological replicates were performed, with plants grown independently, and with samples collected,

processed, and analyzed at different times. Unpaired t-test was performed for the statistical analyses between cryptochrome mutants and wild-type samples. ** p-value<0.01, and ns: not significant.

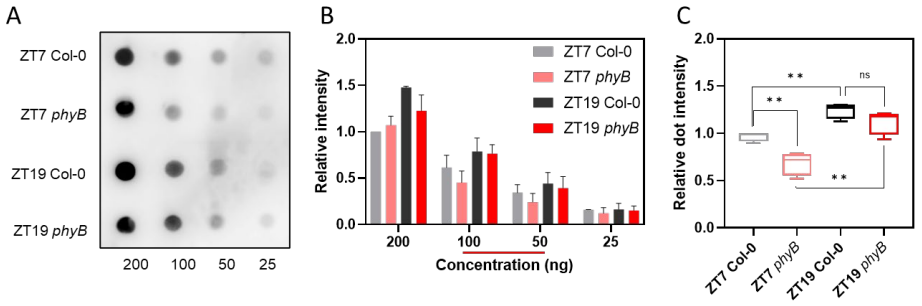


Figure 17. R-loop accumulation is reduced in *phyB* mutants during the day under red light/dark conditions. (A) Dot-blot analyses of R-loop accumulation in wild-type and *phyB* mutant seedlings. Plants were grown under a 12-hour red light (100 µmol/m^2/s) and 12 hours dark cycle for 10 days, and samples were collected at ZT7 and ZT19. (B) Quantification of signals detected by the S9.6 antibody. The values were normalized against the ZT7 wild-type sample. Data are shown as means + SEM. (C) Statistical analyses were conducted on the quantified signals from 100 ng and 50 ng, highlighted by the red line in panel B. Box plots show median and 25th and 75th percentiles with whiskers showing minimum and maximum values. Two biological replicates were performed, with plants grown independently, and with samples collected, processed, and analyzed at different times. Unpaired t-test was performed for the statistical analyses between *phyB* mutant and wild-type samples. ** p-value<0.01, and ns: not significant.

2.2 CCA1 represses R-loop accumulation during the day

To examine whether the diurnal accumulation of R-loops is controlled by the circadian clock, we performed dot-blot assays with plants miss-expressing the morning-expressed clock component CCA1. Our studies showed that compared to the wild-type, R-loop enrichment was significantly increased in the *cca1/lhy* double mutant and significantly decreased in *CCA1-ox* plants, particularly during the day (Figure 18A-C). The changes were much reduced and non-significant during the night (Figure 18C), which is consistent with the morning specific

function of CCA1. The results thus suggest that CCA1 represses R-loop formation mostly during the day.

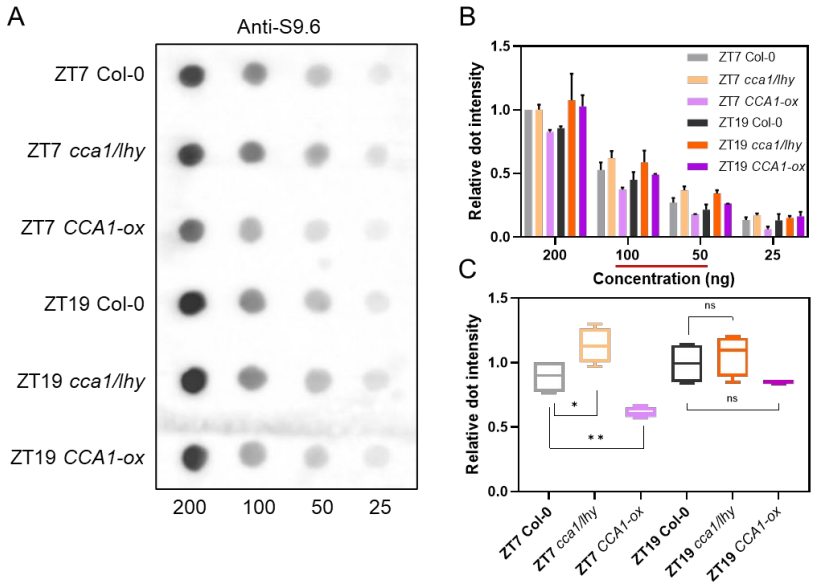


Figure 18. CCA1 represses R-loop accumulation during the day. (A) Dot-blot analyses of R-loop accumulation in wild-type, *CCA1-ox*, and *cca1/lhy* double mutant seedlings. Plants were grown under a 12-hour light and 12-hour dark cycle for 10 days, and samples were collected at ZT7 and ZT19. (B) Quantification of signals detected by the S9.6 antibody. The values were normalized against the ZT7 wild-type sample. Data are shown as means + SEM. (C) Statistical analyses were conducted on the quantified signals from 100 ng and 50 ng, highlighted by the red line in panel B. Box plots show median and 25th and 75th percentiles with whiskers showing minimum and maximum values. Two biological replicates were performed, with plants grown independently, and with samples collected, processed, and analyzed at different times. Unpaired t-test was performed for the statistical analyses between each sample. ** p-value<0.01, * p-value<0.05, and ns: not significant.

2.3 PRRs are required for R-loop accumulation during the day

To determine if other clock components are also important for the diurnal regulation of R-loops, we examined R-loop enrichment in mutant plants of the

members of the PRR (PSEUDO-RESPONSE REGULATOR) protein family, *prr9-10 prr7-11 prr5-11* triple mutant (*prr579*) (Nakamichi et al., 2005). The results showed that contrary to the increased R-loop accumulation in *cca1/lhy* double mutant plants, R-loop enrichment was significantly decreased in the *prr579* mutant during the day but not during the night (Figure 19A-C). The results are consistent with the PRR function during the day and suggest that while CCA1 represses R-loop accumulation, the morning-expressed PRRs positively contribute to R-loop accumulation.

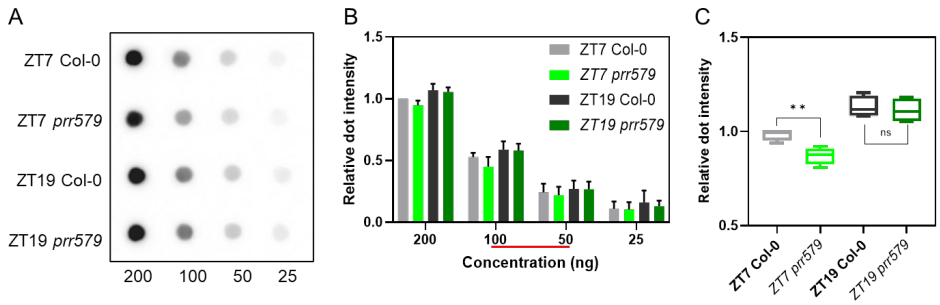


Figure 19. Reduced R-loop accumulation in the *prr579* triple mutant during the day. (A) Dot-blot analyses of R-loop accumulation in wild-type and *prr579* triple mutant seedlings. Plants were grown under a 12-hour light and 12-hour dark cycle for 10 days, and samples were collected at ZT7 and ZT19. (B) Quantification of signals detected by the S9.6 antibody. The values were normalized against the ZT7 wild-type sample. Data are shown as means + SEM. (C) Statistical analyses were conducted on the quantified signals from 100 ng and 50 ng, highlighted by the red line in panel B. Box plots show median and 25th and 75th percentiles with whiskers showing minimum and maximum values. Two biological replicates were performed, with plants grown independently, and with samples collected, processed, and analyzed at different times. Unpaired t-test was performed for the statistical analyses between the *prr579* triple mutant and wild-type samples. ** p-value<0.01, and ns: not significant.

2.4 ELF3 represses R-loop accumulation at both day and night

We next investigated whether clock components acting during the night also affected R-loop accumulation. Thus, we performed dot-blot assays using plants

miss-expressing the evening-expressed clock component ELF3. The results showed decreased R-loop accumulation in *ELF3-ox* (Herrero et al., 2012) at both day and night (Figure 20A-C). The *elf3-2* mutant (Hicks et al., 2001) exhibited a slightly increased R-loop accumulation although the statistical analysis revealed no significant differences compared to the wild-type (Figure 20A-C). The results suggest that evening-expressed clock components such as ELF3 also contribute to proper diurnal accumulation of R-loops.

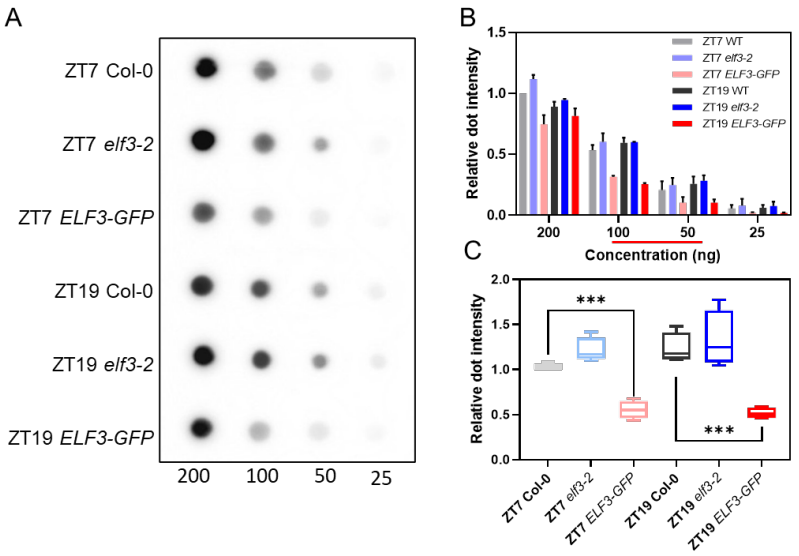


Figure 20. Reduced R-loop accumulation in *ELF3-GFP* compared to wild-type. (A) Dot-blot analyses of R-loop accumulation in wild-type, *ELF3-GFP*, and *elf3-2* mutant seedlings. Plants were grown under a 12-hour light and 12-hour dark cycle for 10 days, and samples were collected at ZT7 and ZT19. (B) Quantification of signals detected by the S9.6 antibody. The values were normalized against the ZT7 wild-type sample. Data are shown as means + SEM. (C) Statistical analyses were conducted on the quantified signals from 100 ng and 50 ng, highlighted by the red line in panel B. Box plots show median and 25th and 75th percentiles with whiskers showing minimum and maximum values. Two biological replicates were performed, with plants grown independently, and with samples collected, processed, and analyzed at different times. Unpaired t-test was performed for the statistical analyses between each sample. *** p-value<0.001.

3. Connection of transcription and R-loop accumulation

3.1 Mutation of LNKs reduces R-loop accumulation in Arabidopsis

LNKs are clock-related proteins that are important for the rhythmic recruitment of the RNA Pol II to clock loci, facilitating the rhythmic transcription (Ma et al., 2018). To investigate the connection between transcription and the formation of R-loops, we performed dot-blot assays using *lnk1lnk2* double mutant plants (Rugnone et al., 2013). Our results showed that compared to wild-type plants, R-loop abundance was significantly decreased in the *lnk1lnk2* double mutant at both day and night (Figure 21A-C). The reduction was more pronounced during the night than during the day such that the diurnal regulation of R-loops in wild-type was lost in *lnk1lnk2* double mutant plants (Figure 21C). These results suggest that LNKs positively regulate R-loop accumulation and are required for the proper diurnal accumulation of R-loops.

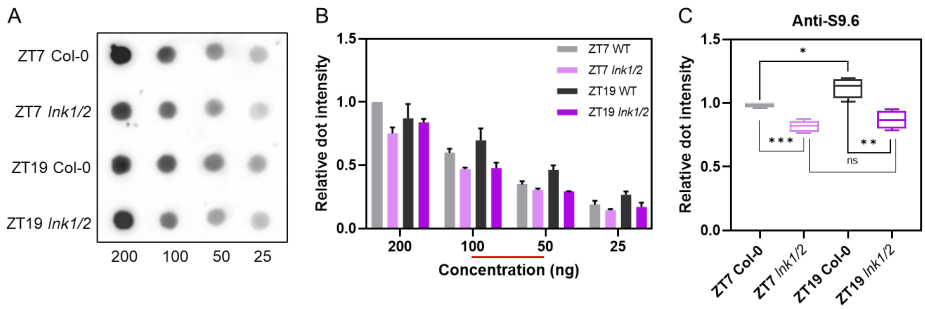


Figure 21. Reduced R-loop accumulation in *lnk1lnk2* double mutant compared to wild-type. (A) Dot-blot analyses of R-loop accumulation in wild-type and *lnk1lnk2* double mutant seedlings. Plants were grown under a 12-hour light and 12-hour dark cycle for 10 days, and samples were collected at ZT7 and ZT19. (B) Quantification of signals detected by S9.6 antibody. The values were normalized against the ZT7 wild-type sample. Data are shown as means + SEM. (C) Statistical analyses on the quantified signals from 100 ng and 50 ng, highlighted by the red line in panel B. Box plots show median and 25th and 75th percentiles with whiskers showing minimum and maximum

values. Two biological replicates were performed, with plants grown independently, and with samples collected, processed, and analyzed at different times. Unpaired t-test was performed for the statistical analyses between *lnk1lnk2* double mutant and wild-type samples. * p-value <0.05, ** p-value<0.01, *** p-value<0.001, and ns: not significant.

3.2 Decreased accumulation of RNA Pol II at genomic loci correlates with reduced R-loop abundance

To further examine the connection of transcription with R-loop accumulation, we used flavopiridol (FLAP), an inhibitor of transcription (Ding et al., 2011). Chromatin immunoprecipitation followed by qPCR (ChIP-qPCR) allowed us to examine the enrichment of RNA Pol II S5P in untreated (Mock) and FLAP-treated wild-type plants. We randomly selected genes accumulating R-loops using datasets from previous publications (Xu et al., 2017) and from ssDRIP-seq analyses (single-strand DNA ligation-based library preparation from DNA:RNA hybrid immunoprecipitation, followed by sequencing) performed in the Mas Lab. Our results showed that RNA Pol II S5P enrichment was significantly decreased in FLAP-treated samples compared to the untreated samples while no significant differences were observed when the transcriptionally inactive retrotransposon TA3 was examined (Figure 22A). These results confirmed that FLAP treatment effectively reduced RNA Pol II S5P abundance at expressed genes.

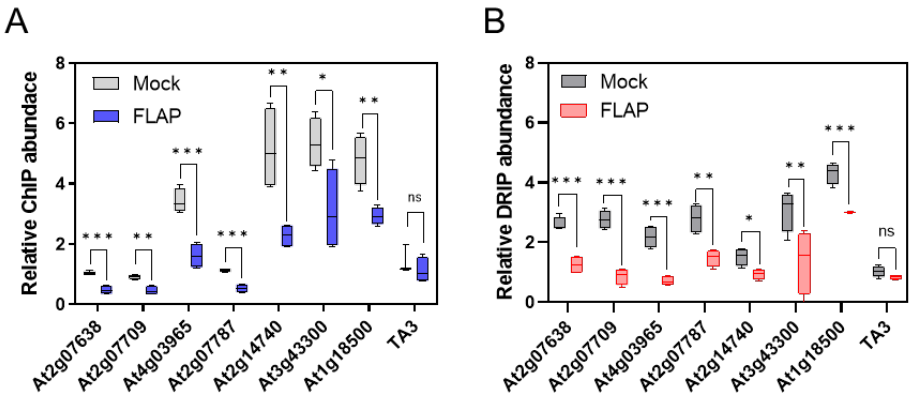


Figure 22. Flavopiridol (FLAP) treatment reduces the abundance of RNA Pol II S5P and R-loop accumulation in wild-type. (A) RNA Pol II S5P enrichment at selected genes by chromatin immunoprecipitation followed by qPCR (ChIP-qPCR) in untreated and FLAP-treated wild-type plants. (B) DNA-RNA immunoprecipitation followed by qPCR (DRIP-qPCR) analyses R-loop enrichment in both untreated and FLAP-treated wild-type plants. Plants were grown under a 12-hour light and 12-hour dark cycle for 10 days, and samples were collected at ZT7. TA3 was used as the negative control. Enrichment was calculated relative to the input values. Box plots show median and 25th and 75th percentiles with whiskers showing the minimum and maximum values. Two biological replicates were performed, with plants grown independently, and with samples collected, processed, and analyzed at different times. Unpaired t-test was performed for the statistical analyses between untreated samples and FLAP-treated wild-type samples. * P-value < 0.05, ** P-value < 0.01, *** P-value < 0.001, and ns: not significant.

We next performed DRIP-qPCR analyses of R-loop accumulation in untreated (mock) and FLAP-treated samples using the randomly selected genes analyzed in Figure 22A. R-loop enrichment was significantly reduced in FLAP-treated samples compared to the mock while no significant differences were observed when the transcriptionally inactive retrotransposon TA3 was examined (Figure 22B). Furthermore, correlation analyses (Figure 23) also showed a positive correlation between RNA Pol II abundance and the accumulation of R-loops in

Arabidopsis.

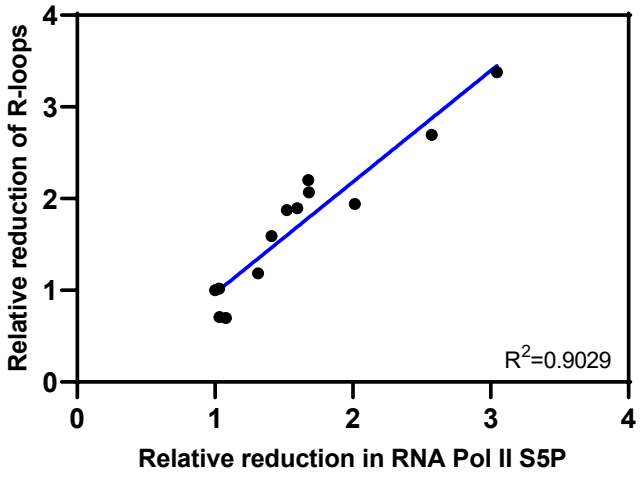


Figure 23. Correlation analyses of RNA Pol II S5P abundance and R-loop accumulation at randomly selected genes. Correlation analysis and linear regression line fitting comparing changes in R-loop accumulation and RNA Pol II S5P abundance after FLAP treatment. R^2=0.9029.

3.3 The diurnal changes in R-loop levels correlate with the accumulation of RNA Pol II-CTD S2P and S5P

To further examine the correlation between RNA Pol II abundance and R-loop accumulation, we performed Western-blots assays to analyze RNA Pol II S5P and S2P accumulation during the day and night. The results showed that the overall global accumulation of both RNA Pol II S5P and S2P increased during the night compared to the day (Figure 24A-C). The results are consistent with the FLAP treatment experiments and indicate that transcriptional activity might be higher during the night than during the day. The higher transcriptional activity might correlate with the increased R-loop accumulation at night.

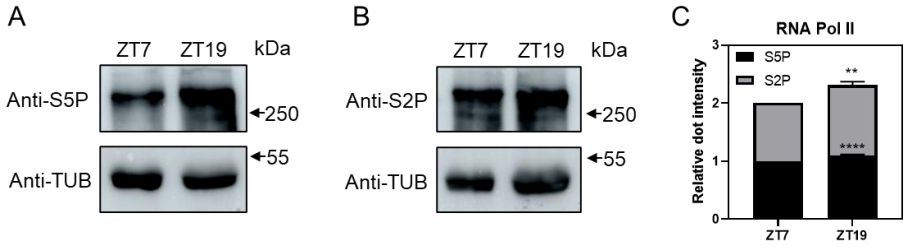


Figure 24. Increased global accumulation of RNA Pol II S2P and S5P at night. (A, B) RNA Pol II S5P and S2P accumulation at ZT7 and ZT19 was assayed by western-blot analyses with plants grown under a 12-hour light and 12-hour dark cycle for 10 days. Detection was performed using the anti-S5P, anti-S2P, and anti-Tubulin antibodies. (C) Quantification of signals detected by anti-S5P, anti-S2P, and anti-Tubulin antibodies. The values were quantified relative to the ZT7 value for each blot after normalization to the tubulin. Data are represented as the mean + SEM. Two biological replicates were performed, with plants grown independently, and with samples collected, processed, and analyzed at different times. Unpaired t-test was performed for the statistical analyses between day and night samples. **** P-value < 0.0001, ** P-value < 0.01.

3.4 Diurnal changes in chromatin compaction

Euchromatin is overall associated with transcriptionally active genome, while heterochromatic domains are usually transcriptionally repressed (Sun and Elgin, 1999; Donze and Kamakaka, 2002). Based on our results on the diurnal regulation of R-loops and its connection with transcription, we examined changes in chromocenters, typically characterized by highly compacted chromatin containing repetitive sequences and concentrated heterochromatin, which are typically transcriptionally inactive. To that end, the number of chromocenters was counted in cotyledon cells of 10-day-old wild-type seedlings grown under LD conditions. Staining with 4′,6-diamidino-2-phenylindole (DAPI) showed that the heterochromatic foci or chromocenters significantly decreased during the night compared to the day (Figure 25A-C). The results suggest that the

euchromatic/heterochromatin ratio might be diurnally regulated, with decreased heterochromatin at night. The reduced heterochromatic domains at night coincide with the increased RNA Pol II and R-loop accumulation also at night.

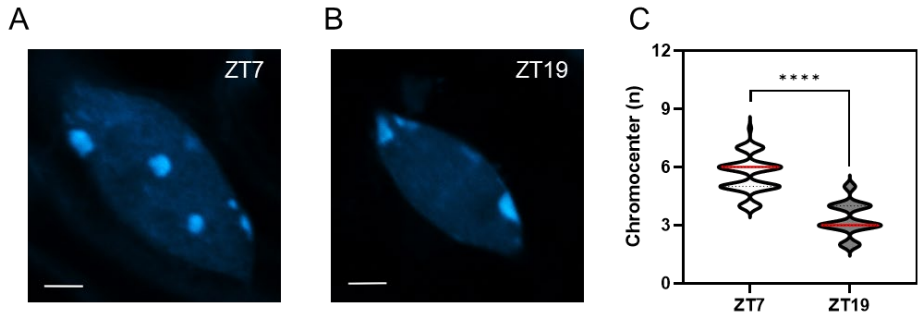


Figure 25. The number of chromocenters is reduced at night in wild-type cotyledon cells. (A, B) Representative images of DAPI-stained cotyledon nuclei in wild-type samples (Scale bar, 2 μm). Plants were grown under a 12-hour light and 12-hour dark cycle for 10 days, and samples were collected at ZT7 and ZT19. (C) The violin graph represented the number of chromocenters per nucleus in DAPI-stained wild-type cotyledons. Two biological replicates were performed, with plants grown independently, and with samples collected, processed, and analyzed at different times. The black dotted lines indicate the interquartile range and medians are shown as red horizontal line. Unpaired t-test was performed for the statistical analyses between the day and night samples. **** P-value < 0.0001, with a sample size n > 50.

3.5 Mutation of the transcription elongation factor *TFIIs* increases R-loop accumulation

We next focused on the identification of molecular components that connect transcription and R-loop abundance. Mutation of the transcription elongation factor *TFIIs* in human cells induces increased RNA Pol II pausing, and/or backtracking, which correlates with increased R-loop accumulation (Zatreanu et al., 2019). TFIIS is highly conserved, and the expression of the *TFIIS* mutant variant (*TFIIsmut*) efficiently inhibits the RNA cleavage activity of RNA Pol II,

resulting in transcriptional arrest (Antosz et al., 2020). To identify whether *TFIIs* could regulate R-loop accumulation in Arabidopsis, we analyzed R-loop enrichment in wild-type and *tfiis* mutant (SALK_056755) plants. The results showed that compared to the wild-type, the *tfiis* mutant exhibited significantly increased R-loop accumulation at both day and night (Figure 26A-C). However, R-loop accumulation was still diurnally regulated in *tfiis* mutant plants, with an increased accumulation at night, suggesting that TFIIs reduces R-loop accumulation at both day and night but it does not have a prevalent function specifically controlling R-loop diurnal abundance.

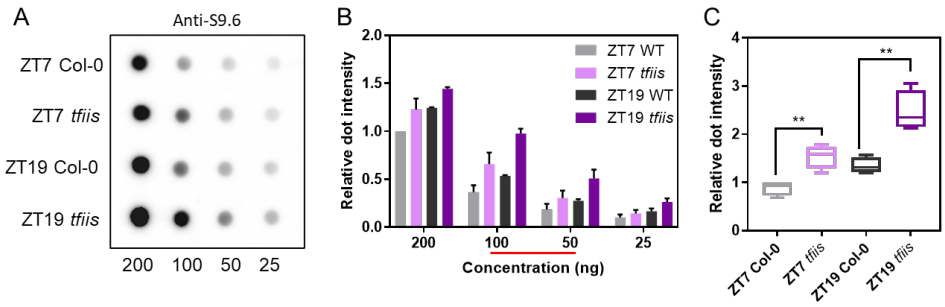


Figure 26. Mutation of *TFIIs* increases R-loop accumulation at both day and night. (A) Dot-blot analyses of R-loop accumulation in wild-type and *tfiis* mutant seedlings. Plants were grown under a 12-hour light and 12-hour dark cycle for 10 days, and samples were collected at ZT7 and ZT19. (B) Quantification of signals detected by S9.6 antibody. The values were normalized against the ZT7 wild-type sample. Data are shown as means + SEM. (C) Statistical analyses were conducted on the quantified signals from 100 ng and 50 ng, highlighted by the red line in panel B. Box plots show median and 25th and 75th percentiles with whiskers showing minimum and maximum values. Two biological replicates were performed, with plants grown independently, and with samples collected, processed, and analyzed at different times. Unpaired t-test was performed for the statistical analyses between *tfiis* mutant and wild-type samples. ** p-value < 0.01.

4. Identifying the molecular link between transcription and the diurnal accumulation of R-loops

4.1 SSRP1 sustains the diurnal accumulation of R-loops

The FACT complex is another key component of the transcriptional machinery involved in transcription elongation (Van Lijsebettens and Grasser, 2014). Mutation of *ssrp1* in yeast increases R-loop accumulation (Herrera-Moyano et al., 2014). In plants, the FACT complex regulates circadian clock gene expression through direct interaction with clock-related proteins (Perales and Mas, 2007; Ma et al., 2018). Knock-out mutants of SSRP1 (*ssrp1-1*) (Lolas et al., 2010) are embryo-lethal, while a T-DNA insertion line in the last exon (*ssrp1-2*) reduces SSRP1 function but the plants are viable (Lolas et al., 2010) (Figure 27A). We used the *ssrp1-2* mutant and confirmed the reduced expression of *SSRP1* by RT-qPCR (Figure 27B).

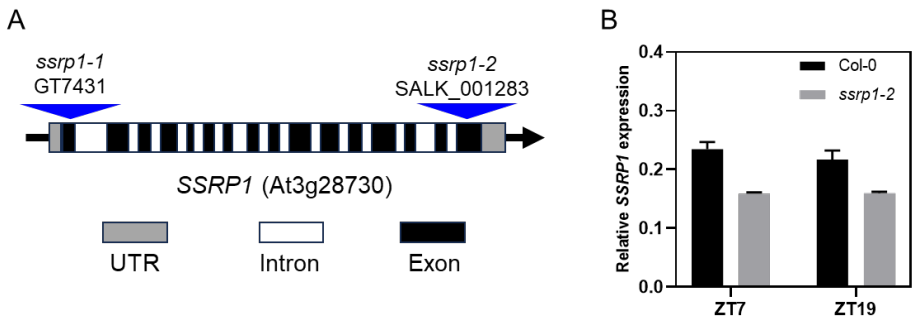


Figure 27. Characterization of Arabidopsis *ssrp1* mutant. (A) Schematic representation of the *SSRP1* gene. Black boxes represent exons, grey-filled boxes represent UTRs, and white boxes indicate introns. The blue triangles indicate the T-DNA insertions. (B) RT-qPCR analyses of *SSRP1* expression in *ssrp1-2* mutant and wild-type plants grown in a 12-hour light and 12-hour dark cycle for 10 days. Samples were collected at ZT7 and ZT19. Values were normalized to *IPP2*. Data are represented as the mean + SEM. Two biological replicates were performed, with plants grown independently, with samples collected, processed, and analyzed at different times.

We then compared R-loop accumulation in wild-type and *ssrp1-2* mutant plants. Our results showed that R-loops were increased both at day and night, although the increment was statistically significant only at ZT7 (Figure 28A-C). Overall, R-loops accumulated in *ssrp1-2* mutant at a similar degree at both time points (ZT7 and ZT19) (Figure 28A-C). Calculating the ratio of change verified that the effect on R-loop accumulation in *ssrp1-2* mutant plants was more severe during the day than during the night as opposed to the similar R-loop increments in the *tfiis* mutants at both time points (Figure 28D). Therefore, the diurnal regulation of R-loops persists in *tfiis* mutant plants but was lost in *ssrp1-2*. The results suggest that SSRP1 might have a prevalent role contributing to the reduced R-loop abundance during the day compared to the night, and thus proper SSRP1 function is required for the diurnal regulation of R-loops observed in wild-type plants.

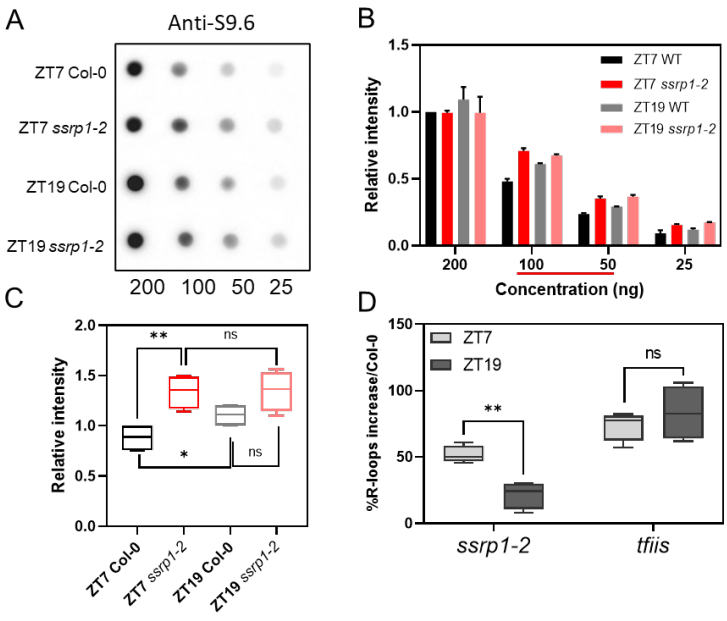


Figure 28. Increased R-loop accumulation in the *ssrp1-2* mutant. (A) Dot-blot analyses of R-loop accumulation in wild-type and *ssrp1-2* seedlings. Plants were grown under a 12-hour light and

12-hour dark cycle for 10 days, and samples were collected at ZT7 and ZT19. (B) Quantification of signals detected with the S9.6 antibody. The values were normalized against the ZT7 wild-type sample. Data are shown as means + SEM. (C) Statistical analyses were conducted on the quantified signals from 100 ng and 50 ng, highlighted by the red line in panel B. (D) Comparison analysis of the increments of R-loops in *ssrp1*-2 and *tfiis* mutant during the day and night. Box plots show median and 25th and 75th percentiles with whiskers showing the minimum and maximum values. Two biological replicates were performed, with plants grown independently, and with samples collected, processed, and analyzed at different times. Unpaired t-test was performed for the statistical analyses between *ssrp1-2* mutant and wild-type samples. * p-value <0.05, ** p-value<0.01, and ns: not significant.

4.2 Mutation of *SSRP1* alters the chromatin compaction

As R-loops and the RNA Pol II transcriptional function are affected in *ssrp1* mutant plants (Li et al., 2007b; Herrera-Moyano et al., 2014), then, chromatin compaction might be also altered in the mutant. We utilized DAPI staining to analyze the chromocenter numbers in wild-type and *ssrp1-2* mutant plants. Our studies showed a significantly decreased number of chromocenters in the mutant compared to wild-type (Figure 29A-C). These results confirm the reduced chromatin compaction in *ssrp1-2* mutant plants.

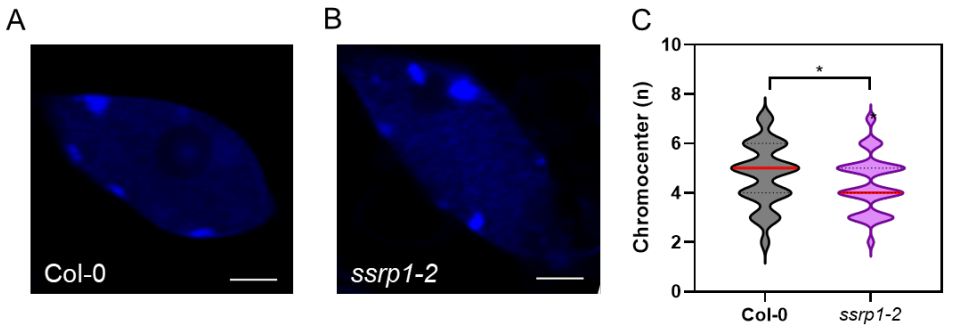


Figure 29. *SSRP1* mutation decreases chromocenter number in cotyledons. (A, B) Representative DAPI-stained cotyledon nuclei of wild-type and *ssrp1-2* mutant. Plants were grown under a 12-hour light and 12-hour dark cycle for 10 days, and samples were collected at ZT7. (C)

The violin graph represented the number of chromocenters per nucleus in wild-type and *ssrp1-2* mutant cotyledons. Two biological replicates were performed, with measurements taken from independent samples grown and processed at different times. The black dotted lines indicate the interquartile range and medians are shown as red horizontal line. Unpaired t-test was performed for the statistical analyses between the wild-type and *ssrp1-2* mutant samples. * P-value < 0. 05 and ns: not significant, with a sample size n > 50.

4.3 Mutation of *SSRP1* induces changes in histone modifications

Active transcription relies at its bases on a permissive chromatin state that facilitates the accessibility of the transcriptional machinery (Kornberg and Lorch, 2002; Ishihara et al., 2021). As histone modifications are closely associated with transcription, we examined by Western-blot analyses the global accumulation of histone marks, specifically H3K4, H3K36, and H3K27 tri-methylation. Our results showed a significant increase in the abundance of both activating marks (H3K4me3 and H3K36me3) in the *ssrp1-2* mutant compared to the wild-type (Figure 30A-D). Conversely, the abundance of the repressing mark H3K27me3 was significantly decreased in the *ssrp1-2* mutant compared to the wild-type (Figure 30E and F). The results suggest that the accumulation of R-loops in the *ssrp1-2* mutant positively correlates with the abundance of active histone marks and negatively with repressive histone marks.

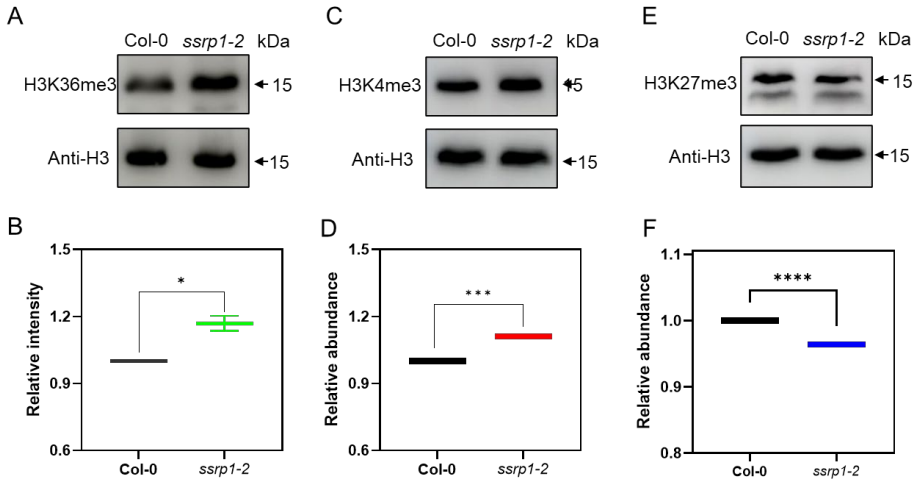


Figure 30. *ssrp1* mutant plants globally increase H3K36me3, H3K4me3, and H3K27me3 accumulation. (A, C, and E) Western blotting analyses the abundance of chromatin marks H3K36me3, H3K4me3, and H3K27me3 in wild-type and *ssrp1-2* mutant samples. Plants were grown under a 12-hour light and 12-hour dark cycle for 10 days, and samples were collected at ZT7. (B, D, and F) Quantification of signals detected by anti-H3K36me3, anti-H3K4me3, anti-H3K27me3, and anti-H3 antibodies. The values were quantified relative to the wild-type value for each blot after normalization to the H3. Box plots show median and 25th and 75th percentiles with whiskers showing minimum and maximum values. Two biological replicates were performed, with plants grown independently, and with samples collected, processed, and analyzed at different times. Unpaired t-test was performed for the statistical analyses between *ssrp1-2* mutant and wild-type samples. **** p-value<0.0001, *** p-value<0.001 and * p-value <0.05.

4.4 Mutation of *SSRP1* increases RNA Pol II S5P and S2P accumulation

We next examined whether the changes in R-loop accumulation in *ssrp1-2* mutant plants might correlate with changes in RNA Pol II abundance. We thus examined by Western-blot analyses, the RNA Pol II S5P and S2P global accumulation in wild-type and *ssrp1-2* mutant plants. The results showed that both S5P and S2P accumulation increased in the *ssrp1-2* mutant compared to wild-type (Figure 31A

and B). Thus, the increased accumulation of R-loops and active histone marks also correlated well with the increased abundance of S5P and S2P. Altogether, the results suggest that active transcription correlates with the accumulation of R-loops in Arabidopsis.

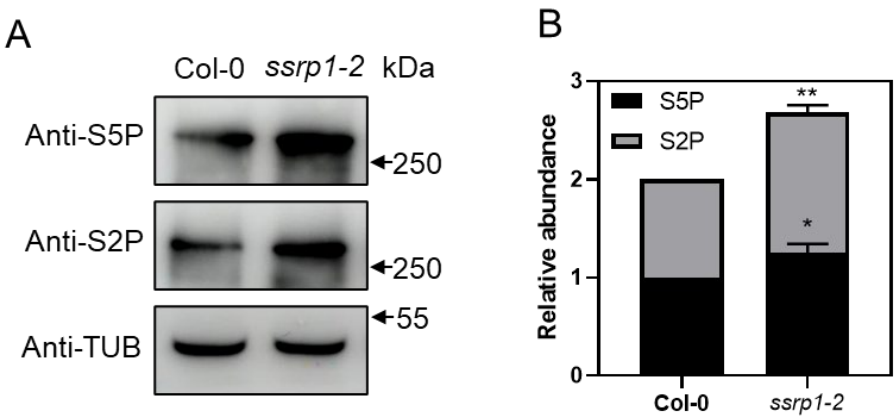


Figure 31. Mutation of *SSRP1* alters the accumulation of RNA Pol II CTD S5P and S2P. (A) Western blotting analyses the abundance of RNA Pol II S5P and S2P in wild-type and *ssrp1-2* mutant samples. Plants were grown under a 12-hour light and 12-hour dark cycle for 10 days, and samples were collected at ZT7. Detection was performed using the anti-S5P, anti-S2P, and anti-Tubulin antibodies. (B) Quantification of signals detected by anti-S5P, anti-S2P, and anti-Tubulin antibodies. The values were quantified relative to the wild-type value for each blot after normalization to the tubulin. Data are represented as the mean + SEM. Two biological replicates were performed, with plants grown independently, and with samples collected, processed, and analyzed at different times. Unpaired t-test was performed for the statistical analyses between wild-type and *ssrp1-2* mutant samples. ** p-value<0.01 and * p-value <0.05.

4.5 Mutation of *SSRP1* suppresses m^{6}A accumulation

The accumulation of m^{6}A modification occurs co-transcriptionally, and the efficiency of transcription influences the m^{6}A methyltransferase catalytic activity (Akhtar et al., 2021). Furthermore, m^{6}A marks mediate R-loop removal in human

cells (Abakir et al., 2020; Boulias and Greer, 2023). To investigate whether R-loops correlated with the m^{6}A modification, we analyzed RNA m^{6}A accumulation in wild-type and *ssrp1-2* mutant plants. RNA m^{6}A accumulation was analyzed by dot-blot assays (Shen et al., 2017a) using a specific m^{6}A antibody (Synaptic Systems). Our results showed that the RNA m^{6}A mark was significantly reduced in the *ssrp1-2* mutant compared to wild-type (Figure 32A and B), while the loading of total RNA was similar in both samples as assayed by methylene blue staining (Figure 32C). Further, our results showed that the changes in m^{6}A abundance were inversely correlated with the accumulation of R-loops in the *ssrp1-2* mutant (Figure 32D).

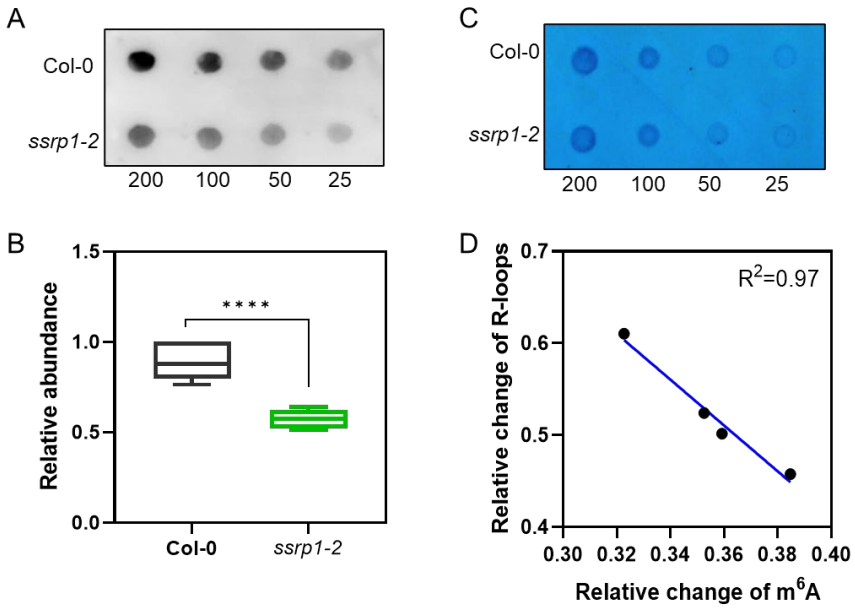


Figure 32. Reduced RNA m^{6}A modification level in *ssrp1-2* mutant compared to the wild-type. (A) Dot-blot analyses of m^{6}A accumulation in wild-type and *ssrp1-2* mutant seedlings. Plants were grown under a 12-hour light and 12-hour dark cycle for 10 days, and samples were collected at ZT7. Detection was performed using m^{6}A antibody. (B) Statistical analyses were conducted on the quantified signals from 100 ng and 50 ng. The values were normalized against the wild-type sample.

Box plots show median and 25th and 75th percentiles with whiskers showing the minimum and maximum values. (C) Methylene blue staining was used as the loading control. Three biological replicates were performed, with plants grown independently, with samples collected, processed, and analyzed at different times. (D) Correlation analysis and linear regression line fitting comparing changes in R-loops accumulation and abundance of m^{6}A in *ssrp1-2* mutant. R^2=0.97. Unpaired t-test was performed for the statistical analyses between *ssrp1-2* mutant and wild-type samples. **** p-value<0.0001.

4.6 Mutation of *SSRP1* affects leaf emergence after DNA damage

Alteration of R-loop accumulation has been associated with genome instability in human cells (Patel et al., 2021). To examine whether this is also the case in Arabidopsis, we used bleomycin (BLM, Abcam Biochemicals), a glycopeptide known to induce DNA double-strand breaks (DSBs). The response to BLM treatment was monitored by quantifying the emergence of the first pair of true leaves. Mock, untreated wild-type, and *ssrp1-2* mutant plants showed no differences in leaf emergence (Figure 33A and B). Treatment with BLM resulted in a pronounced delay in the emergence of true leaves compared to untreated plants in both wild-type and *ssrp1-2* mutant plants (Figure 33A and B). However, the *ssrp1-2* mutant displayed an increased number of true leaves compared to wild-type (Figure 33B). These results suggest that the DNA damage might be reduced, and/or the repair efficiency increased in the *ssrp1-2* mutant compared to wild-type.

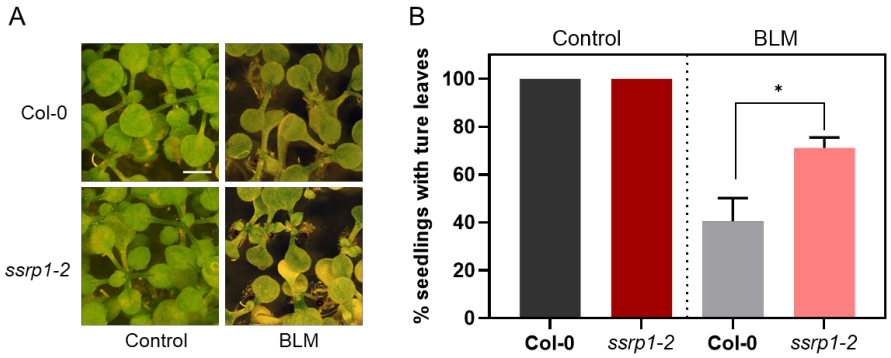


Figure 33. *SSRP1* expression correlates with true leave emergence in response to bleomycin (BLM) induced DSB. (A) Pictures of wild-type and *ssrp1-2* untreated and BLM-treated wild-type plants after 21 days after germination. (B) The percentage of true leaf emergence. The scale bar represents 0.5 cm. Unpaired t-test was performed to evaluate the statistical significance of differences between the *ssrp1-2* mutant and wild-type. * p-value<0.05.

DISCUSSION

To understand the dynamics of R-loop accumulation and the factors involved in their homeostasis is essential to develop appropriate methods to detect R-loops in a rapid and specific way. By developing dot-blot assays, we have been able to unravel the dynamics of Arabidopsis R-loop accumulation during the day and night cycle. The dot-blot assays have also allowed us to identify molecular components required for the proper diurnal changes in R-loop accumulation. The use of dot-blot and western-blot analyses has also uncovered the connection of diurnal R-loop dynamics with RNA Pol II accumulation and active transcription in Arabidopsis. We have also identified the component of the FACT complex SSRP1 as a molecular link functionally connecting the diel R-loop abundance with transcription.

Although R-loops were initially considered rare by-products resulting from transcription, increasing evidence supports the notion of functional R-loops that are prevalently distributed in the genomes of eukaryotic organisms (Amon and Koshland, 2016; Xu et al., 2017). Proper regulation of R-loops is important in the control of multiple biological processes in both plants and animals (Costantino and Koshland, 2015; Allison and Wang, 2019; Zheng et al., 2022). For instance, miss-regulation of R-loops has been connected with alteration of gene expression, replication, DNA damage and repair, and genome integrity (Hatchi et al., 2015; Santos-Pereira and Aguilera, 2015; Yang et al., 2017; Niehrs and Luke, 2020; Rinaldi et al., 2020; Gao et al., 2021; Wei and He, 2021).

Due to the importance of R-loop homeostasis, research studies were initially focused on the development of several methods for specific R-loop detection.

Thus, over the years, a number of methods have been reported. For instance, the DRIP (DNA-RNA immunoprecipitation) technique uses the S9.6 antibody to specifically detect R-loops from purified genomic DNA. The DRIP technique can be followed by qPCR or sequencing (DRIP- qPCR or DRIP-Seq) (Sun et al., 2013; Shafiq et al., 2017; Xu et al., 2017). DRIP-Seq offers high specificity and enables the identification of R-loop accumulation and genomic position. However, it is technically challenging and requires complex data analysis. Immunofluorescence staining with the S9.6 antibody allows for the visualization of R-loops within cells, providing valuable spatial information (Skourti-Stathaki et al., 2014), but it cannot provide a specific view of R-loop accumulation within the genome. More recently, another method, known as MapR (R-loop mapping strategy) utilized the RNase H enzyme to identify R-loops. The method was combined with a CUT&RUN (cleavage under targets and release using nuclease) approach (Yan et al., 2019). The spKAS-seq (strand-specific kethoxal-assisted single-stranded DNA (ssDNA) sequencing) technique is an alternative approach for R-loop mapping, which does not use the S9.6 antibody or RNase H but it is rather based on the high specificity of N3-kethoxal-assisted labeling of ssDNA (Wu et al., 2022). The spKAS-seq allows rapid, sensitive, and genome-wide capture and mapping of R-loops although complex informatic analyses are required to identify canonical R-loops.

For our screenings of R-loop accumulation in plants, we have performed dot-blot assays using the S9.6 antibody. Although these dot-blots are semi-quantitative, their simplicity, versatility, and sensitivity are key advantages for analyzing global R-loop accumulation. In our studies, we have observed comparable results using multiple S9.6 antibodies from different manufacturers. The specificity of our results was also confirmed by the reduced signals in samples treated with RNase

H, which specifically degrades the RNA within R-loops (Shen et al., 2017b). This strongly suggests that the dot-blot is a robust method for R-loop detection and quantification in *Arabidopsis thaliana*.

Although our results showed reliable and reproducible accumulation of R-loops using different S9.6 antibodies, the affinity of the S9.6 antibody could be slightly affected by the sequence context (Konig et al., 2017), which raises the possibility of a potential sequence-related bias of R-loop recognition. We have also observed some residual signals remaining in the RNase H-treated samples. It is possible that commercial RNase H cannot effectively remove all the RNA from the R-loops. The commercial RNase H is produced in *E. coli*, utilizing the *RNase H* gene of *E. coli*. However, unlike the RNase H1 in *Arabidopsis thaliana*, the RNase H in *E. coli* lacks the DNA:RNA hybrid binding domain (Gaidamakov et al., 2005; Yang et al., 2017). Deletion of this domain in humans and mouse reduces the activity of RNase H1, resulting in proteins that exhibit deficiencies in RNase H1 activity (Gaidamakov et al., 2005; Nowotny et al., 2008). Therefore, a reduced RNase H activity might be responsible for the remaining signals detected in RNase H-treated samples. Several studies in both plants and animals using immunoblotting or spKAS-seq approaches have also shown the presence of residual signals in RNase H-treated samples (Yang et al., 2017; Zatreanu et al., 2019; Wu et al., 2022). In our studies, plants over-expressing the nuclear-localized Arabidopsis RNase H1A are also able to reduce R-loops although not to background levels. It is possible that RNase H1A might work in concert with other proteins so that just by solely over-expressing RNase H1 (and not other components of the complex) is not sufficient to fully reduce the R-loops. It is also possible that other pathways contributing to R-loop homeostasis (Masse et al., 1997; Yang et al., 2023)

compensate for the increased activity of RNase H1.

Regarding the formation of R-loops, several factors have been involved in the generation and regulation of R-loop accumulation in plants (Xu et al., 2020). In Arabidopsis, R-loops remain relatively stable during the vegetative stage and in response to different environmental stimuli (Xu et al., 2020a). However, significant differences in R-loop accumulation were observed between plants grown under continuous white light compared to continuous darkness (Xu et al., 2020a). Instead of constant conditions, we used plants grown under more natural environmental conditions (24-hour light: dark cycles) and analyzed R-loop accumulation during the light and dark periods. We found that R-loops accumulated significantly higher during the night compared to the day. Therefore, rapid changes in R-loop accumulation are already evident in a 24-hour cycle. Our results suggest that both the circadian clock and light signaling contribute to the diurnal regulation of R-loops.

The diurnal regulation of R-loops is consistent with our studies showing a role for photoreceptors controlling the accumulation of R-loops. We found that both cryptochromes and PHYB activate the formation of R-loops both day and night. Several studies have shown that open chromatin may facilitate R-loop formation in mammals (Ginno et al., 2012; Sanz et al., 2016; Chen et al., 2017b; Dumelie and Jaffrey, 2017). CRY2 acts as an activator of chromatin decompaction in a process requiring light and PHYB (van Zanten et al., 2010). Thus, it is possible that PHYB and CRYs regulate R-loop accumulation by influencing the state of chromatin compaction. Both *cry2* and *phyB* mutants exhibited an increase in heterochromatic regions (van Zanten et al., 2010). Thus, there might be a negative

correlation between heterochromatin and R-loop accumulation. This aligns with our results showing the correlation between increased R-loop accumulation and reduced number of chromocenters. The results are further supported by studies in mammals, which show a positive correlation between open chromatin and R-loops (Powell et al., 2013).

We did not observe a significant difference in R-loop accumulation during the night in cryptochrome mutants compared to wild-type under BL/D conditions. Similarly, R-loop accumulation in *phyB* mutants during the night was similar to wild-type plants assayed under RL/D conditions. It is possible that the defective function of cryptochrome and PHYB occurs under monochromatic light conditions. PHYB interacts directly with CRY2 in a light-dependent manner (Mas et al., 2000), and PHYA physically interacts with CRY1 (Ahmad et al., 1998). These highly dynamic interactions may lead to the formation of varied protein complexes, which confer plants the plasticity to adapt to the varied light conditions in nature (Xu et al., 2016; Mao et al., 2020). This suggests that the full function of cryptochrome and PHYB in the regulation of R-loops is only apparent when they are simultaneously exposed to multiple wavelengths of light. Further studies are still required to fully elucidate the cellular and molecular mechanisms underlying the function of CRYs and PHYB in the accumulation of R-loops.

Light signaling pathways together with the circadian clock are responsible for perceiving and responding to the day and night cycle (Roenneberg and Foster, 1997; Xiong et al., 2022). Consistently, proper expression of the clock genes is crucial for proper R-loop accumulation in plants. We found that CCA1 represses the accumulation of R-loops, mostly during the day. These results fit quite well

with the general CCA1 repressing function of oscillator gene expression and with CCA1 main peak of expression and activity. The fact that CCA1 is also over-expressed at night, but the effects on R-loops are only minor at this time, suggests that other factors only expressed during the day or regulated by CCA1 during the day contribute to the R-loop accumulation. It is possible that CCA1 regulates the accumulation of R-loops by controlling the morning-expressed *PRRs*. It is also possible that post-translational modifications that activate CCA1 function occur only during the day. In this regard, the protein kinase CK2 can phosphorylate CCA1, and this phosphorylation is essential for the proper transcriptional activity of CCA1 (Sugano et al., 1998; Daniel et al., 2004; Portoles and Mas, 2010).

Our studies also showed that the PRRs enhance the accumulation of R-loops during the day. These results are consistent with their morning peak of expression and activity. However, PRR5, PRR7, and PRR9 have been described mostly as transcriptional repressors in Arabidopsis (Nakamichi et al., 2010). It is possible that the effect of PRRs on R-loop accumulation relies on CCA1, as PRRs are strong repressors of *CCA1* (Nakamichi et al., 2010). Thus, the increased accumulation of *CCA1* in the *prr* mutant will result in decreased accumulation of R-loops.

Not only morning-acting clock components regulate R-loops. The clock component ELF3, which functions as a transcriptional repressor at night also regulates R-loops. Over-expression of *ELF3* repressed the accumulation of R-loops both during the day and night. Thus, the reduced R-loop is consistent with the repressive function of ELF3 during the night. The effect of ELF3-ox during the day might also be due to the function of CCA1 since *CCA1* expression is up-

regulated in *ELF3-ox* plants (Lu et al., 2012). However, no significant difference was observed in R-loop accumulation in the *elf3-2* mutant compared to the wild-type. It is possible that other components of the EC, such as ELF4 and LUX, are also involved in the regulation of R-loops. Previous studies have shown that R-loops increased following high-temperature treatment and declined after switching to control temperature, suggesting that R-loops are responsive to temperature changes (Xu et al., 2020a). Notably, ELF3 has been identified as a thermosensor (Jung et al., 2020). It will be interesting to examine the temperature-dependent changes in R-loop accumulation mediated by ELF3.

LNK (*NIGHT LIGHT–INDUCIBLE AND CLOCK-REGULATED* genes) were identified as key circadian components with an important role connecting light regulation of gene expression (Xie et al. 2014, Perez-Garcia et al. 2015). In Arabidopsis, LNKs act as molecular hubs connecting the DNA binding specificity provided by RVEs (REVEILLEs) with transcription initiation and elongation due to the recruitment of RNA Pol II and the FACT complex (Ma et al., 2018). Our studies showed that the LNKs enhance the accumulation of R-loops during both day and night. The decreased R-loops in *lnk1lnk2* double mutant during the day fit well with the general LNKs function and with their main peak of expression and activity. The reduced R-loop accumulation during the night in *lnk1lnk2* mutants may be due to altered transcription of evening-expressed genes. In this regard, *LNK1* and *LNK2* integrate early light signals with temporal information provided by core oscillator components to control the expression of afternoon and night genes (Rugnone et al., 2013). In Arabidopsis, the transcription of afternoon-expressed *PRR5* and evening-expressed *TOC1* was clearly repressed in the *lnk1lnk2* double mutant (Ma et al., 2018). Overall, the R-loop regulation by LNKs

are likely connected with their role in the control of transcription (Ma et al., 2018). Consistently, studies in mammals have shown that the accumulation of R-loops was decreased when cells were treated with a transcription initiation inhibitor, while washing the inhibitor after treatment lead to the progressive reappearance of R-loops (Sanz et al., 2016). In plants, genes with sense and antisense R-loops exhibit higher expression levels (Fang et al., 2019), suggesting a positive correlation between transcription and the accumulation of R-loops. Consistent with this idea, R-loops have the capacity to promote *de nove* transcript synthesis in mammals (Tan-Wong et al., 2019), and facilitate transcription termination (Yang et al., 2019). In our studies, we have observed that the increased R-loops during the night correlated with the increased accumulation of RNA Pol II S5P and S2P. The correlation suggests a parallelism between the accumulation of R-loops and the transcription activity. Transcription is finely regulated by chromatin marks (Berger, 2007). Consistent with the previous findings in both plants and mammals (Chen et al., 2015; Xu et al., 2017), our results showed that R-loop accumulation positively correlated with active chromatin marks and negatively with repressive marks.

The TFII-type transcription factors are components of the RNA Pol II transcriptional pre-initiation complex (Nikolov and Burley, 1997; Bong Kim et al., 2007; Freytes et al., 2024). Following transcription initiation, RNA Pol II associates with various transcription elongation factors, facilitating efficient messenger RNA (mRNA) synthesis (Adelman and Lis, 2012). Several studies showed that TFIIs is one of the TFII-type transcription factors required for both efficient pre-initiation complex formation (Bong Kim et al., 2007) and transcriptional elongation (Zatreanu et al., 2019). In human cells, mutation of

TFIIs induces increased levels of RNA Pol II pausing arrest and/or RNA Pol II backtracking (Zatreanu et al., 2019). Thus, TFIIs might play an essential role maintaining the fidelity and efficiency of RNA synthesis during transcription. Notably, RNA Pol II backtracking was associated with increased R-loop accumulation (Zatreanu et al., 2019). As TFIIs is highly conserved among eukaryotes (Shimasaki and Kane, 2000; Antosz et al., 2020), we found increased accumulation of R-loops in *tfiis* mutant during both day and night. The accumulation of R-loops in *tfiis* mutation might be due to transcriptional arrest caused by the inhibition of RNA Pol II-mediated transcription cleavage (Antosz et al., 2020).

The FACT (FAcilitates Chromatin Transcription) complex plays a crucial role in transcription regulation by facilitating the passage of RNA polymerase II through nucleosomes (Orphanides et al., 1998; Orphanides et al., 1999; Belotserkovskaya et al., 2004). In mammals, FACT accompanies RNA Pol II during transcription elongation (Saunders et al., 2003), and mutation of *SSRP1* led to increased R-loop accumulation (Herrera-Moyano et al., 2014). The FACT complex is highly conserved among eukaryotes (Sims et al., 2004), and consistently, we found that SSRP1 suppresses the formation of R-loops mostly during the daytime. In *Saccharomyces cerevisiae,* FACT mutants show cryptic transcription (Mason and Struhl, 2003; Myers et al., 2011) with increased RNA Pol II, and TATA-binding protein (TBP) occupancy at the 3' coding regions (Mason and Struhl, 2003). Thus, altered regulation of transcription in Arabidopsis *ssrp1* mutant plants might lead to accumulation of R-loops. In agreement with this view, the Arabidopsis FACT complex efficiently represses intragenic transcriptional initiation (Nielsen et al., 2019), which is consistent with the increased RNA Pol II abundance observed in

the *ssrp1* mutant. Increased transcription-replication conflicts in the *ssrp1* mutant might also result in increased accumulation of R-loops (Herrera-Moyano et al., 2014).

Together, our results show that both TFIIs and SSRP1 are important for R-loop accumulation and suggest a tight connection between R-loops and transcriptional activity in Arabidopsis. However, there is an important difference between TFIIs and SSRP1 function: while TFIIs represses R-loop accumulation during both day and night, SSRP1 decreases R-loop accumulation mainly during the day. The results indicate that the diurnal regulation of R-loops is lost in the *ssrp1* mutant plants but still in place in the *tfiis* mutant. Thus, SSPR1 plays an important role reducing R-loop accumulation during the day. Improved precision of RNA Pol II-mediated transcription, avoiding the excessive formation of R-loops might be more important during the day, when the possibility of DNA damage is increased due to ultraviolet (UV) light. Indeed, miss-regulation of R-loops has been shown to compromise genome integrity (Sollier and Cimprich, 2015).

Studies in human cells have shown that the N 6-methyladenosine (m^6A) RNA modification (Sun et al., 2023) is prevalent in the RNA strands of RNA-DNA hybrids (Abakir et al., 2020). These results connect, directly or indirectly, the m^6A modification with R-loops (Yang et al., 2019). Consistently, m^6A is present on the majority of R-loops in human cells, and knockout of the m^6A reader, YTH N6-methyladenosine RNA binding protein 2 (YTHDF2) (Abakir et al., 2020) or the methyltransferase METTL3 (methyltransferase 3) lead to increased R-loop levels (Kang et al., 2021). In our studies, we found that the accumulation of R-loops is inversely correlated with the abundance of m^6A modification. The modifications

of m^{6}A are also closely related to transcription and chromatin states (Akhtar et al., 2021). Studies in mouse showed that knockout of the m^{6}A writer *Mettl3* or reader *Ythdc1* increases chromatin accessibility, activates transcription (Liu et al., 2020a), and prolongs the activation of stress genes (Ji et al., 2021). The results suggest that m^{6}A may influence the accumulation of R-loops by modifying transcription processes or chromatin states.

As mentioned above, proper R-loop homeostasis is important for maintaining genome integrity (Sollier and Cimprich, 2015; Brambati et al., 2020). However, the increased accumulation of R-loops during the day in *ssrp1-2* mutant correlates with improved responses to double-stranded breaks after bleomycin treatment. In yeast, R-loops have the potential to promote DNA repair (Wahba et al., 2013). Similarly, the accumulation of active histone marks such as H3K4me3 and H3K36me3 is required for effective DNA repair (Pena et al., 2008; Faucher and Wellinger, 2010; Miller and Jackson, 2012; Aymard et al., 2014; Pfister et al., 2014; Li et al., 2018; Sun et al., 2020). Thus, it is possible that these and some other, yet unknown factors and mechanisms contribute to *ssrp1-2* improved response to bleomycin treatment.

Although R-loops have been described as stable genomic structures in both animal and plant systems (Sanz et al., 2016; Xu et al., 2020a), our studies have shown that R-loops dynamically change during the day and night. Photoreceptors and circadian clock components directly or indirectly contribute to the diurnal regulation of R-loop accumulation. We also found that R-loop homeostasis is linked to transcription in Arabidopsis, and that SSPR1, the component of the FACT complex acts as a functional hub connecting transcription with the diurnal

regulation of R-loops. Understanding the components and mechanisms behind R-loop generation, stability, and degradation could provide useful tools to manipulate and improve transcription, gene expression, genome integrity, growth, and development. Our study incorporates the importance of proper timing for orchestrating R-loop dynamics and suggests a complex interplay between photoreceptors, circadian clock components and the transcriptional machinery.

CONCLUSIONS

This Doctoral Thesis advances our understanding of R-loop dynamics in *Arabidopsis thaliana* and the connection with proper regulation of transcription. We have identified the diurnal changes in R-loop accumulation and the contribution of photoreceptors and clock components on R-loop homeostasis. We have established a positive correlation between the diurnal accumulation of R-loops and transcriptional activity, with SSRP1 functioning as a molecular link connecting these processes. The primary conclusions drawn from our study can be outlined as follows:

1. The dot-blot assay using the S9.6 antibody is a reliable and reproducible method for R-loop detection in *Arabidopsis thaliana*. This method offers a valuable tool for further studies of R-loop dynamics in plants.

2. R-loops in *Arabidopsis thaliana* accumulate in a diurnal fashion with a significant enrichment during the night compared to the day. This suggests dynamic light- and diurnal responsive pathways for R-loop regulation.

3. Arabidopsis photoreceptors (PHYTOCHROME B and CRYPTOCHROME 1 and 2), and morning- and evening-expressed clock components differentially contribute to the diurnal accumulation of R-loops. The results highlight the intricate interplay between light signaling and the circadian clock in the control of R-loop homeostasis.

4. R-loops in Arabidopsis correlate with active transcription as assayed by RNA Polymerase II accumulation, pharmacological inhibition of transcription, chromatin compaction and analyses of transcription-related mutants. The results

pave the way for manipulating transcription to intervene on R-loop dynamics.

5. The Arabidopsis transcription elongation factor TFIIs (transcription elongation factor IIs) contributes to proper R-loop accumulation at both day and night. The findings reinforce a connection between proper regulation of transcription and R-loop accumulation.

6. The component of the FACT complex, SSRP1 (structure-specific recognition protein 1), contributes to proper RNA Polymerase II accumulation, chromatin compaction, abundance of histone marks and responses to DNA damage. The results suggest that SSRP1 likely plays a multifaceted role in the regulation of transcription-associated processes.

7. SSRP1 contributes to the diurnal regulation of R-loops by reducing R-loop accumulation predominantly (albeit not exclusively) during the day. This finding directly links transcription and the diurnal accumulation of R-loops through SSRP1 function.

RESUMEN EN CASTELLANO

Resumen en Castellano

El reloj circadiano es un mecanismo celular endógeno que sincroniza procesos biológicos en coordinación con los ciclos de 24 horas del día y la noche. La función circadiana es esencial para la regulación rítmica de procesos fundamentales en plantas, incluyendo entre otros, el crecimiento, el desarrollo y las respuestas al estrés. El sistema circadiano requiere la regulación precisa de la transcripción rítmica de genes del oscilador central. Desde hace algunos años se ha correlacionado la transcripción con estructuras genómicas denominadas R-loops, compuestas por el híbrido DNA-RNA y el DNA monocatenario que no sirve de molde. Basándonos en la correlación que existe entre la transcripción con el sistema circadiano y con los R-loops, planteamos en esta Tesis Doctoral descubrir la posible regulación diurna de los R-loops e identificar los componentes moleculares y mecanismos subyacentes que controlan su homeostasis en *Arabidopsis thaliana*. Utilizando ensayos tipo dot-blot, observamos que los R-loops presentaban una regulación diurna, con un enriquecimiento significativo durante la noche en comparación con el día. Los fotoreceptores (PHYTOCHROME B y CRYPTOCHROME 1 y 2), así como genes del reloj que se expresan tanto durante el día como por la noche, contribuían diferencialmente a la acumulación diurna de los R-loops. Estos resultados resaltan la intricada interacción entre la señalización lumínica y el reloj circadiano en el control de la homeostasis de los R-loops en *Arabidopsis thaliana*. Adicionalmente, observamos que los R-loops se correlacionaban positivamente con la transcripción, evaluada mediante la acumulación de la RNA polimerasa II, la inhibición farmacológica de la transcripción, la compactación de la cromatina y el análisis de plantas mutantes de genes relacionados con la transcripción. Encontramos además que SSRP1 (structure-specific recognition protein 1), un componente del complejo FACT

(FAcilitates Chromatin Transcription), era necesario para la correcta acumulación de la RNA polimerasa II, la compactación de la cromatina, la abundancia de marcas de histonas y las respuestas al daño del DNA. Adicionalmente, la expresión y función de SSRP1 resultaban esenciales para la regulación diurna de los R-loops, contribuyendo a su menor acumulación principalmente durante el día. En conjunto, nuestros estudios establecen una conexión directa de la función de SSRP1 con la transcripción y la acumulación diurna de los R-loops, y abren nuevas vías de manipulación de la transcripción y regulación circadiana.

SUMMARY IN ENGLISH

Summary in English

The circadian clock is an endogenous timing mechanism that synchronizes biological processes with the 24-hour day and night cycles. Proper circadian function is essential for the rhythmic regulation of fundamental processes in plants, including among others, growth, development, and responses to stress. At its bases, the circadian function relies on the precise regulation of the rhythmic transcription of core oscillator genes. Active transcription also generates in many organisms the so-called R-loops, three-stranded nucleic acid structures composed of the DNA-RNA hybrid and the non-template single-stranded DNA. Based on the correlation of transcription with both the circadian system and R-loops, in this Doctoral Thesis, we aimed to uncover the potential diurnal regulation of R-loops and identify the molecular components and mechanisms underlying R-loop homeostasis in *Arabidopsis thaliana*. By using dot-blot assays, we found that indeed R-loops accumulated in a diurnal fashion with a significant enrichment during the night compared to the day. The photoreceptors (PHYTOCHROME B and CRYPTOCHROME 1 and 2), as well as morning- and evening-expressed clock components differentially contributed to the diurnal accumulation of R-loops, highlighting the intricate interplay between light signaling and the circadian clock in the control of R-loop homeostasis. R-loops also positively correlated with active transcription as assayed by RNA Polymerase II accumulation, pharmacological inhibition of transcription, chromatin compaction, and analyses of transcription-related mutant plants. We found that the component of the FACT (FAcilitates Chromatin Transcription) complex, SSRP1 (structure-specific recognition protein 1) also contributed to proper RNA Polymerase II accumulation, chromatin compaction, abundance of histone marks, and responses to DNA damage. SSRP1 was also responsible for the diurnal regulation of R-loops by

reducing their accumulation predominantly during the day. Altogether, our studies establish a direct connection of SSRP1 function with transcription and the diurnal accumulation of R-loops. Our results open up possible new avenues for the manipulation of transcription and circadian regulation.

MATERIALS AND METHODS

1. Plant material and growth conditions

The *Arabidopsis thaliana* lines used in this study are listed in Table I. Seeds were surface sterilized for 10-15 minutes using a sterilization solution [(75% ethanol (v/v) and 0.1% (v/v) Triton X-100)]. After several washes with sterile water in a flow hood, the seeds were placed on agar plates containing half-strength Murashige and Skoog (½MS-) medium without sucrose. Seeds were then stratified for 2-4 days in darkness at 4ºC. Seedlings were grown under entraining light:dark cycles [12 hours of light/12 hours of dark (LD), 22ºC] in environmentally controlled chambers (INKOA S. L., Percival, or AraLab) with 50 μmol/m^2/s of cool white fluorescent light. For experiments involving blue or red light, seedlings were grown under 12-hour blue or red light and 12-hour dark conditions. Plants were grown under blue or red light light-emitting diode (LED) intensities of 5 μmol/m^2/s for blue light and 100 μmol/m^2/s for red light.

2. Dot-blot assay for R-loops analysis

Approximately 2 g of 10-day-old seedlings were collected at Zeitgeber Time 7 (ZT7, 7 hours after lights-on) and ZT19 (7 hours after lights-off) under LD cycles, and immediately frozen in liquid nitrogen. The samples were ground into a fine powder in liquid nitrogen in a mortar and then resuspended in 20 mL of cold-extraction buffer (0.44 M sucrose, 1.25% Ficoll, 2.5% Dextran, 20 mM HEPES-KOH, pH 7.4, 10 mM $MgCl_2$, and 0.5% Triton X-100) by vortexing. Detailed information on chemicals and reagents used in our studies is listed in Table II. The samples were then kept on ice for 5 minutes. After filtration through two layers of miracloth, the extracts were centrifuged at 1500 g at 4°C for 15 minutes. The pellets were washed twice with 3 mL of cold washing buffer (0.25 M sucrose, 10

mM Tris-HCl, pH 8, 1 mM EDTA, 10 mM $MgCl_2$, 1% Triton X-100, and 5 mM β-mercaptoethanol) by inverting the tube. The washed pellets were then resuspended in 1 mL of lysis buffer (10 mM Tris-HCl pH 8, 1 mM EDTA, and 0.5% SDS) by pipetting, followed by the addition of 40 µL of 2.5 mg/mL proteinase K. The mixture was then incubated at 37°C with shaking at 300 rpm for at least 5 hours. After incubation, 1/4 volume of 5 M KAc was added, and the mixture was kept on ice for 15 minutes to agglutinate proteins. Genomic DNA (gDNA) was isolated using the phenol: chloroform extraction method. A volume of phenol: chloroform: isoamyl alcohol (25:24:1) was added to the lysed sample. The mixture was thoroughly mixed by vortexing or inverting the tube to ensure proper extraction. The mixture was then centrifuged at 12000 g at 4°C for 5 minutes. The aqueous phase (upper layer) was carefully transferred to a new tube, being cautious not to disturb the interphase. The extraction process was repeated by adding fresh chloroform: isoamyl alcohol (24:1), mixing, and centrifuging at 12000 g at 4°C for 5 minutes. Aqueous phases were transferred to a new tube, and the gDNA was precipitated by adding 1/10 volumes of 5 M NaCl supplemented with one volume of isopropanol, followed by incubation for 1 hour at -80°C. The mixture was then centrifuged at 12000 g at 4°C for 15 minutes, and the supernatant was carefully removed without disturbing the pellet. The pellets were washed with cold 70% ethanol and dissolved in 200 µL of nuclease-free water. For RNase H treatment, half of the gDNA volume was incubated with 25 U of RNase H at 37°C for 12 to 16 hours without shaking. The RNase H treated gDNA was purified using the phenol: chloroform extraction method detailed above. The concentration of the gDNA was measured using the Nanodrop (Thermo Fisher Scientific). Subsequently, a series of gDNA dilutions were prepared to achieve concentrations of 100 ng/µL, 50 ng/µL, 25 ng/µL, and 12.5 ng/µL by adding RNase-free water.

The Immobilon-P membrane was prepared following the instructions. The membrane was wetted by placing it on the surface of methanol for 15 seconds, without immersion. Then, the membrane was carefully placed in ultrapure water and soaked for 2 minutes. Subsequently, the membrane was placed in TBST buffer (20 mM Tris-HCl pH 7.5, 150 mM NaCl, 0.1% Tween 20) and allowed to equilibrate for at least 5 minutes. The membrane was placed on two sheets of TBST-moistened filter paper. Subsequently, 2 µL of each dilution was spotted onto two separate membranes. After UV light crosslinking at 1200 µJ for 20 minutes, the membranes were incubated in a blocking solution (5% milk in TBST) for 1 hour at room temperature on a shaker at 150 rpm. Following a wash with TBST, one of the membranes was incubated with an anti-dsDNA antibody while the other was incubated with an anti-S9.6 antibody (1:2,000 dilution). The membranes were incubated overnight at 4°C with shanking (150 rpm). After three washes with TBST, the membranes were incubated with horseradish peroxidase (HRP)-conjugated secondary antibody (1:10,000 dilution) for 1 hour at room temperature on a shaker at 150 rpm. The signal was detected using the ImageQuant 800 chemiluminescence imaging system (Amersham™). Signal intensity was quantified using Image J software. At least two biological replicates were performed per experiment.

3. Plasmid construction and plant transformation

The coding sequence (CDS) of the *RNase H1A* (At3g01410) gene was initially amplified by polymerase chain reaction (PCR) and inserted into the pENTR/D-TOPO vector following the manufacturer's recommendations. The obantied entry vector was transformed into chemically competent *Escherichia coli* (One Shot®

TOP10, Gateway®). Resistant bacterial colonies were obtained after overnight incubation at 37°C on 50 µg/ml kanamycin selection plates. Selected resistant colonies were amplified overnight in Luria-Bertani (LB) liquid medium containing 50 µg/ml kanamycin antibiotic at 37°C shaker at 200 rpm. Liquid colony PCR was used to detect colonies containing the *RNase H1A* CDS. Plasmids from two positive colonies were purified using a QIAprep Spin Miniprep Kit (Qiagen) following the manufacturer's recommendations. The correct sequence of *RNase H1A* CDS was confirmed by capillary sequencing with M13 forward (Fw) and reverse (Rv) primers (Gateway®). The entry vector was used to clone the *RNase H1A* CDS into the plant destination vector pGWB602 (featuring a 35S promoter without tag) (Nakagawa et al., 2007) using the LR reaction (Gateway™ LR Clonase™ II Enzyme mix, Invitrogen) following the manufacturer's recommendations. The obtained vector was amplified in *Escherichia coli* and further introduced into *Agrobacterium tumefaciens* strain GV3101 using a heat shock method. Transformed Agrobacteria were grown for 48 hours at 28°C on a solid yeast extract beef (YEB) plate containing three selection antibiotics (gentamycin 30 µg/ml, spectinomycin 100 µg/ml, and rifampicin 100 µg/ml). After confirmation by PCR using the *RNase H1A* cloning primer, the positive colonies were transferred to a liquid YEB medium with the same selection of antibiotics and grown at 28°C with 200 rpm shaking until OD_{600}≈2.0. After centrifugation, the pellet containing the bacteria was resuspended by vortexing in 100 mL solution containing 10% sucrose, and 40 µL Sliwet L-77. The *TOC1:LUC* plants, which express the luciferase reporter gene under the control of the *TOC1* promoter, were transformed through *Agrobacterium tumefaciens*-mediated DNA transfer (Clough and Bent, 1998) by dipping the inflorescences. Briefly, the inflorescences were dipped into the Agrobacterium suspension for 30 seconds.

The plants were kept under dark conditions at 22°C for 24 hours and then transferred to the greenhouse. The collected seeds were sown on 1/2 MS- medium plates with 10 mg/L phosphinotricin (PPT) antibiotic, and T1 positive lines were obtained. At least 50 seeds from each T1 line were sown on the PPT selection plates, and the segregation patterns of the T2 lines were observed. The lines that exhibited a Mendelian segregation ratio, indicating a single insertion, were transferred to soil for seed collection. At least 100 seeds from independent T2 lines were sown on the PPT selection plates, and T3 homozygous lines were obtained with all the seedlings having PPT resistance. The expression levels were checked by using qPCR with primers designed from the CDS of *RNase H1A*, following the procedure as described in the "*RNA extraction and real-time quantitative PCR analysis*" section. A list of primers used in our studies is shown in Table III.

4. RNA extraction and real-time quantitative PCR analysis

For gene expression analyses, 8-10 seedlings were collected at ZT7 under LD conditions. Total plant RNA was extracted using the Maxwell RSC Plant RNA Kit (Promega) following the manufacturer's recommendations. The RNA concentration was measured using a Nanodrop spectrophotometer (Thermo Fisher). First-strand cDNA synthesis was performed using either iScript™ Reverse Transcription Supermix for RT-qPCR or PrimeScript RT Master Mix for RT-qPCR with 1 µg of RNA. The obtained cDNA was diluted tenfold with nuclease-free water. Quantitative polymerase chain reaction (qPCR) mixture comprised of 2 µL of diluted cDNA, 0.5 µL of forward (Fw) and 0.5µl of Reverse (Rv) primers both at 10 mM, 2 µL nuclease-free water, and 5 µl of the Brilliant III Ultra-Fast SYBR Green qPCR Master Mix or the TB Green™ Premix Ex Taq™

II Tli RNase H Plus. RT-qPCR was performed on a 96-well CFX96 Touch Real-Time PCR detection system (Bio-Rad). Three technical replicates were performed for each sample and gene tested. Gene expression data were normalized to *IPP2* (*ISOPENTENYL PYROPHOSPHATE: DIMETHYL-ALLYL PYROPHSPHATE ISOMERASE*). Relative transcript levels were calculated using the $2^{-\Delta\Delta CT}$ method (Livak and Schmittgen, 2001). A list of primers used in our studies is shown in Table III.

5. Flavopiridol (FLAP) treatments

Pharmacological inhibition of transcription treatments were conducted using a water-diluted solution of flavopiridol (FLAP). Ten-day-old wild-type Arabidopsis seedlings grown on 12 cm x 12 cm square plates under LD conditions, were treated at ZT7 in the fume hood with 10 mL of 10 µM FLAP solution via vacuum infiltration for 10 minutes. Control mock-treated samples were similarly processed, except that water without FLAP was used. After treatment, plants were kept under LD conditions for 24 hours, and samples were collected at ZT7 for subsequent analysis.

6. DRIP (DNA-RNA Immunoprecipitation)-qPCR assay

DRIP-qPCR analyses were conducted following a previously described protocol (Xu et al., 2017) with minor modifications. Briefly, 2 g of ten-day-old Arabidopsis seedlings grown under LD conditions were collected at ZT7. The samples were ground in liquid nitrogen in a mortar and then homogenized in 20 mL of cold extraction buffer (0.44 M sucrose, 20 mM HEPES-KOH, pH 7.4, 2.5% Dextran, 1.25% Ficoll, 10 mM MgCl2, and 0.5% Triton X-100). The mixture was filtered

through miracloth. After centrifugation at 1000 g for 20 minutes at 4°C, the pellets were washed twice with cold washing buffer (0.25 M sucrose, 1 mM EDTA, 10 mM Tris pH 8, 1% Triton X-100, 10 mM $MgCl_2$, 5 mM β-mercaptoethanol) by inverting the tube and centrifuged at 1000 g for 20 minutes at 4°C. The pellets were incubated with 0.1 mg/mL of proteinase K in lysis buffer (10 mM Tris-HCl pH 8, 0.5% SDS, 1 mM EDTA) with shaking (350 rpm) for at least 5 hours at 37ºC. The gDNA was subsequently purified using the phenol: chloroform extraction procedure as described above in the "*Dot-blot assay for R-loops analysis*" section. The extracted gDNA was sonicated for 8 minutes (30 s ON, 30 s OFF, low intensity) using a sonicator (Bioruptor, Diagnode). The DNA concentration was measured using a Nanodrop spectrophotometer (Thermo Fisher). Next, 5 µg of the fragmented DNA was incubated with 4 µL of S9.6 antibody (reference ENH001, Karefast) in DRIP buffer (100 mM $NaPO_4$, 1.4 M NaCl, 0.5% Triton X-100) overnight at 4ºC on a rotator at 15 rpm. The antibody-DNA:RNA hybrid complexes were collected by incubating with 50 µL of equilibrated slurry protein G beads for 4 hours in a cold room with rotation at 15 rpm. The complexes were washed three times with cold 1x DRIP buffer by rotating for 5 minutes at 15 rpm in a cold room. The DNA-RNA hybrids were then eluted by incubating with 250 µL of elution buffer (50 mM Tris-HCl, pH 8, 0.5% SDS, 10 mM EDTA, 0.1 mg/mL Proteinase K) for 1 hour at 60ºC with 950 rpm shaking, followed by DNA purification using the phenol: chloroform extraction method. The DNA pellets were dissolved in 200 µL of nuclease-free water. The qPCR was performed using 2 µL of DRIP DNA, 0.5 µL of 10 mM forward and reverse primers for each, 2 µL nuclease-free water, and 5 µL either Brilliant III Ultra-Fast SYBR Green qPCR Master Mix or TB Green™ Premix Ex Taq™ II Tli RNase H Plus on a 96-well CFX96 Touch Real-Time PCR detection system

(Bio-Rad). At least two technical replicates were performed for each region and gene. *TA3* retrotransposon was used as a negative control. Relative enrichment was calculated using the $2^{-\Delta\Delta CT}$ method (Livak and Schmittgen, 2001). DRIP-qPCR values were normalized to 5% of input values. A list of primers used in our studies is shown in Table III.

7. Chromatin Immunoprecipitation (ChIP)

ChIP assays were performed as previously described (Ma et al., 2018) with minor modifications. Briefly, 2 g of seedlings were collected under LD conditions at ZT7 and fixed using vacuum infiltration with PBS (131 mM NaCl, 7 mM Na_2HPO_4, 3 mM NaH_2PO_4) solution containing 1% formaldehyde for 15 minutes in the fume hood at room temperature. Formaldehyde was removed in the fume hood with the pipette and 10 mL of 0.125 M glycine solution was added (which quenched the cross-linker) and vacuumed for 5 minutes. Samples were washed three times with cold PBS solution by inverting the tube in a cold room, subsequently frozen in liquid nitrogen, and stored at -80°C. Fixed samples were processed by grinding to a fine powder in liquid nitrogen in a mortar and homogenizing in 30 mL of cold extraction buffer I (10 mM Tris-HCl, pH 8.0, 0.4 M sucrose, 5 mM EDTA, 5 mM β-mercaptoethanol, 1 mM PMSF, 5 mg/mL leupeptin, 1 mg/mL aprotinin, 1 mg/mL E-64, 5 mg/mL antipain, 1 mg/mL pepstatin, 5 mg/mL chymostatin, and 50 mM MG-132) and filtered through two layers miracloth. After centrifugation at 1000 g at 4°C for 20 minutes, the pellets were washed with cold extraction buffer II (10 mM Tris-HCl, pH 8.0, 0.25 M sucrose, 10 mM $MgCl_2$, 1% Triton X-100, 5 mM EDTA, 5 mM β-mercaptoethanol, 1 mM PMSF, 5 mg/mL leupeptin, 1 mg/mL aprotinin, 1 mg/mL E-64, 5 mg/mL antipain, 1 mg/mL pepstatin, 5 mg/mL

chymostatin, and 50 mM MG-132) by inverting the tube in a cold room and centrifuged at 1000 g for 20 minutes at 4ºC. The pellet was resuspended in 1 mL of lysis buffer (10 mM Tris-HCl, pH 8.0, 10 mM EDTA, 1% SDS, 1 mM PMSF, 5 mg/mL leupeptin, 1 mg/mL aprotinin, 1 mg/mL E-64, 5 mg/mL antipain, 1 mg/mL pepstatin, 5 mg/mL chymostatin, and 50 mM MG-132) by pipetting and sonicated for 8 minutes (30 s ON, 30 s OFF, low intensity) with a sonicator (Bioruptor, Diagnode). Nuclear debris (pellet) was removed by centrifugation at 13000 g for 5 minutes at 4°C and the supernatant containing the chromatin was collected. Sonicated chromatin was diluted in 700 µL of cold ChIP dilution buffer (15 mM Tris-HCl, pH 8.0, 167 mM NaCl, 1 mM EDTA, 1.1% Triton X-100, 1 mM PMSF, 5 mg/mL leupeptin, 1 mg/mL aprotinin, 1 mg/mL antipain, 1 mg/mL pepstatin, 5 mg/mL chymostatin, and 50 mM MG-132) and incubated with the RNA Pol II S5P antibody overnight on a rotator at 15 rpm at 4°C. The protein-DNA complexes were collected by incubating with 50 µL of equilibrated protein G beads (Invitrogen) for 4 hours at 4°C on a rotator at 15 rpm at 4°C. The complexes were washed twice with different washing buffers, each time for 5 minutes, on a rotator set at 15 rpm in a cold room: low-salt buffer (20 mM Tris-HCl, pH 8.0, 0.1% SDS, 1% TritonX-100, 2 mM EDTA, 150 mM NaCl, 1 mM PMSF, 1 mg/mL aprotinin, 5 mg/mL leupeptin, 1 mg/mL antipain, 1 mg/mL E-64, 1 mg/mL pepstatin, 50 mM MG-132, and 5 mg/mL chymostatin), high-salt buffer (20 mM Tris-HCl, pH 8.0, 500 mM NaCl, 2 mM EDTA, 1% Triton X-100, 0.1% SDS, 1 mM PMSF, 1 mg/mL aprotinin, 5 mg/mL leupeptin, 1 mg/mL antipain, 1 mg/mL E-64, 1 mg/mL pepstatin, 50 mM MG-132, and 5 mg/mL chymostatin), LiCl buffer (10 mM Tris-HCl, pH 8.0, 250 mM LiCl, 1 mM EDTA, 1% IGEPAL® CA-630, 1% sodium deoxycholate, 1 mM PMSF, 1 mg/mL aprotinin, 5 mg/mL leupeptin, 1 mg/mL antipain, 1 mg/mL E-64, 1 mg/mL pepstatin, 50 mM MG-132,

and 5 mg/mL chymostatin), and TE buffer (10 mM Tris-HCl, pH 8.0, 1 mM EDTA). The complexes of protein-DNA were separated from the beads by incubating at 65°C with 950 rpm shaking for 1 hour in 300 µL of lysis buffer (10 mM Tris-HCl, pH 8.0, 1% SDS, 10 mM EDTA, 1 mM PMSF, 1 mg/mL aprotinin, 5 mg/mL leupeptin, 1 mg/mL antipain, 1 mg/mL E-64, 1 mg/mL pepstatin, 50 mM MG-132, and 5 mg/mL chymostatin). The reverse crosslinking was performed by adding NaCl to a final concentration of 0.2 M and incubating at 65°C overnight with shaking at 950 rpm. DNA was purified using QIAquick Kit (QIAGEN) following the manufacturer's recommendations. The DNA was eluted in 200 µL of nuclease-free water. The qPCR was performed using 2 µL of ChIP DNA, 0.5 µL of 10 mM forward and reverse primers for each, 2 µL nuclease-free water, and 5 µL either Brilliant III Ultra-Fast SYBR Green qPCR Master Mix or TB Green™ Premix Ex Taq™ II Tli RNase H Plus on a 96-well CFX96 Touch Real-Time PCR detection system (Bio-Rad). At least two technical replicates were performed for each region and gene. *TA3* retrotransposon was used as a negative control. Relative enrichment was calculated using the $2^{-\Delta\Delta CT}$ method (Livak and Schmittgen, 2001). ChIP-qPCR values were normalized to 2% of input values. The primers used for ChIP-qPCR are detailed in Table III.

8. Western blot analyses

Approximately 100 mg of seedlings under LD conditions were sampled at ZT7 and ZT19 and ground in liquid nitrogen in a mortar, followed by resuspension in 100 µL of cold protein extraction buffer (6 M urea, 125 mM Tris-HCl pH 7.4, 2% SDS, 20% glycerol, 1% β-mercaptoethanol, 1% protease inhibitor cocktail). After centrifugation for 10 minutes at 13000 g at 4ºC, the supernatant was collected.

Protein concentration was quantified using standard curves with the Pierce BCA (bicinchoninic acid) protein assay kit following the manufacturer's recommendations. A total of 40 μg of protein was mixed with 4x SDS loading buffer (200 mM Tris-HCl, pH 6.8, 0.4% bromophenol blue, 8% SDS, 40% glycerol, 10% β-mercaptoethanol) and heated at 95°C for 10 minutes without shaking. For chromatin-related protein analysis, total proteins were separated using 15% SDS-PAGE gel. The 0.2 μm pore size Immobilon-P membrane was wetted by placing it on the surface of methanol for 15 seconds, without immersion. Then, the membrane was carefully placed in ultrapure water and soaked for 2 minutes. Subsequently, the membrane was placed in transfer buffer (48 mM Tris-HCl, pH 9, 39 mM glycine, 20% methanol, 10% SDS) and allowed to equilibrate for at least 5 minutes. Proteins were transferred from the gel to a fully prepared PVDF membrane using a semi-dry transfer system. The membrane was incubated with block solution (5% milk in TBST) for 1 hour at room temperature with shaking at 150 rpm. After three times washing with TBST with shaking at 150 rpm at room temperature, the membrane was incubated overnight with primary antibody at 4°C with 150 rpm shaking. The primary antibodies used in our studies included the anti-trimethyl-Histone H3 Lysine4 antibody at a 1:3000 dilution, the anti-trimethyl-Histone H3 Lysine27 antibody at a 1:3000 dilution, the anti-trimethyl-Histone H3 Lysine36 antibody at a 1:3000 dilution, and the anti-Histone H3 antibody at a 1:5000 dilution. After washing three times with TBST with shaking at 150 rpm in a cold room, the membrane was incubated with goat anti-rabbit IgG (H+L) HRP (1:10,000 dilution) secondary antibody for 1 hour at room temperature with shaking at 150 rpm.

For RNA Pol II S5P and S2P analyses, proteins were separated using 7% SDS-

PAGE gel. The 0.45 μm pore size Immobilon-P PVDF membrane was prepared, and proteins were transferred following the same procedure as described above in this section. The membrane was incubated with block solution (5% milk in TBST) for 1 hour at room temperature with shaking at 150 rpm. After three washes with shaking at 150 rpm at room temperature, the membrane was immunoblotted overnight with primary antibody at 4°C with 150 rpm shaking. The primary antibodies used for RNA Pol II analyses were the anti-RNA Pol II CTD repeat YSPTSPS (phospho S2) antibody at a 1:1000 dilution, the anti-RNA Pol II CTD repeat YSPTSPS (phospho S5) antibody at a 1:1000 dilution, and the monoclonal anti-α-Tubulin antibody at a 1:5000 dilution, which was used as a loading control. After washing with TBST buffer 3 to 5 times with shaking at 150 rpm in a cold room, the membrane was incubated with goat anti-mouse IgG (H+L) HRP (reference 31430, Invitrogen) (1:10,000 dilution) secondary antibody for 1 hour at room temperature with shaking 150 rpm. The signal was detected using the ImageQuant 800 chemiluminescence imaging system (Amersham™). The intensity of individual bands was quantified using Image J software. At least two biological replicates were performed per experiment.

9. DAPI staining and image acquisition

Ten-day-old Arabidopsis seedlings grown under LD conditions were fixed in 4% paraformaldehyde in PBS (131 mM NaCl, 7 mM Na2HPO4, 3 mM NaH2PO4) buffer and vacuumed for 3 hours. The fixed seedlings were treated with a solution containing 0.5% cellulose Onozuka R10 (Yakult), 0.25% macerozyme R10 (Duchefa), and 0.1% Triton X-100 for 90 minutes at 37ºC without shaking. Subsequently, the seedlings were incubated with PEMSB buffer (50 mM PIPES,

pH 7.3, 5 mM EGTA, pH 7.1, 5 mM $MgSO_4$, 0.05% saponin, 5% BSA) supplemented with 2 µg/mL of 4′,6′-diamidino-2-phenylindole (DAPI) (reference D9542, Sigma-Aldrich) at room temperature for 15 minutes without shaking. After three washes with PEMSB buffer at room temperature, the cotyledon cells were observed using the Zeiss 980 Elyra with an Airyscan microscope (excitation, 359 nm; emission, 457 nm) with a 63x oil objective to detect the DAPI signals.

10. Dot-blot analysis of N6-methyladenosine RNA modification

Approximately 20-25 seedlings grown under LD conditions were collected at ZT7 and immediately frozen in liquid nitrogen. The samples were ground with a TissueLyser II (Qiagen). Total RNA was extracted using the Maxwell® RSC Plant RNA Kit (Promega) following the manufacturer's recommendations. The RNA concentration was measured using a NanoDrop spectrophotometer (Thermo Fisher). Subsequently, a series of RNA dilutions were prepared by adding RNase-free water to achieve concentrations of 100 ng/µL, 50 ng/µL, 25 ng/µL, and 12.5 ng/µL. The dilutions were incubated at 95°C for 3 minutes and then immediately transferred to ice for 5 minutes to disrupt secondary structures. Immobilon®-P PVDF membranes were prepared following the same procedure as described above in the "*Dot-blot assay for R-loops analysis*" section. Two µL of denatured RNA dilutions were directly loaded onto the fully prepared membrane. Following UV crosslinking at 1,200 microjoules for 50 seconds, the membrane was washed with 10 mL of TBST buffer (150 mM NaCl, 20 mM Tris, pH 7.5, 0.1% Tween 20) for 5 minutes at room temperature, with gentle shaking to eliminate unbound RNA. The membrane was then incubated with blocking buffer (5% non-fat milk in TBST) for at least 1 hour at 4°C with 150 rpm shaking. After three washes with

TBST buffer at 4°C for 5 minutes each with shaking at 150 rpm, the membrane was incubated with the m^6A antibody (reference 202-003, Synaptic Systems) (1:2,000 dilution) overnight at 4°C with 150 rpm shaking. The primary antibody was removed, and the membrane was washed with TBST three times for 5 minutes each, at 4°C with shaking at 150 rpm. The membrane was then incubated with goat anti-rabbit IgG (H+L) HRP secondary antibody (diluted 1:10,000) for 1 hour at room temperature with shaking at 150 rpm. The signal was detected using the ImageQuant 800 chemiluminescence imaging system (Amersham™). The intensity of individual dots was quantified using Image J software. At least two biological replicates were performed per experiment. For methylene blue staining, following blocking, the membranes were incubated with a 0.02% methylene blue solution at room temperature for 5 minutes with gentle shaking at 150 rpm, then washed twice with TBST buffer before imaging.

11. Leaf emergence analyses

Sterilized seeds were sown directly on ½MS- plates, with or without 4 µM bleomycin. After 2-3 days of stratification in darkness at 4°C, the seeds were grown under LD conditions. Three weeks post-germination, the emergence of the first true leaves was monitored with an optical magnifying microscope paired with an Olympus digital camera DP71. Analyses were performed by calculating the percentage of seedlings with true leaves compared to the total number of seedlings for each condition.

Table I. *Arabidopsis thaliana* lines used in this study

Line	Ecotype	Reference
Wild-Type	Col-0	From NASC (N1093)
RNase H1A-ox G4	Col-0	This study
RNase H1A-ox B7	Col-0	This study
cca1-1/lhy-20	Col-0	(Nitschke et al., 2016)
CCA1-ox	Col-0	(Wang and Tobin, 1998)
YFP-ELF3-ox	Col-0	(Herrero et al., 2012)
elf3-2	Col-0	(Hicks et al., 2001)
prr579	Col-0	(Nakamichi et al., 2005)
lnk1lnk2	Col-0	(Rugnone et al., 2013)
cry2cry1	Col-0	(Mockler et al., 1999)
cry2-1	Col-0	(Lin et al., 1998)
phyB	Col-0	(Seo et al., 2006)
tfiis	Col-0	(Antosz et al., 2020)
ssrp1-2	Col-0	(Lolas et al., 2010)

Table II. List of the chemicals or reagents used in this study

Chemicals or reagents	Source	Product No.
Ethanol	Scharlab	ET00071000
Triton X-100	Sigma-Aldrich	T9284
Murashige and Skoog	Duchefa Biochemie	M0221
Sucrose	Duchefa Biochemie	S0809
Ficoll® PM 400	Sigma-Aldrich	F4375
Dextran	Sigma-Aldrich	D1662
HEPES	Sigma-Aldrich	H4034
$MgCl_2$	Sigma-Aldrich	M9272
Tris	Cytiva	GE17-1321-01
EDTA	Sigma-Aldrich	E5134
β-mercaptoethanol	Sigma-Aldrich	M3148
SDS	Sigma-Aldrich	L3771
Proteinase K	Roche	3115836001
KAc	Sigma-Aldrich	P1190
NaCl	Fisher	BP358
Phenol: Chloroform: Isoamyl Alcohol 25:24:1	Sigma-Aldrich	08168
Chloroform: isoamyl alcohol 24:1	Sigma-Aldrich	C0549
Isopropanol	Fisher Scientific	BP2618500
RNase H	New England Biolabs	M0297S
RNase H	Thermo Fisher	EN0201
Immobilon-P PVDF membrane 0.2 µm	Millipore	ISEQ00010
Immobilon-P PVDF membrane 0.45 µm	Millipore	IPVH00010
16% Formaldehyde	Thermo Fisher	28908
Glycine	Thermo Fisher	17-1323-01
Dynabeads® Protein G beads	Invitrogen	10004D
LiCl	Merck	1.05679
IGEPAL® CA-630	Sigma-Aldrich	I8896
Sodium deoxycholate	Sigma-Aldrich	D6750
Cellulase R10	Yakult	9012-54-8
Macerozyme R10	Duchefa	9023-75-1
PIPES	Carl Roth	9156
EGTA	Sigma-Aldrich	E3889

$MgSO_4$	Sigma-Aldrich	63138
Bovine Serum Albumin	Sigma-Aldrich	A3912
DAPI (4',6-diamidino-2-phenylindole)	Sigma-Aldrich	D9542
Methylene blue	Sigma-Aldrich	03978
Methanol	Scharlab	ME03021000
PMSF	Panreac Química	A0999
Leupeptin	Panreac Química	A2183
Aprotinin	Panreac Química	A2132
E-64	Panreac Química	A2157
Pepstatin	Panreac Química	PT318
Antipain	Sigma-Aldrich	10791
Chymostatin	Calbiochem	230790
MG-132	Calbiochem	133407-82-6
Urea	Supelco	PHR1406
Glycerol	Merck	A2926
Silwet L-77	Biogen Cientifica	P10233
Protease inhibitor cocktail	Sigma-Aldrich	P8340
Na_2HPO_4	Millipore	567547
NaH_2PO_4	Supelco	106346
Tween-20	Sigma-Aldrich	P1379
Miracloth	Millipore	475855
Bleomycin	Abcam	ab142977
Flavopiridol	Selleck Chemicals	S1230
pENTR/D-TOPO vector	Invitrogen	K240020
Gateway™ LR Clonase™ II Enzyme mix	Invitrogen	11791100
Brilliant III Ultra-Fast SYBR Green qPCR Master Mix	Agilent	600883
TB Green™ Premix Ex Taq™ II Tli RNase H Plus	TAKARA	RR82WR
QIAquick PCR & Gel Cleanup Kit	Qiagen	28506
Pierce™ BCA protein assay kit	Thermo Scientific	23227
Maxwell® RSC Plant RNA Kit	Promega	AS1500
QIAprep Spin Miniprep Kit	QIAGEN	27106
iScript™ Reverse Transcription Supermix	BioRad	1708841
PrimeScript RT Master Mix for RT-qPCR	TAKARA	RR036B
S9.6 antibody	Karefast	ENH001

S9.6 antibody	Abcam	ab234957
S9.6 antibody	Bio-Rad	MCA6391
Anti-dsDNA antibody	Abcam	ab27156
Anti-RNA Pol II CTD repeat YSPTSPS (phospho S2)	Abcam	ab5095
Anti-RNA Pol II CTD repeat YSPTSPS (phospho S5)	Abcam	ab5131
Anti-α-Tubulin antibody	Merck	T5168
Anti-trimethyl-Histone H3 (Lys4) Antibody	Millipore	04-745
Anti-trimethyl-Histone H3 (Lys27) antibody	Millipore	07-449
Anti-trimethyl-Histone H3 (Lys36) antibody	Abcam	ab282596
Anti-Histone H3 antibody	Abcam	ab1791
Goat anti-rabbit IgG (H+L) HRP	Invitrogen	31460
Goat anti-mouse IgG (H+L) HRP	Invitrogen	31430
m^6A antibody	Synaptic Systems	202-003

Table III. List of primers used in this study

Name		Sequence (5' --> 3')	Experiment
RNase H1A	Forward	CACCATGGGTTCCACAATGGAGGATG	Cloning
(AT3G01410)	Reverse	CTAGCCGCCTGAAATCACTTGC	Cloning
M13	Forward	GTAAAACGACGGCCAG	Sequencing
	Reverse	CAGGAAACAGCTATGAC	Sequencing
RNase H1A	Forward	AATGTGCACGTCTTAGGCGA	Gene expression
(AT3G01410)	Reverse	TAGCCTGTTTGCACAGCTCA	Gene expression
SSRP1	Forward	GGACAAGCTGGAGCGATCAT	Gene expression
(AT3G28730)	Reverse	CTTTGCACCAGACAGCCAAC	Gene expression
IPP2	Forward	CCAGGACAATGCACTAGGTGTG	Gene expression
(AT3G02780)	Reverse	AGGGAGTGAACTCATCGACTGG	Gene expression
AT2G07638	Forward	ATAGGGAGCTGGCAATGTCG	ChIP/DRIP-qPCR
	Reverse	CGGTTGGCTAAAGACATGGG	ChIP/DRIP-qPCR
AT2G07709	Forward	TTTGCGAATGAATGCTGGGC	ChIP/DRIP-qPCR
	Reverse	TCAGTCCCTCTAGTCGGGTG	ChIP/DRIP-qPCR
AT4G03965	Forward	GGGTCGGATCATGTAACGGG	ChIP/DRIP-qPCR
	Reverse	CCGTTTCCTCCGTTCGGTAA	ChIP/DRIP-qPCR
AT2G07787	Forward	AGACCTGGCCGATGTCTACT	ChIP/DRIP-qPCR
	Reverse	AAGGACCAGGTCGGGATAGG	ChIP/DRIP-qPCR
VSR3	Forward	CATGGACTCAGAGATCAGAGCC	ChIP/DRIP-qPCR
(AT2G14740)	Reverse	GGCGCGTTCATCATTCACG	ChIP/DRIP-qPCR
BEN1	Forward	GAGAGTGTTTTGCTTTGCCAC	ChIP/DRIP-qPCR
(AT3G43300)	Reverse	GGAGATAAGAGGTGCACTAGCC	ChIP/DRIP-qPCR
IPMS1	Forward	GCAGGAGCAACAACTCTCAAC	ChIP/DRIP-qPCR
(AT1G18500)	Reverse	ATCCCCGGAGTATTGGCCT	ChIP/DRIP-qPCR
TA3	Forward	CTGCGTGGAAGTCTGTCAAA	ChIP/DRIP-qPCR
(AT1G37110)	Reverse	CTATGCCACAGGGCAGTTTT	ChIP/DRIP-qPCR

Table IV. List of solutions or buffers used in this study

Solutions or Buffers	Chemicals	Concentration
Seed sterilization solution	Ethanol	75% (v/v)
	Triton X-100	0.1% (v/v)
Extraction buffer (For dot-blot analysis of R-loops and DRIP-qPCR)	Sucrose	0.44 M
	Ficoll	1.25%
	Dextran	2.5%
	HEPES-KOH, pH 7.4	20 mM
	Triton X-100	10 mM
	$MgCl_2$	0.5%
Washing buffer (For dot-blot analysis of R-loops and DRIP-qPCR)	Sucrose	0.25 M
	Tris-HCl, pH 8, 1	10 mM
	EDTA	1 mM
	MgCl2	10 mM
	Triton X-100	1% (v/v)
	β-mercaptoethanol	5 mM
Lysis buffer (For dot-blot analysis of R-loops and DRIP-qPCR)	Tris-HCl, pH 8, 1	10 mM
	EDTA	1 mM
	SDS	0.5% (v/v)
TBST buffer	Tris-HCl pH 7.5	20 mM
	NaCl	150 mM
	Tween 20	0.1% (v/v)
DRIP buffer	$NaPO_4$	100 mM
	NaCl	1.4 M
	Triton X-100	0.5% (v/v)
Elution buffer	Tris-HCl, pH 8	50 mM
	EDTA	10 mM
	SDS	0.5% (v/v)
	Proteinase K	0.1 mg/mL
PBS buffer	NaCl	131 mM
	Na2HPO4	7 mM
	NaH2PO4	3 mM

Extraction buffer I (For ChIP-qPCR)	Tris-HCl, pH 8.0	10 mM
	Sucrose	0.4 M
	EDTA	5 mM
	β-mercaptoethanol	5 mM
	PMSF	1 mM
	Leupeptin	5 mg/mL
	Aprotinin	1 mg/mL
	E-64	1 mg/mL
	Antipain	1 mg/mL
	Pepstatin	1 mg/mL
	Chymostatin	5 mg/mL
	MG-132	50 mM
Extraction buffer II (For ChIP-qPCR)	Tris-HCl, pH 8.0	10 mM
	Sucrose	0.25 M
	$MgCl_2$	10 mM
	Triton X-100	1%
	EDTA	5 mM
	β-mercaptoethanol	5 mM
	PMSF	1 mM
	Leupeptin	5 mg/mL
	Aprotinin	1 mg/mL
	E-64	1 mg/mL
	Antipain	1 mg/mL
	Pepstatin	1 mg/mL
	Chymostatin	5 mg/mL
	MG-132	50 mM
Lysis buffer (For ChIP-qPCR)	Tris-HCl, pH 8	10 mM
	EDTA	10 mM
	SDS	1% (v/v)
	PMSF	1 mM
	Leupeptin	5 mg/mL
	Aprotinin	1 mg/mL
	E-64	1 mg/mL
	Antipain	1 mg/mL

	Pepstatin	1 mg/mL
	Chymostatin	5 mg/mL
	MG-132	50 mM
ChIP dilution buffer	Tris-HCl, pH 8.0	15 mM
	NaCl	167 mM
	EDTA	1 mM
	Triton X-100	1.1%
	PMSF	1 mM
	Leupeptin	5 mg/mL
	Aprotinin	1 mg/mL
	E-64	1 mg/mL
	Antipain	1 mg/mL
	Pepstatin	1 mg/mL
	Chymostatin	5 mg/mL
	MG-132	50 mM
Low-salt buffer	Tris-HCl, pH 8.0	20 mM
	NaCl	150 mM
	TritonX-100	1%
	EDTA	2 mM
	SDS	0.1% (v/v)
	PMSF	1 mM
	Leupeptin	5 mg/mL
	Aprotinin	1 mg/mL
	E-64	1 mg/mL
	Antipain	1 mg/mL
	Pepstatin	1 mg/mL
	Chymostatin	5 mg/mL
	MG-132	50 mM
High-salt buffer	Tris-HCl, pH 8.0	20 mM
	NaCl	500 mM
	TritonX-100	1%
	EDTA	2 mM
	SDS	0.1% (v/v)
	PMSF	1 mM

	Leupeptin	5 mg/mL
	Aprotinin	1 mg/mL
	E-64	1 mg/mL
	Antipain	1 mg/mL
	Pepstatin	1 mg/mL
	Chymostatin	5 mg/mL
	MG-132	50 mM
LiCl buffer	Tris-HCl, pH 8.0	10 mM
	LiCl	250 mM
	IGEPAL® CA-630	1%
	EDTA	1 mM
	Sodium deoxycholate	1%
	PMSF	1 mM
	Leupeptin	5 mg/mL
	Aprotinin	1 mg/mL
	E-64	1 mg/mL
	Antipain	1 mg/mL
	Pepstatin	1 mg/mL
	Chymostatin	5 mg/mL
	MG-132	50 mM
TE buffer	Tris-HCl, pH 8.0	10 mM
	EDTA	1 mM
Protein extraction buffer	Urea	6 M
	Tris-HCl pH 7.4	125 mM
	SDS	2% (v/v)
	Glycerol	20%
	β-mercaptoethanol	1%
	Protease inhibitor cocktail	1%
4x SDS loading buffer	Tris-HCl, pH 6.8	200 mM
	SDS	8% (v/v)
	Bromophenol blue	0.4%
	Glycerol	40%
	β-mercaptoethanol	10%
Transfer buffer	Tris-HCl, pH 9	48 mM

	Glycine	39 mM
	Methanol	20 %
	SDS	10% (v/v)
PEMSB buffer	PIPES, pH 7.3	50 mM
	EGTA	5 mM
	$MgSO_4$	5 mM
	Saponin	0.05%
	BSA	5%

REFERENCES

Abakir, A., Giles, T.C., Cristini, A., Foster, J.M., Dai, N., Starczak, M., Rubio-Roldan, A., Li, M., Eleftheriou, M., Crutchley, J., Flatt, L., Young, L., Gaffney, D.J., Denning, C., Dalhus, B., Emes, R.D., Gackowski, D., Correa, I.R., Jr., Garcia-Perez, J.L., Klungland, A., Gromak, N., and Ruzov, A. (2020). N(6)-methyladenosine regulates the stability of RNA:DNA hybrids in human cells. Nat Genet **52,** 48-55.

Adelman, K., and Lis, J.T. (2012). Promoter-proximal pausing of RNA polymerase II: emerging roles in metazoans. Nat Rev Genet **13,** 720-731.

Ahmad, M., and Cashmore, A.R. (1993). HY4 gene of A. thaliana encodes a protein with characteristics of a blue-light photoreceptor. Nature **366,** 162-166.

Ahmad, M., Jarillo, J.A., Smirnova, O., and Cashmore, A.R. (1998). The CRY1 blue light photoreceptor of Arabidopsis interacts with phytochrome A in vitro. Molecular cell **1,** 939-948.

Akhtar, J., Lugoboni, M., and Junion, G. (2021). m(6)A RNA modification in transcription regulation. Transcription **12,** 266-276.

Akinori Matsushika, Seiya Makino, Kojima，, M., and Mizuno., T. (2000). Circadian Waves of Expression of the APRR1/TOC1 Family of PseudoResponse Regulators in Arabidopsis thaliana: Insight into the Plant Circadian Clock. Plant Cell Physiol **41,** 1002-1012.

Alabadí, D., Yanovsky, M.J., Más, P., Harmer, S.L., and Kay, S.A. (2002). Critical role for CCA1 and LHY in maintaining circadian rhythmicity in Arabidopsis. Current Biology **12,** 757-761.

Alabadí, D., Oyama, T., Yanovsky, M.J., Harmon, F.G., Más, P., and Kay, S.A. (2001). Reciprocal Regulation Between TOC1 and LHY/CCA1 Within the Arabidopsis Circadian Clock. Science **293,** 880-883.

Allen, T., Koustenis, A., Theodorou, G., Somers, D.E., Kay, S.A., Whitelam, G.C., and Devlin, P.F. (2006). Arabidopsis FHY3 specifically gates phytochrome signaling to the circadian clock. Plant Cell **18,** 2506-2516.

Allison, D.F., and Wang, G.G. (2019). R-loops: formation, function, and relevance to cell stress. Cell Stress **3,** 38-46.

Allison, L.A., Moyle, M., Shales, M., and Ingles, C.J. (1985). Extensive homology among the largest subunits of eukaryotic and prokaryotic RNA polymerases. Cell **42,** 599-610.

Amon, J.D., and Koshland, D. (2016). RNase H enables efficient repair of R-loop induced DNA damage. Elife **5**.

Antosch, M., Mortensen, S.A., and Grasser, K.D. (2012). Plant proteins containing high mobility group box DNA-binding domains modulate different nuclear processes. Plant Physiol **159,** 875-883.

Antosz, W., Deforges, J., Begcy, K., Bruckmann, A., Poirier, Y., Dresselhaus, T., and Grasser, K.D. (2020). Critical Role of Transcript Cleavage in Arabidopsis RNA Polymerase II Transcriptional Elongation. The Plant Cell **32,** 1449-1463.

Antosz, W., Pfab, A., Ehrnsberger, H.F., Holzinger, P., Kollen, K., Mortensen, S.A., Bruckmann, A., Schubert, T., Langst, G., Griesenbeck, J., Schubert, V., Grasser, M., and Grasser, K.D. (2017). The Composition of the Arabidopsis RNA Polymerase II Transcript Elongation Complex Reveals the Interplay between Elongation and mRNA Processing Factors. Plant Cell **29,** 854-870.

Ariel, F., Lucero, L., Christ, A., Mammarella, M.F., Jegu, T., Veluchamy, A., Mariappan, K., Latrasse, D., Blein, T., Liu, C., Benhamed, M., and Crespi, M. (2020). R-Loop Mediated trans Action of the APOLO Long Noncoding RNA. Mol Cell **77,** 1055-1065 e1054.

Aschoff, J. (1979). Circadian rhythms: influences of internal and external factors on the period measured in constant conditions 1. Zeitschrift für Tierpsychologie **49,** 225-249.

Aschoff, J. (1999). Masking and parametric effects of high-frequency light-dark cycles. The Japanese journal of physiology **49,** 11-18.

Atkins, K.A., and Dodd, A.N. (2014). Circadian regulation of chloroplasts. Current opinion in plant biology **21,** 43-50.

Aton, S.J., and Herzog, E.D. (2005). Come together, right… now: synchronization of rhythms in a mammalian circadian clock. Neuron **48,** 531-534.

Aukerman, M.J., Hirschfeld, M., Wester, L., Weaver, M., Clack, T., Amasino, R.M., and Sharrock, R.A. (1997). A deletion in the PHYD gene of the Arabidopsis Wassilewskija ecotype defines a role for phytochrome D in red/far-red light sensing. The Plant Cell **9,** 1317-1326.

Aymard, F., Bugler, B., Schmidt, C.K., Guillou, E., Caron, P., Briois, S., Iacovoni, J.S., Daburon, V., Miller, K.M., Jackson, S.P., and Legube, G. (2014). Transcriptionally active chromatin recruits homologous recombination at DNA double-strand breaks. Nat Struct Mol Biol **21,** 366-374.

Bagnall, D.J., King, R.W., and Hangarter, R.P. (1996). Blue-light promotion of flowering is absent in hy4 mutants of Arabidopsis. Planta **200,** 278-280.

Beaulé, C. (2009). Aschoff's Rules. In Encyclopedia of Neuroscience, M.D. Binder, N.

Hirokawa, and U. Windhorst, eds (Berlin, Heidelberg: Springer Berlin Heidelberg), pp. 190-193.

Belotserkovskaya, R., Saunders, A., Lis, J.T., and Reinberg, D. (2004). Transcription through chromatin: understanding a complex FACT. Biochimica Et Biophysica Acta (BBA)-Gene Structure and Expression **1677,** 87-99.

Belotserkovskaya, R., Oh, S., Bondarenko, V.A., Orphanides, G., Studitsky, V.M., and Reinberg, D. (2003). FACT facilitates transcription-dependent nucleosome alteration. Science **301,** 1090-1093.

Belotserkovskii, B.P., Tornaletti, S., D'Souza, A.D., and Hanawalt, P.C. (2018). R-loop generation during transcription: Formation, processing and cellular outcomes. DNA Repair (Amst) **71,** 69-81.

Berger, S.L. (2007). The complex language of chromatin regulation during transcription. Nature **447,** 407-412.

Bieniawska, Z., Espinoza, C., Schlereth, A., Sulpice, R., Hincha, D.K., and Hannah, M.A. (2008). Disruption of the Arabidopsis circadian clock is responsible for extensive variation in the cold-responsive transcriptome. Plant Physiol **147,** 263-279.

Bird, A. (2002). DNA methylation patterns and epigenetic memory. Genes & development **16,** 6-21.

Bognar, L.K., Hall, A., Adam, E., Thain, S.C., Nagy, F., and Millar, A.J. (1999). The circadian clock controls the expression pattern of the circadian input photoreceptor, phytochrome B. Proc Natl Acad Sci U S A **96,** 14652-14657.

Bong Kim, Alexey I. Nesvizhskii, P. Geetha Rani, Steven Hahn, Ruedi Aebersold, and Ranish, J.A. (2007). The transcription elongation factor TFIIS is a component of RNA polymerase II preinitiation complexes. PNAS **104,** 16068–16073.

Bou-Nader, C., Bothra, A., Garboczi, D.N., Leppla, S.H., and Zhang, J. (2022). Structural basis of R-loop recognition by the S9.6 monoclonal antibody. Nat Commun **13,** 1641.

Boule, J.B., and Zakian, V.A. (2007). The yeast Pif1p DNA helicase preferentially unwinds RNA DNA substrates. Nucleic Acids Res **35,** 5809-5818.

Boulias, K., and Greer, E.L. (2023). Biological roles of adenine methylation in RNA. Nat Rev Genet **24,** 143-160.

Boyko, A., Filkowski, J., and Kovalchuk, I. (2005). Homologous recombination in plants is temperature and day-length dependent. Mutat Res **572,** 73-83.

Brambati, A., Zardoni, L., Nardini, E., Pellicioli, A., and Liberi, G. (2020). The dark side of RNA:DNA hybrids. Mutat Res Rev Mutat Res **784,** 108300.

Brewster, N.K., Johnston, G.C., and Singer, R.A. (1998). Characterization of the CP complex, an abundant dimer of Cdc68 and Pob3 proteins that regulates yeast transcriptional activation and chromatin repression. Journal of Biological Chemistry **273,** 21972-21979.

Briggs, W.R., and Huala, E. (1999). Blue-light photoreceptors in higher plants. Annual review of cell and developmental biology **15,** 33-62.

Britt, A. (2002). Repair of damaged bases. The Arabidopsis Book/American Society of Plant Biologists **1**.

Brown, S.A., Zumbrunn, G., Fleury-Olela, F., Preitner, N., and Schibler, U. (2002). Rhythms of mammalian body temperature can sustain peripheral circadian clocks. Current biology **12,** 1574-1583.

Butler, W.L., Norris, K., Siegelman, H., and Hendricks, S. (1959). Detection, assay, and preliminary purification of the pigment controlling photoresponsive development of plants. Proceedings of the National Academy of Sciences **45,** 1703-1708.

Canal, B., Duch, A., Posas, F., and de Nadal, E. (2018). A novel mechanism for the prevention of transcription replication conflicts. Mol Cell Oncol **5,** e1451233.

Cao, S., Bendall, H., Hicks, G.G., Nashabi, A., Sakano, H., Shinkai, Y., Gariglio, M., Oltz, E.M., and Ruley, H.E. (2003). The high-mobility-group box protein SSRP1/T160 is essential for cell viability in day 3.5 mouse embryos. Mol Cell Biol **23,** 5301-5307.

Capovilla, G., Pajoro, A., Immink, R.G., and Schmid, M. (2015). Role of alternative pre-mRNA splicing in temperature signaling. Current opinion in plant biology **27,** 97-103.

Carr, I.A. (2001). Day-length perception and the photoperiodic regulation of flowering in Arabidopsis. Journal of Biological Rhythms **16,** 415-423.

Casati, P., Campi, M., Chu, F., Suzuki, N., Maltby, D., Guan, S., Burlingame, A.L., and Walbot, V. (2008). Histone acetylation and chromatin remodeling are required for UV-B-dependent transcriptional activation of regulated genes in maize. Plant Cell **20,** 827-842.

Ceriani, M.F., Darlington, T.K., Staknis, D., Más, P., Petti, A.A., Weitz, C.J., and Kay, S.A. (1999). Light-dependent sequestration of TIMELESS by CRYPTOCHROME. Science **285,** 553-556.

Cervela-Cardona, L., Alary, B., and Mas, P. (2021a). The Arabidopsis Circadian Clock

and Metabolic Energy: A Question of Time. Front Plant Sci **12,** 804468.

Cervela-Cardona, L., Yoshida, T., Zhang, Y., Okada, M., Fernie, A., and Mas, P. (2021b). Circadian Control of Metabolism by the Clock Component TOC1. Front Plant Sci **12,** 683516.

Chapman, R.D., Heidemann, M., Albert, T.K., Mailhammer, R., Flatley, A., Meisterernst, M., Kremmer, E., and Eick, D. (2007). Transcribing RNA polymerase II is phosphorylated at CTD residue serine-7. Science **318,** 1780-1782.

Chen, C., Zhang, Z., Cui, P., Liao, Y., Zhang, Y., Yao, L., Rui, R., and Ju, S. (2017a). Phosphorylation of histone H3 on Ser-10 by Aurora B is essential for chromosome condensation in porcine embryos during the first mitotic division. Histochemistry and Cell Biology **148,** 73-83.

Chen, L., Chen, J.Y., Zhang, X., Gu, Y., Xiao, R., Shao, C., Tang, P., Qian, H., Luo, D., Li, H., Zhou, Y., Zhang, D.E., and Fu, X.D. (2017b). R-ChIP Using Inactive RNase H Reveals Dynamic Coupling of R-loops with Transcriptional Pausing at Gene Promoters. Mol Cell **68,** 745-757 e745.

Chen, P.B., Chen, H.V., Acharya, D., Rando, O.J., and Fazzio, T.G. (2015). R loops regulate promoter-proximal chromatin architecture and cellular differentiation. Nat Struct Mol Biol **22,** 999-1007.

Chen, W.W., Takahashi, N., Hirata, Y., Ronald, J., Porco, S., Davis, S.J., Nusinow, D.A., Kay, S.A., and Mas, P. (2020). A mobile ELF4 delivers circadian temperature information from shoots to roots. Nature plants **6,** 416-426.

Cheng, L., Wang, W., Yao, Y., and Sun, Q. (2021). Mitochondrial RNase H1 activity regulates R-loop homeostasis to maintain genome integrity and enable early embryogenesis in Arabidopsis. PLoS Biol **19,** e3001357.

Chory, J. (1993). Out of darkness: mutants reveal pathways controlling light-regulated development in plants. Trends in Genetics **9,** 167-172.

Clapier, C.R., and Cairns, B.R. (2009). The biology of chromatin remodeling complexes. Annual review of biochemistry **78,** 273-304.

Cloix, C., Kaiserli, E., Heilmann, M., Baxter, K.J., Brown, B.A., O'Hara, A., Smith, B.O., Christie, J.M., and Jenkins, G.I. (2012). C-terminal region of the UV-B photoreceptor UVR8 initiates signaling through interaction with the COP1 protein. Proceedings of the National Academy of Sciences **109,** 16366-16370.

Clough, S.J., and Bent, A.F. (1998). Floral dip: a simplified method for Agrobacterium-mediated transformation of Arabidopsis thaliana. The plant journal **16,** 735-743.

Comas, M., Beersma, D.G., Hut, R.A., and Daan, S. (2008). Circadian phase resetting in response to light-dark and dark-light transitions. J Biol Rhythms **23,** 425-434.

Conn, V.M., Hugouvieux, V., Nayak, A., Conos, S.A., Capovilla, G., Cildir, G., Jourdain, A., Tergaonkar, V., Schmid, M., Zubieta, C., and Conn, S.J. (2017). A circRNA from SEPALLATA3 regulates splicing of its cognate mRNA through R-loop formation. Nat Plants **3,** 17053.

Corden, J.L., Cadena, D.L., Ahearn Jr, J.M., and Dahmus, M.E. (1985). A unique structure at the carboxyl terminus of the largest subunit of eukaryotic RNA polymerase II. Proceedings of the National Academy of Sciences **82,** 7934-7938.

Costantino, L., and Koshland, D. (2015). The Yin and Yang of R-loop biology. Current opinion in cell biology **34,** 39-45.

Covington, M.F., Maloof, J.N., Straume, M., Kay, S.A., and Harmer, S.L. (2008). Global transcriptome analysis reveals circadian regulation of key pathways in plant growth and development. Genome Biol **9,** R130.

Daniel, X., Sugano, S., and Tobin, E.M. (2004). CK2 phosphorylation of CCA1 is necessary for its circadian oscillator function in Arabidopsis. Proceedings of the National Academy of Sciences **101,** 3292-3297.

de Lucas, M., Daviere, J.M., Rodriguez-Falcon, M., Pontin, M., Iglesias-Pedraz, J.M., Lorrain, S., Fankhauser, C., Blazquez, M.A., Titarenko, E., and Prat, S. (2008). A molecular framework for light and gibberellin control of cell elongation. Nature **451,** 480-484.

de Montaigu, A., Toth, R., and Coupland, G. (2010). Plant development goes like clockwork. Trends Genet **26,** 296-306.

Devlin, P.F. (2002). Signs of the time: environmental input to the circadian clock. J Exp Bot **53,** 1535-1550.

Devlin, P.F., and Kay, S.A. (2000). Cryptochromes Are Required for Phytochrome Signaling to the Circadian Clock but Not for Rhythmicity. The Plant Cell **12,** 2499-2509.

Devlin, P.F., Patel, S.R., and Whitelam, G.C. (1998). Phytochrome E influences internode elongation and flowering time in Arabidopsis. The Plant Cell **10,** 1479-1487.

Devlin, P.F., Robson, P.R., Patel, S.R., Goosey, L., Sharrock, R.A., and Whitelam, G.C. (1999). Phytochrome D acts in the shade-avoidance syndrome in Arabidopsis by controlling elongation growth and flowering time. Plant physiology **119,** 909-916.

Ding, Y., Avramova, Z., and Fromm, M. (2011). Two distinct roles of ARABIDOPSIS

HOMOLOG OF TRITHORAX1 (ATX1) at promoters and within transcribed regions of ATX1-regulated genes. Plant Cell **23,** 350-363.

Dixon, L.E., Knox, K., Kozma-Bognar, L., Southern, M.M., Pokhilko, A., and Millar, A.J. (2011). Temporal repression of core circadian genes is mediated through EARLY FLOWERING 3 in Arabidopsis. Current Biology **21,** 120-125.

Dodd, A.N., Salathia, N., Hall, A., Kévei, E., Tóth, R., Nagy, F., Hibberd, J.M., Millar, A.J., and Webb, A.A.R. (2005). Plant Circadian Clocks Increase Photosynthesis, Growth, Survival, and Competitive Advantage. Science **309,** 630-633.

Donze, D., and Kamakaka, R.T. (2002). Braking the silence: how heterochromatic gene repression is stopped in its tracks. Bioessays **24,** 344-349.

Drury, G.E., Dowle, A.A., Ashford, D.A., Waterworth, W.M., Thomas, J., and West, C.E. (2012). Dynamics of plant histone modifications in response to DNA damage. Biochem J **445,** 393-401.

Dumelie, J.G., and Jaffrey, S.R. (2017). Defining the location of promoter-associated R-loops at near-nucleotide resolution using bisDRIP-seq. Elife **6**.

Duroux, M., Houben, A., Ruzicka, K., Friml, J., and Grasser, K.D. (2004). The chromatin remodelling complex FACT associates with actively transcribed regions of the Arabidopsis genome. Plant J **40,** 660-671.

Edgar, R.C. (2004). MUSCLE: multiple sequence alignment with high accuracy and high throughput. Nucleic Acids Res **32,** 1792-1797.

Egloff, S., and Murphy, S. (2008). Cracking the RNA polymerase II CTD code. Trends Genet **24,** 280-288.

Eichenberg, K., Bäurle, I., Paulo, N., Sharrock, R.A., Rüdiger, W., and Schäfer, E. (2000). Arabidopsis phytochromes C and E have different spectral characteristics from those of phytochromes A and B. Febs Letters **470,** 107-112.

El Hage, A., French, S.L., Beyer, A.L., and Tollervey, D. (2010). Loss of Topoisomerase I leads to R-loop-mediated transcriptional blocks during ribosomal RNA synthesis. Genes Dev **24,** 1546-1558.

Espinos, E., Le Van Thaï, A., Pomiès, C., and Weber, M.J. (1999). Cooperation between phosphorylation and acetylation processes in transcriptional control. Molecular and cellular biology.

Ezer, D., Jung, J.H., Lan, H., Biswas, S., Gregoire, L., Box, M.S., Charoensawan, V., Cortijo, S., Lai, X., Stockle, D., Zubieta, C., Jaeger, K.E., and Wigge, P.A. (2017). The

evening complex coordinates environmental and endogenous signals in Arabidopsis. Nat Plants **3,** 17087.

Fang, Y., Chen, L., Lin, K., Feng, Y., Zhang, P., Pan, X., Sanders, J., Wu, Y., Wang, X.-e., Su, Z., Chen, C., Wei, H., and Zhang, W. (2019). Characterization of functional relationships of R-loops with gene transcription and epigenetic modifications in rice. Genome Research **29,** 1287-1297.

Fankhauser, C., and Staiger, D. (2002). Photoreceptors in Arabidopsis thaliana: light perception, signal transduction and entrainment of the endogenous clock. Planta **216,** 1-16.

Farinas, B., and Mas, P. (2011). Functional implication of the MYB transcription factor RVE8/LCL5 in the circadian control of histone acetylation. Plant J **66,** 318-329.

Farré, E.M., Harmer, S.L., Harmon, F.G., Yanovsky, M.J., and Kay, S.A. (2005). Overlapping and distinct roles of PRR7 and PRR9 in the Arabidopsis circadian clock. Current Biology **15,** 47-54.

Faucher, D., and Wellinger, R.J. (2010). Methylated H3K4, a transcription-associated histone modification, is involved in the DNA damage response pathway. PLoS Genet **6**.

Feher, B., Kozma-Bognar, L., Kevei, E., Hajdu, A., Binkert, M., Davis, S.J., Schafer, E., Ulm, R., and Nagy, F. (2011). Functional interaction of the circadian clock and UV RESISTANCE LOCUS 8-controlled UV-B signaling pathways in Arabidopsis thaliana. Plant J **67,** 37-48.

Filichkin, S.A., Priest, H.D., Givan, S.A., Shen, R., Bryant, D.W., Fox, S.E., Wong, W.K., and Mockler, T.C. (2010). Genome-wide mapping of alternative splicing in Arabidopsis thaliana. Genome Res **20,** 45-58.

Fonouni-Farde, C., Christ, A., Blein, T., Legascue, M.F., Ferrero, L., Moison, M., Lucero, L., Ramirez-Prado, J.S., Latrasse, D., Gonzalez, D., Benhamed, M., Quadrana, L., Crespi, M., and Ariel, F. (2022). The Arabidopsis APOLO and human UPAT sequence-unrelated long noncoding RNAs can modulate DNA and histone methylation machineries in plants. Genome Biol **23,** 181.

Formosa, T. (2012). The role of FACT in making and breaking nucleosomes. Biochim Biophys Acta **1819,** 247-255.

Formosa, T., Eriksson, P., Wittmeyer, J., Ginn, J., Yu, Y., and Stillman, D.J. (2001). Spt16-Pob3 and the HMG protein Nhp6 combine to form the nucleosome-binding factor SPN. EMBO J **20,** 3506-3517.

Freytes, S.N., Gobbini, M.L., and Cerdan, P.D. (2024). The Plant Mediator Complex in

the Initiation of Transcription by RNA Polymerase II. Annu Rev Plant Biol.

Frost, J.M., Kim, M.Y., Park, G.T., Hsieh, P.H., Nakamura, M., Lin, S.J.H., Yoo, H., Choi, J., Ikeda, Y., Kinoshita, T., Choi, Y., Zilberman, D., and Fischer, R.L. (2018). FACT complex is required for DNA demethylation at heterochromatin during reproduction in Arabidopsis. Proc Natl Acad Sci U S A **115,** E4720-E4729.

Fuchs, J., Demidov, D., Houben, A., and Schubert, I. (2006). Chromosomal histone modification patterns--from conservation to diversity. Trends Plant Sci **11,** 199-208.

Fukushima, A., Kusano, M., Nakamichi, N., Kobayashi, M., Hayashi, N., Sakakibara, H., Mizuno, T., and Saito, K. (2009). Impact of clock-associated Arabidopsis pseudo-response regulators in metabolic coordination. Proceedings of the National Academy of Sciences **106,** 7251-7256.

Gaidamakov, S.A., Gorshkova, II, Schuck, P., Steinbach, P.J., Yamada, H., Crouch, R.J., and Cerritelli, S.M. (2005). Eukaryotic RNases H1 act processively by interactions through the duplex RNA-binding domain. Nucleic Acids Res **33,** 2166-2175.

Gan, W., Guan, Z., Liu, J., Gui, T., Shen, K., Manley, J.L., and Li, X. (2011). R-loop-mediated genomic instability is caused by impairment of replication fork progression. Genes Dev **25,** 2041-2056.

Gao, J., Zhang, P., Li, X., Wu, W., Wei, H., and Zhang, W. (2021). Toward an understanding of the detection and function of R-loops in plants. J Exp Bot **72,** 6110-6122.

Gao, Y., Li, C., Wei, L., Teng, Y., Nakajima, S., Chen, X., Xu, J., Leger, B., Ma, H., Spagnol, S.T., Wan, Y., Dahl, K.N., Liu, Y., Levine, A.S., and Lan, L. (2017). SSRP1 Cooperates with PARP and XRCC1 to Facilitate Single-Strand DNA Break Repair by Chromatin Priming. Cancer Res **77,** 2674-2685.

García-Muse, T., and Aguilera, A. (2016). Transcription–replication conflicts: how they occur and how they are resolved. Nature reviews Molecular cell biology **17,** 553-563.

Gendron, J.M., Pruneda-Paz, J.L., Doherty, C.J., Gross, A.M., Kang, S.E., and Kay, S.A. (2012). Arabidopsis circadian clock protein, TOC1, is a DNA-binding transcription factor. Proc Natl Acad Sci U S A **109,** 3167-3172.

Gerhart-Hines, Z., and Lazar, M.A. (2015). Circadian metabolism in the light of evolution. Endocr Rev **36,** 289-304.

Ginno, P.A., Lott, P.L., Christensen, H.C., Korf, I., and Chedin, F. (2012). R-loop formation is a distinctive characteristic of unmethylated human CpG island promoters. Mol Cell **45,** 814-825.

Ginno, P.A., Lim, Y.W., Lott, P.L., Korf, I., and Chedin, F. (2013). GC skew at the 5' and 3' ends of human genes links R-loop formation to epigenetic regulation and transcription termination. Genome Res **23,** 1590-1600.

Golden, S.S., and Canales, S.R. (2003). Cyanobacterial circadian clocks—timing is everything. Nature Reviews Microbiology **1,** 191-199.

Golubov, A., Yao, Y., Maheshwari, P., Bilichak, A., Boyko, A., Belzile, F., and Kovalchuk, I. (2010). Microsatellite instability in Arabidopsis increases with plant development. Plant Physiol **154,** 1415-1427.

Gonzalo, L., Tossolini, I., Gulanicz, T., Cambiagno, D.A., Kasprowicz-Maluski, A., Smolinski, D.J., Mammarella, M.F., Ariel, F.D., Marquardt, S., Szweykowska-Kulinska, Z., Jarmolowski, A., and Manavella, P.A. (2022). R-loops at microRNA encoding loci promote co-transcriptional processing of pri-miRNAs in plants. Nat Plants **8,** 402-418.

Goswami, I., Sandlesh, P., Stablewski, A., Toshkov, I., Safina, A.F., Magnitov, M., Wang, J., and Gurova, K. (2022). FACT maintains nucleosomes during transcription and stem cell viability in adult mice. EMBO Rep **23,** e53684.

Goto, N., Kumagai, T., and Koornneef, M. (1991). Flowering responses to light-breaks in photomorphogenic mutants of Arabidopsis thaliana, a long-day plant. Physiologia Plantarum **83,** 209-215.

Gould, P.D., Locke, J.C., Larue, C., Southern, M.M., Davis, S.J., Hanano, S., Moyle, R., Milich, R., Putterill, J., Millar, A.J., and Hall, A. (2006). The molecular basis of temperature compensation in the Arabidopsis circadian clock. Plant Cell **18,** 1177-1187.

Grasser, K.D. (2020). The FACT Histone Chaperone: Tuning Gene Transcription in the Chromatin Context to Modulate Plant Growth and Development. Front Plant Sci **11,** 85.

Grasser, M., and Grasser, K.D. (2018). The plant RNA polymerase II elongation complex: A hub coordinating transcript elongation and mRNA processing. Transcription **9,** 117-122.

Green, R., and Tobin, E. (1999). Loss of the circadian clock-associated protein 1 in Arabidopsis results in altered clock-regulated gene expression. Proceedings of the National Academy of Sciences **96,** 4176-4179.

Groh, M., and Gromak, N. (2014). Out of balance: R-loops in human disease. PLoS genetics **10,** e1004630.

Guo, H., Yang, H., Mockler, T.C., and Lin, C. (1998). Regulation of flowering time by Arabidopsis photoreceptors. Science **279,** 1360-1363.

Gurova, K., Chang, H.-W., Valieva, M.E., Sandlesh, P., and Studitsky, V.M. (2018). Structure and function of the histone chaperone FACT–Resolving FACTual issues. Biochimica et Biophysica Acta (BBA)-Gene Regulatory Mechanisms **1861,** 892-904.

Hamperl, S., Bocek, M.J., Saldivar, J.C., Swigut, T., and Cimprich, K.A. (2017). Transcription-Replication Conflict Orientation Modulates R-Loop Levels and Activates Distinct DNA Damage Responses. Cell **170,** 774-786 e719.

Harmer, S.L., and Kay, S.A. (2005). Positive and negative factors confer phase-specific circadian regulation of transcription in Arabidopsis. Plant Cell **17,** 1926-1940.

Hasanova, Z., Klapstova, V., Porrua, O., Stefl, R., and Sebesta, M. (2023). Human senataxin is a bona fide R-loop resolving enzyme and transcription termination factor. Nucleic Acids Res **51,** 2818-2837.

Hatchi, E., Skourti-Stathaki, K., Ventz, S., Pinello, L., Yen, A., Kamieniarz-Gdula, K., Dimitrov, S., Pathania, S., McKinney, K.M., Eaton, M.L., Kellis, M., Hill, S.J., Parmigiani, G., Proudfoot, N.J., and Livingston, D.M. (2015). BRCA1 recruitment to transcriptional pause sites is required for R-loop-driven DNA damage repair. Mol Cell **57,** 636-647.

Haussmann, I.U., Bodi, Z., Sanchez-Moran, E., Mongan, N.P., Archer, N., Fray, R.G., and Soller, M. (2016). m6A potentiates Sxl alternative pre-mRNA splicing for robust Drosophila sex determination. Nature **540,** 301-304.

Hayama, R., and Coupland, G. (2003). Shedding light on the circadian clock and the photoperiodic control of flowering. Curr Opin Plant Biol **6,** 13-19.

Hazen, S.P., Schultz, T.F., Pruneda-Paz, J.L., Borevitz, J.O., Ecker, J.R., and Kay, S.A. (2005). LUX ARRHYTHMO encodes a Myb domain protein essential for circadian rhythms. Proceedings of the National Academy of Sciences **102,** 10387-10392.

He, Y., Yu, Y., Wang, X., Qin, Y., Su, C., and Wang, L. (2022). Aschoff's rule on circadian rhythms orchestrated by blue light sensor CRY2 and clock component PRR9. Nat Commun **13,** 5869.

Hegazy, Y.A., Fernando, C.M., and Tran, E.J. (2020). The balancing act of R-loop biology: The good, the bad, and the ugly. J Biol Chem **295,** 905-913.

Heidemann, M., Hintermair, C., Voß, K., and Eick, D. (2013). Dynamic phosphorylation patterns of RNA polymerase II CTD during transcription. Biochimica et Biophysica Acta (BBA)-Gene Regulatory Mechanisms **1829,** 55-62.

Helfer, A., Nusinow, D.A., Chow, B.Y., Gehrke, A.R., Bulyk, M.L., and Kay, S.A. (2011). LUX ARRHYTHMO encodes a nighttime repressor of circadian gene expression

in the Arabidopsis core clock. Curr Biol **21,** 126-133.

Hemmes, H., Henriques, R., Jang, I.C., Kim, S., and Chua, N.H. (2012). Circadian clock regulates dynamic chromatin modifications associated with Arabidopsis CCA1/LHY and TOC1 transcriptional rhythms. Plant Cell Physiol **53,** 2016-2029.

Herrera-Moyano, E., Mergui, X., Garcia-Rubio, M.L., Barroso, S., and Aguilera, A. (2014). The yeast and human FACT chromatin-reorganizing complexes solve R-loop-mediated transcription-replication conflicts. Genes Dev **28,** 735-748.

Herrero, E., Kolmos, E., Bujdoso, N., Yuan, Y., Wang, M., Berns, M.C., Uhlworm, H., Coupland, G., Saini, R., Jaskolski, M., Webb, A., Goncalves, J., and Davis, S.J. (2012). EARLY FLOWERING4 recruitment of EARLY FLOWERING3 in the nucleus sustains the Arabidopsis circadian clock. Plant Cell **24,** 428-443.

Hetzel, J., Duttke, S.H., Benner, C., and Chory, J. (2016). Nascent RNA sequencing reveals distinct features in plant transcription. Proc Natl Acad Sci U S A **113,** 12316-12321.

Hicks, K.A., Albertson, T.M., and Wagner, D.R. (2001). EARLY FLOWERING3 encodes a novel protein that regulates circadian clock function and flowering in Arabidopsis. The Plant Cell **13,** 1281-1292.

Higashi, M., Inoue, S., and Ito, T. (2010). Core histone H2A ubiquitylation and transcriptional regulation. Experimental cell research **316,** 2707-2712.

Hirose, Y., and Manley, J.L. (2000). RNA polymerase II and the integration of nuclear events. Genes & development **14,** 1415-1429.

Hirschfeld, M., Tepperman, J.M., Clack, T., Quail, P.H., and Sharrock, R.A. (1998). Coordination of phytochrome levels in phyB mutants of Arabidopsis as revealed by apoprotein-specific monoclonal antibodies. Genetics **149,** 523-535.

Hobert, O. (2004). Common logic of transcription factor and microRNA action. Trends Biochem Sci **29,** 462-468.

Hondele, M., Stuwe, T., Hassler, M., Halbach, F., Bowman, A., Zhang, E.T., Nijmeijer, B., Kotthoff, C., Rybin, V., and Amlacher, S. (2013). Structural basis of histone H2A–H2B recognition by the essential chaperone FACT. Nature **499,** 111-114.

Hooper, C.M., Castleden, I.R., Tanz, S.K., Aryamanesh, N., and Millar, A.H. (2017). SUBA4: the interactive data analysis centre for Arabidopsis subcellular protein locations. Nucleic Acids Res **45,** D1064-D1074.

Hsieh, F.K., Kulaeva, O.I., Patel, S.S., Dyer, P.N., Luger, K., Reinberg, D., and Studitsky, V.M. (2013). Histone chaperone FACT action during transcription through

chromatin by RNA polymerase II. Proc Natl Acad Sci U S A **110,** 7654-7659.

Hsin, J.-P., and Manley, J.L. (2012). The RNA polymerase II CTD coordinates transcription and RNA processing. Genes & development **26,** 2119-2137.

Hsu, P.Y., and Harmer, S.L. (2014). Wheels within wheels: the plant circadian system. Trends Plant Sci **19,** 240-249.

Hu, W., Franklin, K.A., Sharrock, R.A., Jones, M.A., Harmer, S.L., and Lagarias, J.C. (2013). Unanticipated regulatory roles for Arabidopsis phytochromes revealed by null mutant analysis. Proc Natl Acad Sci U S A **110,** 1542-1547.

Huang, W., Pérez-García, P., Pokhilko, A., Millar, A.J., Antoshechkin, I., Riechmann, J.L., and Mas, P. (2012). Mapping the Core of the Arabidopsis Circadian Clock Defines the Network Structure of the Oscillator. Science **336,** 75-79.

Ikeda, Y., Kinoshita, Y., Susaki, D., Ikeda, Y., Iwano, M., Takayama, S., Higashiyama, T., Kakutani, T., and Kinoshita, T. (2011). HMG domain containing SSRP1 is required for DNA demethylation and genomic imprinting in Arabidopsis. Dev Cell **21,** 589-596.

Inoue, K., Araki, T., and Endo, M. (2017). Integration of Input Signals into the Gene Network in the Plant Circadian Clock. Plant and Cell Physiology **58,** 977-982.

Ishihara, S., Sasagawa, Y., Kameda, T., Yamashita, H., Umeda, M., Kotomura, N., Abe, M., Shimono, Y., and Nikaido, I. (2021). Local states of chromatin compaction at transcription start sites control transcription levels. Nucleic Acids Res **49,** 8007-8023.

Jamai, A., Puglisi, A., and Strubin, M. (2009). Histone chaperone spt16 promotes redeposition of the original h3-h4 histones evicted by elongating RNA polymerase. Mol Cell **35,** 377-383.

James, A.B., Syed, N.H., Brown, J.W., and Nimmo, H.G. (2012). Thermoplasticity in the plant circadian clock: how plants tell the time-perature. Plant Signal Behav **7,** 1219-1223.

Jansen, M.A., Gaba, V., and Greenberg, B.M. (1998). Higher plants and UV-B radiation: balancing damage, repair and acclimation. Trends in plant science **3,** 131-135.

Jeronimo, C., Poitras, C., and Robert, F. (2019). Histone Recycling by FACT and Spt6 during Transcription Prevents the Scrambling of Histone Modifications. Cell Rep **28,** 1206-1218 e1208.

Ji, Q., Zong, X., Mao, Y., and Qian, S.B. (2021). A heat shock-responsive lncRNA Heat acts as a HSF1-directed transcriptional brake via m(6)A modification. Proc Natl Acad Sci U S A **118**.

Jia, G., Fu, Y., Zhao, X., Dai, Q., Zheng, G., Yang, Y., Yi, C., Lindahl, T., Pan, T., Yang, Y.G., and He, C. (2011). N6-methyladenosine in nuclear RNA is a major substrate of the obesity-associated FTO. Nat Chem Biol **7,** 885-887.

Jiang, L., Wang, Y., Bjorn, L.O., and Li, S. (2011). UV-B-induced DNA damage mediates expression changes of cell cycle regulatory genes in Arabidopsis root tips. Planta **233,** 831-841.

Johansson, M., and Staiger, D. (2015). Time to flower: interplay between photoperiod and the circadian clock. Journal of experimental botany **66,** 719-730.

Johnson, C.H. (1992). Phase response curves: what can they tell us about circadian clocks. Circadian clocks from cell to human**,** 209-249.

Johnson, E., Bradley, M., Harberd, N.P., and Whitelam, G.C. (1994). Photoresponses of light-grown phyA mutants of Arabidopsis (phytochrome A is required for the perception of daylength extensions). Plant physiology **105,** 141-149.

Jones, M.A., Hu, W., Litthauer, S., Lagarias, J.C., and Harmer, S.L. (2015). A Constitutively Active Allele of Phytochrome B Maintains Circadian Robustness in the Absence of Light. Plant Physiol **169,** 814-825.

Jung, J.-H., Domijan, M., Klose, C., Biswas, S., Ezer, D., Gao, M., Khattak, A.K., Box, M.S., Charoensawan, V., and Cortijo, S. (2016). Phytochromes function as thermosensors in Arabidopsis. Science **354,** 886-889.

Jung, J.H., Barbosa, A.D., Hutin, S., Kumita, J.R., Gao, M., Derwort, D., Silva, C.S., Lai, X., Pierre, E., Geng, F., Kim, S.B., Baek, S., Zubieta, C., Jaeger, K.E., and Wigge, P.A. (2020). A prion-like domain in ELF3 functions as a thermosensor in Arabidopsis. Nature **585,** 256-260.

Kadumuri, R.V., and Janga, S.C. (2018). Epitranscriptomic Code and Its Alterations in Human Disease. Trends Mol Med **24,** 886-903.

Kang, H.J., Cheon, N.Y., Park, H., Jeong, G.W., Ye, B.J., Yoo, E.J., Lee, J.H., Hur, J.H., Lee, E.A., Kim, H., Lee, K.Y., Choi, S.Y., Lee-Kwon, W., Myung, K., Lee, J.Y., and Kwon, H.M. (2021). TonEBP recognizes R-loops and initiates m6A RNA methylation for R-loop resolution. Nucleic Acids Res **49,** 269-284.

Kemble, D.J., McCullough, L.L., Whitby, F.G., Formosa, T., and Hill, C.P. (2015). FACT Disrupts Nucleosome Structure by Binding H2A-H2B with Conserved Peptide Motifs. Mol Cell **60,** 294-306.

Kidokoro, S., Shinozaki, K., and Yamaguchi-Shinozaki, K. (2022). Transcriptional regulatory network of plant cold-stress responses. Trends in Plant Science.

Kierzek, E., and Kierzek, R. (2003). The thermodynamic stability of RNA duplexes and hairpins containing N6-alkyladenosines and 2-methylthio-N6-alkyladenosines. Nucleic Acids Res **31,** 4472-4480.

Kim, J.A., Kim, H.S., Choi, S.H., Jang, J.Y., Jeong, M.J., and Lee, S.I. (2017). The Importance of the Circadian Clock in Regulating Plant Metabolism. Int J Mol Sci **18**.

King, D.P., Zhao, Y., Sangoram, A.M., Wilsbacher, L.D., Tanaka, M., Antoch, M.P., Steeves, T.D., Vitaterna, M.H., Kornhauser, J.M., and Lowrey, P.L. (1997). Positional cloning of the mouse circadian clock gene. Cell **89,** 641-653.

Kinmonth-Schultz, H.A., Golembeski, G.S., and Imaizumi, T. (2013). Circadian clock-regulated physiological outputs: dynamic responses in nature. Semin Cell Dev Biol **24,** 407-413.

Komarnitsky, P., Cho, E.J., and Buratowski, S. (2000). Different phosphorylated forms of RNA polymerase II and associated mRNA processing factors during transcription. Genes Dev **14,** 2452-2460.

Konig, F., Schubert, T., and Langst, G. (2017). The monoclonal S9.6 antibody exhibits highly variable binding affinities towards different R-loop sequences. PLoS One **12,** e0178875.

Konopka, R.J., and Benzer, S. (1971). Clock mutants of Drosophila melanogaster. Proceedings of the National Academy of Sciences **68,** 2112-2116.

Koornneef, M., Alonso-Blanco, C., Peeters, A.J., and Soppe, W. (1998). Genetic control of flowering time in Arabidopsis. Annual review of plant biology **49,** 345-370.

Kornberg, R.D., and Lorch, Y. (2002). Chromatin and transcription: where do we go from here? Current opinion in genetics & development **12,** 249-251.

Krohn, N.M., Stemmer, C., Fojan, P., Grimm, R., and Grasser, K.D. (2003). Protein kinase CK2 phosphorylates the high mobility group domain protein SSRP1, inducing the recognition of UV-damaged DNA. J Biol Chem **278,** 12710-12715.

Kucinski, J., Chamera, S., Kmera, A., Rowley, M.J., Fujii, S., Khurana, P., Nowotny, M., and Wierzbicki, A.T. (2020). Evolutionary History and Activity of RNase H1-Like Proteins in Arabidopsis thaliana. Plant Cell Physiol **61,** 1107-1119.

Kumar, V., and Sharma, A. (2018). Common features of circadian timekeeping in diverse organisms. Current Opinion in Physiology **5,** 58-67.

Kuno, N., Møller, S.G., Shinomura, T., Xu, X., Chua, N.-H., and Furuya, M. (2003). The novel MYB protein EARLY-PHYTOCHROME-RESPONSIVE1 is a component of a

slave circadian oscillator in Arabidopsis. The Plant Cell **15,** 2476-2488.

Kuzminov, A. (2018). When DNA topology turns deadly–RNA polymerases dig in their R-loops to stand their ground: new positive and negative (super) twists in the replication–transcription conflict. Trends in Genetics **34,** 111-120.

Kwon, Y.-J., Park, M.-J., Kim, S.-G., Baldwin, I.T., and Park, C.-M. (2014). Alternative splicing and nonsense-mediated decay of circadian clock genes under environmental stress conditions in Arabidopsis. BMC Plant Biol **14,** 1-15.

Lau, On S., Huang, X., Charron, J.-B., Lee, J.-H., Li, G., and Deng, Xing W. (2011). Interaction of Arabidopsis DET1 with CCA1 and LHY in Mediating Transcriptional Repression in the Plant Circadian Clock. Molecular Cell **43,** 703-712.

Lee, D.Y., Teyssier, C., Strahl, B.D., and Stallcup, M.R. (2005). Role of protein methylation in regulation of transcription. Endocrine reviews **26,** 147-170.

Legris, M., Klose, C., Burgie, E.S., Rojas, C.C.R., Neme, M., Hiltbrunner, A., Wigge, P.A., Schäfer, E., Vierstra, R.D., and Casal, J.J. (2016). Phytochrome B integrates light and temperature signals in Arabidopsis. Science **354,** 897-900.

Li, B., Carey, M., and Workman, J.L. (2007a). The role of chromatin during transcription. Cell **128,** 707-719.

Li, G., Siddiqui, H., Teng, Y., Lin, R., Wan, X.Y., Li, J., Lau, O.S., Ouyang, X., Dai, M., Wan, J., Devlin, P.F., Deng, X.W., and Wang, H. (2011). Coordinated transcriptional regulation underlying the circadian clock in Arabidopsis. Nat Cell Biol **13,** 616-622.

Li, J., Xing, X., Zhang, X., Liang, B., He, Z., Gao, C., Wang, S., Wang, F., Zhang, H., Zeng, S., Fan, J., Chen, L., Zhang, Z., Zhang, B., Liu, C., Wang, Q., Lin, W., Dong, G., Tang, H., Chen, W., Xiao, Y., and Li, D. (2018). Enhanced H3K4me3 modifications are involved in the transactivation of DNA damage responsive genes in workers exposed to low-level benzene. Environ Pollut **234,** 127-135.

Li, Y., Zeng, S.X., Landais, I., and Lu, H. (2007b). Human SSRP1 Has Spt16-dependent and -independent Roles in Gene Transcription. Journal of Biological Chemistry **282,** 6936-6945.

Li, Y., Ding, L., Zhou, M., Chen, Z., Ding, Y., and Zhu, C. (2023). Transcriptional Regulatory Network of Plant Cadmium Stress Response. International Journal of Molecular Sciences **24,** 4378.

Lichota, J., and Grasser, K.D. (2001). Differential chromatin association and nucleosome binding of the maize HMGA, HMGB, and SSRP1 proteins. Biochemistry **40,** 7860-7867.

Lima, W.F., Murray, H.M., Damle, S.S., Hart, C.E., Hung, G., De Hoyos, C.L., Liang, X.H., and Crooke, S.T. (2016). Viable RNaseH1 knockout mice show RNaseH1 is essential for R loop processing, mitochondrial and liver function. Nucleic Acids Res **44,** 5299-5312.

Lin, C., Ahmad, M., and Cashmore, A.R. (1996). Arabidopsis cryptochrome 1 is a soluble protein mediating blue light-dependent regulation of plant growth and development. Plant J **10,** 893-902.

Lin, C., Yang, H., Guo, H., Mockler, T., Chen, J., and Cashmore, A.R. (1998). Enhancement of blue-light sensitivity of Arabidopsis seedlings by a blue light receptor cryptochrome 2. Proceedings of the National Academy of Sciences **95,** 2686-2690.

Liu, H., Wang, Q., Liu, Y., Zhao, X., Imaizumi, T., Somers, D.E., Tobin, E.M., and Lin, C. (2013). Arabidopsis CRY2 and ZTL mediate blue-light regulation of the transcription factor CIB1 by distinct mechanisms. Proc Natl Acad Sci U S A **110,** 17582-17587.

Liu, J., Dou, X., Chen, C., Chen, C., Liu, C., Xu, M.M., Zhao, S., Shen, B., Gao, Y., and Han, D. (2020a). N 6-methyladenosine of chromosome-associated regulatory RNA regulates chromatin state and transcription. Science **367,** 580-586.

Liu, W., Sun, L., Zhong, M., Zhou, Q., Gong, Z., Li, P., Tai, P., and Li, X. (2012). Cadmium-induced DNA damage and mutations in Arabidopsis plantlet shoots identified by DNA fingerprinting. Chemosphere **89,** 1048-1055.

Liu, X., Gao, Y., Liao, J., Miao, M., Chen, K., Xi, F., Wei, W., Wang, H., Wang, Y., Xu, X., Reddy, A.S.N., and Gu, L. (2021). Genome-wide profiling of circular RNAs, alternative splicing, and R-loops in stem-differentiating xylem of Populus trichocarpa. J Integr Plant Biol **63,** 1294-1308.

Liu, Y., Ma, M., Li, G., Yuan, L., Xie, Y., Wei, H., Ma, X., Li, Q., Devlin, P.F., Xu, X., and Wang, H. (2020b). Transcription Factors FHY3 and FAR1 Regulate Light-Induced CIRCADIAN CLOCK ASSOCIATED1 Gene Expression in Arabidopsis. Plant Cell **32,** 1464-1478.

Livak, K.J., and Schmittgen, T.D. (2001). Analysis of relative gene expression data using real-time quantitative PCR and the $2^{-\Delta\Delta CT}$ method. methods **25,** 402-408.

Lolas, I.B., Himanen, K., Gronlund, J.T., Lynggaard, C., Houben, A., Melzer, M., Van Lijsebettens, M., and Grasser, K.D. (2010). The transcript elongation factor FACT affects Arabidopsis vegetative and reproductive development and genetically interacts with HUB1/2. Plant J **61,** 686-697.

Lu, S.X., Knowles, S.M., Andronis, C., Ong, M.S., and Tobin, E.M. (2009). CIRCADIAN CLOCK ASSOCIATED1 and LATE ELONGATED HYPOCOTYL function synergistically in the circadian clock of Arabidopsis. Plant Physiol **150,** 834-843.

Lu, S.X., Webb, C.J., Knowles, S.M., Kim, S.H., Wang, Z., and Tobin, E.M. (2012). CCA1 and ELF3 Interact in the control of hypocotyl length and flowering time in Arabidopsis. Plant Physiol **158,** 1079-1088.

Lu, W.T., Hawley, B.R., Skalka, G.L., Baldock, R.A., Smith, E.M., Bader, A.S., Malewicz, M., Watts, F.Z., Wilczynska, A., and Bushell, M. (2018). Drosha drives the formation of DNA:RNA hybrids around DNA break sites to facilitate DNA repair. Nat Commun **9,** 532.

Luo, M. (2018). Chemical and biochemical perspectives of protein lysine methylation. Chemical reviews **118,** 6656-6705.

Ma, D., Li, X., Guo, Y., Chu, J., Fang, S., Yan, C., Noel, J.P., and Liu, H. (2016). Cryptochrome 1 interacts with PIF4 to regulate high temperature-mediated hypocotyl elongation in response to blue light. Proc Natl Acad Sci U S A **113,** 224-229.

Ma, Y., Gil, S., Grasser, K.D., and Mas, P. (2018). Targeted Recruitment of the Basal Transcriptional Machinery by LNK Clock Components Controls the Circadian Rhythms of Nascent RNAs in Arabidopsis. The Plant Cell **30,** 907-924.

Malapeira, J., Khaitova, L.C., and Mas, P. (2012). Ordered changes in histone modifications at the core of the Arabidopsis circadian clock. Proc Natl Acad Sci U S A **109,** 21540-21545.

Manzo, S.G., Hartono, S.R., Sanz, L.A., Marinello, J., De Biasi, S., Cossarizza, A., Capranico, G., and Chedin, F. (2018). DNA Topoisomerase I differentially modulates R-loops across the human genome. Genome Biol **19,** 100.

Mao, Z., He, S., Xu, F., Wei, X., Jiang, L., Liu, Y., Wang, W., Li, T., Xu, P., Du, S., Li, L., Lian, H., Guo, T., and Yang, H.Q. (2020). Photoexcited CRY1 and phyB interact directly with ARF6 and ARF8 to regulate their DNA-binding activity and auxin-induced hypocotyl elongation in Arabidopsis. New Phytol **225,** 848-865.

Mas, P., Paul F. Devlin, Panda, S., and Kay, S.A. (2000). Functional interaction of phytochrome B and cryptochrome 2. Nature **408,** 207-211.

Más, P. (2005). Circadian clock signaling in Arabidopsis thaliana: from gene expression to physiology and development. Int J Dev Biol **49,** 491-500.

Más, P., Alabadi, D., Yanovsky, M.J., Oyama, T., and Kay, S.A. (2003). Dual role of TOC1 in the control of circadian and photomorphogenic responses in Arabidopsis. Plant

Cell **15,** 223-236.

Mason, P.B., and Struhl, K. (2003). The FACT complex travels with elongating RNA polymerase II and is important for the fidelity of transcriptional initiation in vivo. Mol Cell Biol **23,** 8323-8333.

Masse, E., Phoenix, P., and Drolet, M. (1997). DNA topoisomerases regulate R-loop formation during transcription of the rrnB operon in Escherichia coli. J Biol Chem **272,** 12816-12823.

Mayer, A., Heidemann, M., Lidschreiber, M., Schreieck, A., Sun, M., Hintermair, C., Kremmer, E., Eick, D., and Cramer, P. (2012). CTD tyrosine phosphorylation impairs termination factor recruitment to RNA polymerase II. Science **336,** 1723-1725.

McClung, C.R. (2014). Wheels within wheels: new transcriptional feedback loops in the Arabidopsis circadian clock. F1000prime reports **6**.

McCullough, L.L., Connell, Z., Xin, H., Studitsky, V.M., Feofanov, A.V., Valieva, M.E., and Formosa, T. (2018). Functional roles of the DNA-binding HMGB domain in the histone chaperone FACT in nucleosome reorganization. J Biol Chem **293,** 6121-6133.

Meyer, K.D., and Jaffrey, S.R. (2017). Rethinking m6A readers, writers, and erasers. Annual review of cell and developmental biology **33,** 319-342.

Michl-Holzinger, P., Mortensen, S.A., and Grasser, K.D. (2019). The SSRP1 subunit of the histone chaperone FACT is required for seed dormancy in Arabidopsis. J Plant Physiol **236,** 105-108.

Michl-Holzinger, P., Obermeyer, S., Markusch, H., Pfab, A., Ettner, A., Bruckmann, A., Babl, S., Langst, G., Schwartz, U., Tvardovskiy, A., Jensen, O.N., Osakabe, A., Berger, F., and Grasser, K.D. (2022). Phosphorylation of the FACT histone chaperone subunit SPT16 affects chromatin at RNA polymerase II transcriptional start sites in Arabidopsis. Nucleic Acids Res **50,** 5014-5028.

Millar, A.J., Straume, M., Chory, J., Chua, N.H., and Kay, S.A. (1995). The regulation of circadian period by phototransduction pathways in Arabidopsis. Science **267,** 1163-1166.

Miller, K.M., and Jackson, S.P. (2012). Histone marks: repairing DNA breaks within the context of chromatin. Biochem Soc Trans **40,** 370-376.

Milman, G., Langridge, R., and Chamberlin, M. (1967). The structure of a DNA-RNA hybrid. Proceedings of the National Academy of Sciences **57,** 1804-1810.

Mizoguchi, T., Wheatley, K., Hanzawa, Y., Wright, L., Mizoguchi, M., Song, H.-R.,

Carré, I.A., and Coupland, G. (2002). LHY and CCA1 are partially redundant genes required to maintain circadian rhythms in Arabidopsis. Developmental cell **2,** 629-641.

Mo, W., Zhang, J., Zhang, L., Yang, Z., Yang, L., Yao, N., Xiao, Y., Li, T., Li, Y., Zhang, G., Bian, M., Du, X., and Zuo, Z. (2022). Arabidopsis cryptochrome 2 forms photobodies with TCP22 under blue light and regulates the circadian clock. Nat Commun **13,** 2631.

Mockler, T.C., Guo, H., Yang, H., Duong, H., and Lin, C. (1999). Antagonistic actions of Arabidopsis cryptochromes and phytochrome B in the regulation of floral induction. Development **126,** 2073-2082.

Moison, M., Pacheco, J.M., Lucero, L., Fonouni-Farde, C., Rodríguez-Melo, J., Mansilla, N., Christ, A., Bazin, J., Benhamed, M., Ibañez, F., Crespi, M., Estevez, J.M., and Ariel, F. (2021). The lncRNA APOLO interacts with the transcription factor WRKY42 to trigger root hair cell expansion in response to cold. Molecular Plant **14,** 937-948.

Mozley, D., and Thomas, B. (1995). Developmental and photobiological factors affecting photoperiodic induction in Arabidopsis thaliana Heynh. Landsberg erecta. Journal of Experimental Botany **46,** 173-179.

Mwimba, M., Karapetyan, S., Liu, L., Marques, J., McGinnis, E.M., Buchler, N.E., and Dong, X. (2018). Daily humidity oscillation regulates the circadian clock to influence plant physiology. Nat Commun **9,** 4290.

Myers, C.N., Berner, G.B., Holthoff, J.H., Martinez-Fonts, K., Harper, J.A., Alford, S., Taylor, M.N., and Duina, A.A. (2011). Mutant versions of the S. cerevisiae transcription elongation factor Spt16 define regions of Spt16 that functionally interact with histone H3. PLoS One **6,** e20847.

Nagel, D.H., Doherty, C.J., Pruneda-Paz, J.L., Schmitz, R.J., Ecker, J.R., and Kay, S.A. (2015). Genome-wide identification of CCA1 targets uncovers an expanded clock network in Arabidopsis. Proceedings of the National Academy of Sciences **112,** E4802-E4810.

Nakagawa, T., Suzuki, T., Murata, S., Nakamura, S., Hino, T., Maeo, K., Tabata, R., Kawai, T., Tanaka, K., Niwa, Y., Watanabe, Y., Nakamura, K., Kimura, T., and Ishiguro, S. (2007). Improved Gateway binary vectors: high-performance vectors for creation of fusion constructs in transgenic analysis of plants. Biosci Biotechnol Biochem **71,** 2095-2100.

Nakamichi, N., Kita, M., Ito, S., Yamashino, T., and Mizuno, T. (2005). PSEUDO-RESPONSE REGULATORS, PRR9, PRR7 and PRR5, together play essential roles close to the circadian clock of Arabidopsis thaliana. Plant Cell Physiol **46,** 686-698.

Nakamichi, N., Kiba, T., Henriques, R., Mizuno, T., Chua, N.H., and Sakakibara, H. (2010). PSEUDO-RESPONSE REGULATORS 9, 7, and 5 are transcriptional repressors in the Arabidopsis circadian clock. Plant Cell **22,** 594-605.

Neff, M.M., and Chory, J. (1998). Genetic interactions between phytochrome A, phytochrome B, and cryptochrome 1 during Arabidopsis development. Plant physiology **118,** 27-35.

Niehrs, C., and Luke, B. (2020). Regulatory R-loops as facilitators of gene expression and genome stability. Nat Rev Mol Cell Biol **21,** 167-178.

Nielsen, M., Ard, R., Leng, X., Ivanov, M., Kindgren, P., Pelechano, V., and Marquardt, S. (2019). Transcription-driven chromatin repression of Intragenic transcription start sites. PLoS Genet **15,** e1007969.

Nikolov, D., and Burley, S. (1997). RNA polymerase II transcription initiation: a structural view. Proceedings of the National Academy of Sciences **94,** 15-22.

Nisa, M.U., Huang, Y., Benhamed, M., and Raynaud, C. (2019). The Plant DNA Damage Response: Signaling Pathways Leading to Growth Inhibition and Putative Role in Response to Stress Conditions. Front Plant Sci **10,** 653.

Nitschke, S., Cortleven, A., Iven, T., Feussner, I., Havaux, M., Riefler, M., and Schmulling, T. (2016). Circadian Stress Regimes Affect the Circadian Clock and Cause Jasmonic Acid-Dependent Cell Death in Cytokinin-Deficient Arabidopsis Plants. Plant Cell **28,** 1616-1639.

Nowotny, M., Cerritelli, S.M., Ghirlando, R., Gaidamakov, S.A., Crouch, R.J., and Yang, W. (2008). Specific recognition of RNA/DNA hybrid and enhancement of human RNase H1 activity by HBD. EMBO J **27,** 1172-1181.

Nusinow, D.A., Helfer, A., Hamilton, E.E., King, J.J., Imaizumi, T., Schultz, T.F., Farré, E.M., and Kay, S.A. (2011a). The ELF4–ELF3–LUX complex links the circadian clock to diurnal control of hypocotyl growth. Nature **475,** 398-402.

Nusinow, D.A., Helfer, A., Hamilton, E.E., King, J.J., Imaizumi, T., Schultz, T.F., Farre, E.M., and Kay, S.A. (2011b). The ELF4-ELF3-LUX complex links the circadian clock to diurnal control of hypocotyl growth. Nature **475,** 398-402.

Oakenfull, R.J., and Davis, S.J. (2017). Shining a light on the Arabidopsis circadian clock. Plant Cell Environ **40,** 2571-2585.

Obermeyer, S., Schrettenbrunner, L., Stockl, R., Schwartz, U., and Grasser, K.D. (2023). Different elongation factors distinctly modulate RNA polymerase II transcription in Arabidopsis. Nucleic Acids Res.

Ohama, N., Sato, H., Shinozaki, K., and Yamaguchi-Shinozaki, K. (2017). Transcriptional regulatory network of plant heat stress response. Trends in plant science **22,** 53-65.

Ohkuma, Y., and Roeder, R.G. (1994). Regulation of TFIIH ATPase and kinase activities by TFIIE during active initiation complex formation. Nature **368,** 160-163.

Orphanides, G., Lagrange, T., and Reinberg, D. (1996). The general transcription factors of RNA polymerase II. Genes & development **10,** 2657-2683.

Orphanides, G., LeRoy, G., Chang, C.-H., Luse, D.S., and Reinberg, D. (1998). FACT, a factor that facilitates transcript elongation through nucleosomes. Cell **92,** 105-116.

Orphanides, G., Wu, W.-H., Lane, W.S., Hampsey, M., and Reinberg, D. (1999). The chromatin-specific transcription elongation factor FACT comprises human SPT16 and SSRP1 proteins. Nature **400,** 284-288.

Oztas, O., Selby, C.P., Sancar, A., and Adebali, O. (2018). Genome-wide excision repair in Arabidopsis is coupled to transcription and reflects circadian gene expression patterns. Nat Commun **9,** 1503.

Park, M.J., Seo, P.J., and Park, C.M. (2012). CCA1 alternative splicing as a way of linking the circadian clock to temperature response in Arabidopsis. Plant Signal Behav **7,** 1194-1196.

Patel, P.S., Abraham, K.J., Guturi, K.K.N., Halaby, M.J., Khan, Z., Palomero, L., Ho, B., Duan, S., St-Germain, J., Algouneh, A., Mateo, F., El Ghamrasni, S., Barbour, H., Barnes, D.R., Beesley, J., Sanchez, O., Berman, H.K., Brown, G.W., Affar, E.B., Chenevix-Trench, G., Antoniou, A.C., Arrowsmith, C.H., Raught, B., Pujana, M.A., Mekhail, K., Hakem, A., and Hakem, R. (2021). RNF168 regulates R-loop resolution and genomic stability in BRCA1/2-deficient tumors. J Clin Invest **131**.

Pena, P.V., Hom, R.A., Hung, T., Lin, H., Kuo, A.J., Wong, R.P., Subach, O.M., Champagne, K.S., Zhao, R., Verkhusha, V.V., Li, G., Gozani, O., and Kutateladze, T.G. (2008). Histone H3K4me3 binding is required for the DNA repair and apoptotic activities of ING1 tumor suppressor. J Mol Biol **380,** 303-312.

Perales, M., and Mas, P. (2007). A functional link between rhythmic changes in chromatin structure and the Arabidopsis biological clock. Plant Cell **19,** 2111-2123.

Pfab, A., Breindl, M., and Grasser, K.D. (2018a). The Arabidopsis histone chaperone FACT is required for stress-induced expression of anthocyanin biosynthetic genes. Plant Mol Biol **96,** 367-374.

Pfab, A., Grønlund, J.T., Holzinger, P., Längst, G., and Grasser, K.D. (2018b). The

Arabidopsis Histone Chaperone FACT: Role of the HMG-Box Domain of SSRP1. Journal of Molecular Biology **430,** 2747-2759.

Pfister, S.X., Ahrabi, S., Zalmas, L.P., Sarkar, S., Aymard, F., Bachrati, C.Z., Helleday, T., Legube, G., La Thangue, N.B., Porter, A.C., and Humphrey, T.C. (2014). SETD2-dependent histone H3K36 trimethylation is required for homologous recombination repair and genome stability. Cell Rep **7,** 2006-2018.

Pittendrigh, C.S. (1960). Circadian rhythms and the circadian organization of living systems. In Cold Spring Harbor symposia on quantitative biology (Cold Spring Harbor Laboratory Press), pp. 159-184.

Poli, J., Gerhold, C.B., Tosi, A., Hustedt, N., Seeber, A., Sack, R., Herzog, F., Pasero, P., Shimada, K., Hopfner, K.P., and Gasser, S.M. (2016). Mec1, INO80, and the PAF1 complex cooperate to limit transcription replication conflicts through RNAPII removal during replication stress. Genes Dev **30,** 337-354.

Portoles, S., and Mas, P. (2010). The functional interplay between protein kinase CK2 and CCA1 transcriptional activity is essential for clock temperature compensation in Arabidopsis. PLoS Genet **6,** e1001201.

Powell, W.T., Coulson, R.L., Gonzales, M.L., Crary, F.K., Wong, S.S., Adams, S., Ach, R.A., Tsang, P., Yamada, N.A., Yasui, D.H., Chedin, F., and LaSalle, J.M. (2013). R-loop formation at Snord116 mediates topotecan inhibition of Ube3a-antisense and allele-specific chromatin decondensation. Proc Natl Acad Sci U S A **110,** 13938-13943.

Promonet, A., Padioleau, I., Liu, Y., Sanz, L., Biernacka, A., Schmitz, A.L., Skrzypczak, M., Sarrazin, A., Mettling, C., Rowicka, M., Ginalski, K., Chedin, F., Chen, C.L., Lin, Y.L., and Pasero, P. (2020). Topoisomerase 1 prevents replication stress at R-loop-enriched transcription termination sites. Nat Commun **11,** 3940.

Proudfoot, N.J. (2016). Transcriptional termination in mammals: Stopping the RNA polymerase II juggernaut. Science **352,** aad9926.

Putterill, J., Robson, F., Lee, K., Simon, R., and Coupland, G. (1995). The CONSTANS gene of Arabidopsis promotes flowering and encodes a protein showing similarities to zinc finger transcription factors. cell **80,** 847-857.

Quail, P.H. (1991). Phytochrome: a light-activated molecular switch that regulates plant gene expression. Annual review of genetics **25,** 389-409.

Rawat, R., Takahashi, N., Hsu, P.Y., Jones, M.A., Schwartz, J., Salemi, M.R., Phinney, B.S., and Harmer, S.L. (2011). REVEILLE8 and PSEUDO-REPONSE REGULATOR5 form a negative feedback loop within the Arabidopsis circadian clock. PLoS Genet **7,**

e1001350.

Rawat, R., Schwartz, J., Jones, M.A., Sairanen, I., Cheng, Y., Andersson, C.R., Zhao, Y., Ljung, K., and Harmer, S.L. (2009). REVEILLE1, a Myb-like transcription factor, integrates the circadian clock and auxin pathways. Proceedings of the national academy of sciences **106,** 16883-16888.

Reed, J.W., Nagpal, P., Poole, D.S., Furuya, M., and Chory, J. (1993). Mutations in the gene for the red/far-red light receptor phytochrome B alter cell elongation and physiological responses throughout Arabidopsis development. The Plant Cell **5,** 147-157.

Reinberg, D., and Sims, R.J., 3rd. (2006). de FACTo nucleosome dynamics. J Biol Chem **281,** 23297-23301.

Rijo-Ferreira, F., and Takahashi, J.S. (2019). Genomics of circadian rhythms in health and disease. Genome Med **11,** 82.

Rinaldi, C., Pizzul, P., Longhese, M.P., and Bonetti, D. (2020). Sensing R-Loop-Associated DNA Damage to Safeguard Genome Stability. Front Cell Dev Biol **8,** 618157.

Robert, F., and Jeronimo, C. (2023). Transcription-coupled nucleosome assembly. Trends Biochem Sci **48,** 978-992.

Robson, F., Costa, M.M., Hepworth, S.R., Vizir, I., Pineiro, M., Reeves, P.H., Putterill, J., and Coupland, G. (2001). Functional importance of conserved domains in the flowering-time gene CONSTANS demonstrated by analysis of mutant alleles and transgenic plants. Plant J **28,** 619-631.

Roeder, R.G. (1991). The complexities of eukaryotic transcription initiation: regulation of preinitiation complex assembly. Trends in biochemical sciences **16,** 402-408.

Roenneberg, T., and Foster, R.G. (1997). Twilight times: light and the circadian system. Photochemistry and photobiology **66,** 549-561.

Roenneberg, T., Hut, R., Daan, S., and Merrow, M. (2010). Entrainment concepts revisited. Journal of Biological Rhythms **25,** 329-339.

Rosa, S., Duncan, S., and Dean, C. (2016). Mutually exclusive sense-antisense transcription at FLC facilitates environmentally induced gene repression. Nat Commun **7,** 13031.

Roy, D., and Lieber, M.R. (2009). G clustering is important for the initiation of transcription-induced R-loops in vitro, whereas high G density without clustering is sufficient thereafter. Mol Cell Biol **29,** 3124-3133.

Rugnone, M.L., Faigon Soverna, A., Sanchez, S.E., Schlaen, R.G., Hernando, C.E.,

Seymour, D.K., Mancini, E., Chernomoretz, A., Weigel, D., Mas, P., and Yanovsky, M.J. (2013). LNK genes integrate light and clock signaling networks at the core of the Arabidopsis oscillator. Proc Natl Acad Sci U S A **110,** 12120-12125.

Saini, R., Jaskolski, M., and Davis, S.J. (2019). Circadian oscillator proteins across the kingdoms of life: structural aspects. BMC Biol **17,** 13.

Sakuraba, Y., Jeong, J., Kang, M.Y., Kim, J., Paek, N.C., and Choi, G. (2014). Phytochrome-interacting transcription factors PIF4 and PIF5 induce leaf senescence in Arabidopsis. Nat Commun **5,** 4636.

Salome, P.A., Weigel, D., and McClung, C.R. (2010). The role of the Arabidopsis morning loop components CCA1, LHY, PRR7, and PRR9 in temperature compensation. Plant Cell **22,** 3650-3661.

Santos-Pereira, J.M., and Aguilera, A. (2015). R loops: new modulators of genome dynamics and function. Nat Rev Genet **16,** 583-597.

Sanz, L.A., Hartono, S.R., Lim, Y.W., Steyaert, S., Rajpurkar, A., Ginno, P.A., Xu, X., and Chedin, F. (2016). Prevalent, Dynamic, and Conserved R-Loop Structures Associate with Specific Epigenomic Signatures in Mammals. Mol Cell **63,** 167-178.

Saunders, A., Werner, J., Andrulis, E.D., Nakayama, T., Hirose, S., Reinberg, D., and Lis, J.T. (2003). Tracking FACT and the RNA polymerase II elongation complex through chromatin in vivo. Science **301,** 1094-1096.

Schaffer, R., Ramsay, N., Samach, A., Corden, S., Putterill, J., Carré, I.A., and Coupland, G. (1998). The late elongated hypocotyl mutation of Arabidopsis disrupts circadian rhythms and the photoperiodic control of flowering. Cell **93,** 1219-1229.

Seo, M., Hanada, A., Kuwahara, A., Endo, A., Okamoto, M., Yamauchi, Y., North, H., Marion-Poll, A., Sun, T.P., Koshiba, T., Kamiya, Y., Yamaguchi, S., and Nambara, E. (2006). Regulation of hormone metabolism in Arabidopsis seeds: phytochrome regulation of abscisic acid metabolism and abscisic acid regulation of gibberellin metabolism. Plant J **48,** 354-366.

Seo, P.J., and Mas, P. (2014). Multiple layers of posttranslational regulation refine circadian clock activity in Arabidopsis. Plant Cell **26,** 79-87.

Seo, P.J., Park, M.J., Lim, M.H., Kim, S.G., Lee, M., Baldwin, I.T., and Park, C.M. (2012). A self-regulatory circuit of CIRCADIAN CLOCK-ASSOCIATED1 underlies the circadian clock regulation of temperature responses in Arabidopsis. Plant Cell **24,** 2427-2442.

Shafiq, S., Chen, C., Yang, J., Cheng, L., Ma, F., Widemann, E., and Sun, Q. (2017).

DNA Topoisomerase 1 Prevents R-loop Accumulation to Modulate Auxin-Regulated Root Development in Rice. Mol Plant **10,** 821-833.

Shang, X., Cao, Y., and Ma, L. (2017). Alternative Splicing in Plant Genes: A Means of Regulating the Environmental Fitness of Plants. Int J Mol Sci **18**.

Sharrock, R.A., and Clack, T. (2002). Patterns of expression and normalized levels of the five Arabidopsis phytochromes. Plant Physiol **130,** 442-456.

Shen, L., Liang, Z., and Yu, H. (2017a). Dot Blot Analysis of N(6)-methyladenosine RNA Modification Levels. Bio Protoc **7,** e2095.

Shen, W., Sun, H., De Hoyos, C.L., Bailey, J.K., Liang, X.H., and Crooke, S.T. (2017b). Dynamic nucleoplasmic and nucleolar localization of mammalian RNase H1 in response to RNAP I transcriptional R-loops. Nucleic Acids Res **45,** 10672-10692.

Shiio, Y., and Eisenman, R.N. (2003). Histone sumoylation is associated with transcriptional repression. Proceedings of the National Academy of Sciences **100,** 13225-13230.

Shilatifard, A. (2006). Chromatin modifications by methylation and ubiquitination: implications in the regulation of gene expression. Annu. Rev. Biochem. **75,** 243-269.

Shimasaki, N.B., and Kane, C.M. (2000). Structural basis for the species-specific activity of TFIIS. J Biol Chem **275,** 36541-36549.

Shor, E., Paik, I., Kangisser, S., Green, R., and Huq, E. (2017). PHYTOCHROME INTERACTING FACTORS mediate metabolic control of the circadian system in Arabidopsis. New Phytol **215,** 217-228.

Sims, R.J., 3rd, Belotserkovskaya, R., and Reinberg, D. (2004). Elongation by RNA polymerase II: the short and long of it. Genes Dev **18,** 2437-2468.

Skourti-Stathaki, K., Kamieniarz-Gdula, K., and Proudfoot, N.J. (2014). R-loops induce repressive chromatin marks over mammalian gene terminators. Nature **516,** 436-439.

Sogaard, T.M., and Svejstrup, J.Q. (2007). Hyperphosphorylation of the C-terminal repeat domain of RNA polymerase II facilitates dissociation of its complex with mediator. J Biol Chem **282,** 14113-14120.

Sollier, J., and Cimprich, K.A. (2015). Breaking bad: R-loops and genome integrity. Trends in cell biology **25,** 514-522.

Sollier, J., Stork, C.T., Garcia-Rubio, M.L., Paulsen, R.D., Aguilera, A., and Cimprich, K.A. (2014). Transcription-coupled nucleotide excision repair factors promote

R-loop-induced genome instability. Mol Cell **56,** 777-785.

Somers, D.E., Devlin, P.F., and Kay, S.A. (1998). Phytochromes and Cryptochromes in the Entrainment of the Arabidopsis Circadian Clock. Science **282,** 1488-1490.

Song, H.R., and Noh, Y.S. (2012). Rhythmic oscillation of histone acetylation and methylation at the Arabidopsis central clock loci. Mol Cells **34,** 279-287.

Spampinato, C.P. (2017). Protecting DNA from errors and damage: an overview of DNA repair mechanisms in plants compared to mammals. Cell Mol Life Sci **74,** 1693-1709.

Stasevich, T.J., Hayashi-Takanaka, Y., Sato, Y., Maehara, K., Ohkawa, Y., Sakata-Sogawa, K., Tokunaga, M., Nagase, T., Nozaki, N., and McNally, J.G. (2014). Regulation of RNA polymerase II activation by histone acetylation in single living cells. Nature **516,** 272-275.

Sterner, D.E., and Berger, S.L. (2000). Acetylation of histones and transcription-related factors. Microbiology and molecular biology reviews **64,** 435-459.

Strayer, C., Oyama, T., Schultz, T.F., Raman, R., Somers, D.E., Más, P., Panda, S., Kreps, J.A., and Kay, S.A. (2000). Cloning of the Arabidopsis Clock Gene *TOC1*, an Autoregulatory Response Regulator Homolog. Science **289,** 768-771.

Struhl, K. (1987). Promoters, activator proteins, and the mechanism of transcriptional initiation in yeast. Cell **49,** 295-297.

Struhl, K. (1998). Histone acetylation and transcriptional regulatory mechanisms. Genes & development **12,** 599-606.

Suarez-Lopez, P., Wheatley, K., Robson, F., Onouchi, H., Valverde, F., and Coupland, G. (2001). CONSTANS mediates between the circadian clock and the control of flowering in Arabidopsis. Nature **410,** 1116-1120.

Suárez-López, P., Wheatley, K., Robson, F., Onouchi, H., Valverde, F., and Coupland, G. (2001). CONSTANS mediates between the circadian clock and the control of flowering in Arabidopsis. Nature **410,** 1116-1120.

Sugano, S., Andronis, C., Green, R.M., Wang, Z.-Y., and Tobin, E.M. (1998). Protein kinase CK2 interacts with and phosphorylates the Arabidopsis circadian clock-associated 1 protein. Proceedings of the National Academy of Sciences **95,** 11020-11025.

Sun, F.-L., and Elgin, S.C. (1999). Putting boundaries on silence. Cell **99,** 459-462.

Sun, H., Li, K., Liu, C., and Yi, C. (2023). Regulation and functions of non-m6A mRNA modifications. Nature Reviews Molecular Cell Biology **24,** 714-731.

Sun, Q., Tibor Csorba, Konstantina Skourti-Stathaki, Nicholas J. Proudfoot, and Dean, C. (2013). R-Loop Stabilization Represses Antisense Transcription at the Arabidopsis FLC Locu. Science **340,** 619-621.

Sun, Z., Zhang, Y., Jia, J., Fang, Y., Tang, Y., Wu, H., and Fang, D. (2020). H3K36me3, message from chromatin to DNA damage repair. Cell Biosci **10,** 9.

Takahashi, N., Hirata, Y., Aihara, K., and Mas, P. (2015). A Hierarchical Multi-oscillator Network Orchestrates the Arabidopsis Circadian System. Cell **163**.

Takeuchi, T., Newton, L., Burkhardt, A., Mason, S., and Farre, E.M. (2014). Light and the circadian clock mediate time-specific changes in sensitivity to UV-B stress under light/dark cycles. J Exp Bot **65,** 6003-6012.

Tan-Wong, S.M., Dhir, S., and Proudfoot, N.J. (2019). R-Loops Promote Antisense Transcription across the Mammalian Genome. Mol Cell **76,** 600-616 e606.

Thines, B., and Harmon, F.G. (2010). Ambient temperature response establishes ELF3 as a required component of the core Arabidopsis circadian clock. Proc Natl Acad Sci U S A **107,** 3257-3262.

Thines, B., and Harmon, F.G. (2011). Four easy pieces: mechanisms underlying circadian regulation of growth and development. Curr Opin Plant Biol **14,** 31-37.

Thomas, M.C., and Chiang, C.-M. (2006). The general transcription machinery and general cofactors. Critical reviews in biochemistry and molecular biology **41,** 105-178.

Tian, Y.Y., Li, W., Wang, M.J., Li, J.Y., Davis, S.J., and Liu, J.X. (2022). REVEILLE 7 inhibits the expression of the circadian clock gene EARLY FLOWERING 4 to fine-tune hypocotyl growth in response to warm temperatures. Journal of Integrative Plant Biology **64,** 1310-1324.

Tripathi, A.K., Singh, K., Pareek, A., and Singla-Pareek, S.L. (2015). Histone chaperones in Arabidopsis and rice: genome-wide identification, phylogeny, architecture and transcriptional regulation. BMC Plant Biol **15,** 42.

Valieva, M.E., Armeev, G.A., Kudryashova, K.S., Gerasimova, N.S., Shaytan, A.K., Kulaeva, O.I., McCullough, L.L., Formosa, T., Georgiev, P.G., Kirpichnikov, M.P., Studitsky, V.M., and Feofanov, A.V. (2016). Large-scale ATP-independent nucleosome unfolding by a histone chaperone. Nat Struct Mol Biol **23,** 1111-1116.

Valverde, F., Mouradov, A., Soppe, W., Ravenscroft, D., Samach, A., and Coupland, G. (2004). Photoreceptor regulation of CONSTANS protein in photoperiodic flowering. Science **303,** 1003-1006.

Van Lijsebettens, M., and Grasser, K.D. (2014). Transcript elongation factors: shaping transcriptomes after transcript initiation. Trends Plant Sci **19,** 717-726.

van Zanten, M., Tessadori, F., McLoughlin, F., Smith, R., Millenaar, F.F., van Driel, R., Voesenek, L.A., Peeters, A.J., and Fransz, P. (2010). Photoreceptors CRYTOCHROME2 and phytochrome B control chromatin compaction in Arabidopsis. Plant Physiol **154,** 1686-1696.

Vitaterna, M.H., Takahashi, J.S., and Turek, F.W. (2001). Overview of circadian rhythms. Alcohol research & health **25,** 85.

Waese, J., Fan, J., Pasha, A., Yu, H., Fucile, G., Shi, R., Cumming, M., Kelley, L.A., Sternberg, M.J., Krishnakumar, V., Ferlanti, E., Miller, J., Town, C., Stuerzlinger, W., and Provart, N.J. (2017). ePlant: Visualizing and Exploring Multiple Levels of Data for Hypothesis Generation in Plant Biology. Plant Cell **29,** 1806-1821.

Wagner, D., Tepperman, J.M., and Quail, P.H. (1991). Overexpression of phytochrome B induces a short hypocotyl phenotype in transgenic Arabidopsis. The Plant Cell **3,** 1275-1288.

Wahba, L., Gore, S.K., and Koshland, D. (2013). The homologous recombination machinery modulates the formation of RNA-DNA hybrids and associated chromosome instability. Elife **2,** e00505.

Wahba, L., Amon, J.D., Koshland, D., and Vuica-Ross, M. (2011). RNase H and multiple RNA biogenesis factors cooperate to prevent RNA:DNA hybrids from generating genome instability. Mol Cell **44,** 978-988.

Wahba, L., Costantino, L., Tan, F.J., Zimmer, A., Koshland, D.J.G., and development. (2016). S1-DRIP-seq identifies high expression and polyA tracts as major contributors to R-loop formation **30,** 1327-1338.

Wang, H., Ma, L.-G., Li, J.-M., Zhao, H.-Y., and Deng, X.W. (2001). Direct interaction of Arabidopsis cryptochromes with COP1 in light control development. Science **294,** 154-158.

Wang, L., Kim, J., and Somers, D.E. (2013). Transcriptional corepressor TOPLESS complexes with pseudoresponse regulator proteins and histone deacetylases to regulate circadian transcription. Proc Natl Acad Sci U S A **110,** 761-766.

Wang, T., Liu, Y., Edwards, G., Krzizike, D., Scherman, H., and Luger, K. (2018). The histone chaperone FACT modulates nucleosome structure by tethering its components. Life Sci Alliance **1,** e201800107.

Wang, W., Li, K., Yang, Z., Hou, Q., Zhao, W.W., and Sun, Q. (2021a). RNase H1C

collaborates with ssDNA binding proteins WHY1/3 and recombinase RecA1 to fulfill the DNA damage repair in Arabidopsis chloroplasts. Nucleic Acids Research **49,** 6771-6787.

Wang, X., Jiang, B., Gu, L., Chen, Y., Mora, M., Zhu, M., Noory, E., Wang, Q., and Lin, C. (2021b). A photoregulatory mechanism of the circadian clock in Arabidopsis. Nat Plants **7,** 1397-1408.

Wang, X., Zhao, B.S., Roundtree, I.A., Lu, Z., Han, D., Ma, H., Weng, X., Chen, K., Shi, H., and He, C. (2015). N(6)-methyladenosine Modulates Messenger RNA Translation Efficiency. Cell **161,** 1388-1399.

Wang, X., Lu, Z., Gomez, A., Hon, G.C., Yue, Y., Han, D., Fu, Y., Parisien, M., Dai, Q., Jia, G., Ren, B., Pan, T., and He, C. (2014). N6-methyladenosine-dependent regulation of messenger RNA stability. Nature **505,** 117-120.

Wang, Y., Wu, J.F., Nakamichi, N., Sakakibara, H., Nam, H.G., and Wu, S.H. (2011). LIGHT-REGULATED WD1 and PSEUDO-RESPONSE REGULATOR9 form a positive feedback regulatory loop in the Arabidopsis circadian clock. Plant Cell **23,** 486-498.

Wang, Z.-Y., and Tobin, E.M. (1998). Constitutive expression of the CIRCADIAN CLOCK ASSOCIATED 1 (CCA1) gene disrupts circadian rhythms and suppresses its own expression. Cell **93,** 1207-1217.

Wang, Z., and Tobin., E.M. (1998). Constitutive Expression of the *CIRCADIAN CLOCK ASSOCIATED 1 (CCA1*) Gene Disrupts Circadian Rhythms and Suppresses Its Own Expression. Cell **93,** 1207–1217.

Waterworth, W.M., Drury, G.E., Bray, C.M., and West, C.E. (2011). Repairing breaks in the plant genome: the importance of keeping it together. New Phytologist **192,** 805-822.

Wei, J., and He, C. (2021). Chromatin and transcriptional regulation by reversible RNA methylation. Curr Opin Cell Biol **70,** 109-115.

Whitelam, G.C., Johnson, E., Peng, J., Carol, P., Anderson, M.L., Cowl, J.S., and Harberd, N.P. (1993). Phytochrome A null mutants of Arabidopsis display a wild-type phenotype in white light. The Plant Cell **5,** 757-768.

Winkler, D.D., Muthurajan, U.M., Hieb, A.R., and Luger, K. (2011). Histone chaperone FACT coordinates nucleosome interaction through multiple synergistic binding events. J Biol Chem **286,** 41883-41892.

Wu, J.F., Tsai, H.L., Joanito, I., Wu, Y.C., Chang, C.W., Li, Y.H., Wang, Y., Hong, J.C., Chu, J.W., Hsu, C.P., and Wu, S.H. (2016). LWD-TCP complex activates the morning gene CCA1 in Arabidopsis. Nat Commun **7,** 13181.

Wu, S.Y., and Chiang, C.M. (2009). Crosstalk between sumoylation and acetylation regulates p53-dependent chromatin transcription and DNA binding. EMBO J **28,** 1246-1259.

Wu, T., Lyu, R., and He, C. (2022). spKAS-seq reveals R-loop dynamics using low-input materials by detecting single-stranded DNA with strand specificity. SCIENCE ADVANCES.

Xiao, Q., Huang, X., Zhang, Y., Xu, W., Yang, Y., Zhang, Q., Hu, Z., Xing, F., Sun, Q., and Li, G. (2022). The landscape of promoter-centred RNA–DNA interactions in rice. Nature Plants **8,** 157-170.

Xiao, T., Kao, C.-F., Krogan, N.J., Sun, Z.-W., Greenblatt, J.F., Osley, M.A., and Strahl, B.D. (2005). Histone H2B ubiquitylation is associated with elongating RNA polymerase II. Molecular and cellular biology **25,** 637-651.

Xie, Q., Wang, P., Liu, X., Yuan, L., Wang, L., Zhang, C., Li, Y., Xing, H., Zhi, L., Yue, Z., Zhao, C., McClung, C.R., and Xu, X. (2014). LNK1 and LNK2 are transcriptional coactivators in the Arabidopsis circadian oscillator. Plant Cell **26,** 2843-2857.

Xin, H., Takahata, S., Blanksma, M., McCullough, L., Stillman, D.J., and Formosa, T. (2009). yFACT induces global accessibility of nucleosomal DNA without H2A-H2B displacement. Mol Cell **35,** 365-376.

Xiong, L., Zhou, W., and Mas, P. (2022). Illuminating the Arabidopsis circadian epigenome: Dynamics of histone acetylation and deacetylation. Curr Opin Plant Biol **69,** 102268.

Xu, C., Wu, Z., Duan, H.C., Fang, X., Jia, G., and Dean, C. (2021). R-loop resolution promotes co-transcriptional chromatin silencing. Nat Commun **12,** 1790.

Xu, L., Zhao, Z., Dong, A., Soubigou-Taconnat, L., Renou, J.P., Steinmetz, A., and Shen, W.H. (2008). Di- and tri- but not monomethylation on histone H3 lysine 36 marks active transcription of genes involved in flowering time regulation and other processes in Arabidopsis thaliana. Mol Cell Biol **28,** 1348-1360.

Xu, P.B., Lian, H.L., Wang, W.X., Xu, F., and Yang, H.Q. (2016). Pivotal Roles of the Phytochrome-Interacting Factors in Cryptochrome Signaling. Mol Plant **9,** 496-497.

Xu, W., Xu, H., Li, K., Fan, Y., Liu, Y., Yang, X., and Sun, Q. (2017). The R-loop is a common chromatin feature of the Arabidopsis genome. Nature plants **3,** 704-714.

Xu, W., Li, K., Li, S., Hou, Q., Zhang, Y., Liu, K., and Sun, Q. (2020a). The R-Loop Atlas of Arabidopsis Development and Responses to Environmental Stimuli. Plant Cell

32, 888-903.

Xu, W., Li, K., Li, S., Hou, Q., Zhang, Y., Liu, K., and Sun, Q. (2020b). The R-loop atlas of Arabidopsis development and responses to environmental stimuli. The Plant Cell **32,** 888-903.

Yadav, P., Owiti, N., and Kim, N. (2016). The role of topoisomerase I in suppressing genome instability associated with a highly transcribed guanine-rich sequence is not restricted to preventing RNA:DNA hybrid accumulation. Nucleic Acids Res **44,** 718-729.

Yan, Q., Shields, E.J., Bonasio, R., and Sarma, K. (2019). Mapping Native R-Loops Genome-wide Using a Targeted Nuclease Approach. Cell Rep **29,** 1369-1380 e1365.

Yang, M., Han, X., Yang, J., Jiang, Y., and Hu, Y. (2021). The Arabidopsis circadian clock protein PRR5 interacts with and stimulates ABI5 to modulate abscisic acid signaling during seed germination. Plant Cell **33,** 3022-3041.

Yang, S., Winstone, L., Mondal, S., and Wu, Y. (2023). Helicases in R-loop Formation and Resolution. J Biol Chem **299,** 105307.

Yang, X., Liu, Q.L., Xu, W., Zhang, Y.C., Yang, Y., Ju, L.F., Chen, J., Chen, Y.S., Li, K., Ren, J., Sun, Q., and Yang, Y.G. (2019). m(6)A promotes R-loop formation to facilitate transcription termination. Cell Res **29,** 1035-1038.

Yang, Z., Li, M., and Sun, Q. (2020). RHON1 Co-transcriptionally Resolves R-Loops for Arabidopsis Chloroplast Genome Maintenance. Cell Rep **30,** 243-256 e245.

Yang, Z., Hou, Q., Cheng, L., Xu, W., Hong, Y., Li, S., and Sun, Q. (2017). RNase H1 Cooperates with DNA Gyrases to Restrict R-Loops and Maintain Genome Integrity in Arabidopsis Chloroplasts. Plant Cell **29,** 2478-2497.

Yanovsky, M.J., and Kay, S.A. (2002). Molecular basis of seasonal time measurement in Arabidopsis. Nature **419,** 308-312.

Yanovsky, M.J., Mazzella, M.A., and Casal, J.J. (2000). A quadruple photoreceptor mutant still keeps track of time. Curr Biol **10,** 1013-1015.

Yao, X., Feng, H., Yu, Y., Dong, A., and Shen, W.H. (2013). SDG2-mediated H3K4 methylation is required for proper Arabidopsis root growth and development. PLoS One **8,** e56537.

Yasuhara, T., Kato, R., Hagiwara, Y., Shiotani, B., Yamauchi, M., Nakada, S., Shibata, A., and Miyagawa, K. (2018). Human Rad52 Promotes XPG-Mediated R-loop Processing to Initiate Transcription-Associated Homologous Recombination Repair. Cell **175,** 558-570 e511.

Yeom, M., Kim, H., Lim, J., Shin, A.Y., Hong, S., Kim, J.I., and Nam, H.G. (2014). How do phytochromes transmit the light quality information to the circadian clock in Arabidopsis? Mol Plant **7,** 1701-1704.

Young, M.W. (2000). Life's 24-hour clock: molecular control of circadian rhythms in animal cells. Trends in biochemical sciences **25,** 601-606.

Yu, Y., Su, C., He, Y., and Wang, L. (2023). B-Box proteins BBX28 and BBX29 interplay with PSEUDO-RESPONSE REGULATORS to fine-tune circadian clock in Arabidopsis. Plant Cell Environ.

Yuan, W., Zhou, J., Tong, J., Zhuo, W., Wang, L., Li, Y., Sun, Q., and Qian, W.J.S.a. (2019a). ALBA protein complex reads genic R-loops to maintain genome stability in Arabidopsis. SCIENCE ADVANCES **5,** eaav9040.

Yuan, W., Zhou, J., Tong, J., Zhuo, W., Wang, L., Li, Y., Sun, Q., and Qian, W. (2019b). ALBA protein complex reads genic R-loops to maintain genome stability in Arabidopsis. SCIENCE ADVANCES **5,** eaav9040.

Yüce, Ö., and West, S.C. (2013). Senataxin, defective in the neurodegenerative disorder ataxia with oculomotor apraxia 2, lies at the interface of transcription and the DNA damage response. Molecular and cellular biology **33,** 406-417.

Zagotta, M.T., Hicks, K.A., Jacobs, C.I., Young, J.C., Hangarter, R.P., and Meeks-Wagner, D.R. (1996). The Arabidopsis ELF3 gene regulates vegetative photomorphogenesis and the photoperiodic induction of flowering. The Plant Journal **10,** 691-702.

Zatreanu, D., Han, Z., Mitter, R., Tumini, E., Williams, H., Gregersen, L., Dirac-Svejstrup, A.B., Roma, S., Stewart, A., Aguilera, A., and Svejstrup, J.Q. (2019). Elongation Factor TFIIS Prevents Transcription Stress and R-Loop Accumulation to Maintain Genome Stability. Molecular Cell **76,** 57-69.e59.

Zhang, C., Chen, L., Peng, D., Jiang, A., He, Y., Zeng, Y., Xie, C., Zhou, H., Luo, X., Liu, H., Chen, L., Ren, J., Wang, W., and Zhao, Y. (2020). METTL3 and N6-Methyladenosine Promote Homologous Recombination-Mediated Repair of DSBs by Modulating DNA-RNA Hybrid Accumulation. Mol Cell **79,** 425-442 e427.

Zhang, D.W., Rodriguez-Molina, J.B., Tietjen, J.R., Nemec, C.M., and Ansari, A.Z. (2012). Emerging Views on the CTD Code. Genet Res Int **2012,** 347214.

Zhang, J.Y., Zheng, K.W., Xiao, S., Hao, Y.H., and Tan, Z. (2014). Mechanism and manipulation of DNA:RNA hybrid G-quadruplex formation in transcription of G-rich DNA. J Am Chem Soc **136,** 1381-1390.

Zhang, X., Bernatavichute, Y.V., Cokus, S., Pellegrini, M., and Jacobsen, S.E. (2009). Genome-wide analysis of mono-, di- and trimethylation of histone H3 lysine 4 in Arabidopsis thaliana. Genome Biol **10,** R62.

Zhang, X., Chen, Y., Wang, Z.Y., Chen, Z., Gu, H., and Qu, L.J. (2007). Constitutive expression of CIR1 (RVE2) affects several circadian-regulated processes and seed germination in Arabidopsis. Plant J **51,** 512-525.

Zhang, Y. (2003). Transcriptional regulation by histone ubiquitination and deubiquitination. Genes Dev **17,** 2733-2740.

Zhang, Y., Fan, S., Hua, C., Teo, Z.W.N., Kiang, J.X., Shen, L., and Yu, H. (2022). Phase separation of HRLP regulates flowering time in Arabidopsis. Science advances **8,** eabn5488.

Zhao, H., Zhu, M., Limbo, O., and Russell, P. (2018). RNase H eliminates R-loops that disrupt DNA replication but is nonessential for efficient DSB repair. EMBO Rep **19**.

Zhao, H., Winogradoff, D., Dalal, Y., and Papoian, G.A. (2019). The Oligomerization Landscape of Histones. Biophys J **116,** 1845-1855.

Zheng, D., Li, M., Yang, Y., Huang, R., and Zhang, W. (2022). R-loops: emerging key regulators in plants. J Exp Bot.

Zhou, J., Wan, J., Gao, X., Zhang, X., Jaffrey, S.R., and Qian, S.B. (2015a). Dynamic m(6)A mRNA methylation directs translational control of heat shock response. Nature **526,** 591-594.

Zhou, K.I., Shi, H., Lyu, R., Wylder, A.C., Matuszek, Z., Pan, J.N., He, C., Parisien, M., and Pan, T. (2019). Regulation of Co-transcriptional Pre-mRNA Splicing by m(6)A through the Low-Complexity Protein hnRNPG. Mol Cell **76,** 70-81 e79.

Zhou, W., Zhu, Y., Dong, A., and Shen, W.H. (2015b). Histone H2A/H2B chaperones: from molecules to chromatin-based functions in plant growth and development. Plant J **83,** 78-95.

Zhu, L., and Zee, P.C. (2012). Circadian rhythm sleep disorders. Neurologic clinics **30,** 1167-1191.

Zippo, A., Serafini, R., Rocchigiani, M., Pennacchini, S., Krepelova, A., and Oliviero, S. (2009). Histone crosstalk between H3S10ph and H4K16ac generates a histone code that mediates transcription elongation. Cell **138,** 1122-1136.